Niemann-Pick C1 Is Essential for Ebola Virus Infection and a Target of Small Molecule Inhibitors

Dissertation Advisor: James Cunningham, M.D. Anna Marie Bruchez

Niemann-Pick C1 is essential for Ebola virus infection and a target of small molecule inhibitors

Abstract

Ebolavirus (EboV) is a highly pathogenic enveloped virus that causes outbreaks of zoonotic infection in Africa. The clinical symptoms are manifestations of the massive production of pro-inflammatory cytokines in response to infection and in many outbreaks, case fatality rate exceeds 75%. The unpredictable onset, ease of transmission, rapid progression of disease, high mortality and lack of effective vaccine or therapy have created a high level of public concern about EboV. Here we report the properties of a benzylpiperazine adamantane diamide-derived compound identified in a screen for inhibitors of EboV infection. We found that the inhibitor is specific, reversible, and that the target(s) for inhibition are present in cells and not in virus particles. The compound is not an inhibitor of acid pH-dependent endosome protease activity, which is required for EboV infection. Treatment of cells with this compound causes accumulation of cholesterol in late endosomes and lysosomes (LE/LY), suggesting it inhibits one or more proteins involved in regulation of cholesterol uptake into cells. Using mutant cell lines and informative derivatives of the inhibitor, we found the inhibitor target is the endosomal membrane protein Niemann-Pick C1 (NPC1). NPC1 is a polytopic LE/LY membrane protein that

mediates uptake of lipoprotein-derived cholesterol into cells. We find that NPC1 is essential for EboV infection, that NPC1 binds to the protease-cleaved GP1 subunit of the EboV glycoprotein, and that the anti-viral compound inhibits infection by targeting NPC1 and interfering with binding to GP1. Furthermore, analysis of viral variants resistant to the anti-viral compound revealed that the residues which confer resistance are located on the surface of the receptor binding domain of GP1. Combined with the results of previous studies of GP structure and function, our findings support a model of EboV infection in which cleavage of the GP1 subunit by endosomal cathepsin proteases removes heavily glycosylated domains to expose the N-terminal domain, which is a ligand for NPC1 and regulates membrane fusion by the GP2 subunit. Thus, NPC1 is essential for EboV entry and a target for anti-viral therapy.

Table of Contents

List of Figures

List of Tables

Acknowledgments

First of all, I'd like to thank my advisor Jim Cunningham for all of his valuable insight, guidance, and enthusiasm for science. Your passion for the process of scientific discovery and virus entry makes discussions always exciting and intellectually stimulating. I'd also like to thank all of the Cunningham lab members, you have helped guide me through graduate school, while making the sometimes-daily monotony that can be science fun, exciting, and, dare I say, pleasant. The environment is collaborative to the fullest extent and I will always treasure the moments where one of us ran in with a new blot and put the still warm exposure on the light box to share and discuss. I always look forward to our scientific conversations because they are a pure joy. Thank you!

I'd also like to thank my friends and family. They have stuck with me through the hard times and the wonderful ones, sharing every success and failure along the way. To my brother Marcel, a scientist to the end, thank-you for all of your help and support throughout my scientific career. But most importantly, thanks for fostering my love of science from a young age and teaching me that I could do anything that I set my sights on, it is because of you that I never doubted for a single moment that I could be both a scientist and a woman at heart. To my brothers, all three of them, thanks for treating me like one of the boys and for never letting me see myself as anything other than a capable and passionate human being. To my mom, who has always encouraged my scientific endeavors, thank you for being there from boiling plants from the backyard for science fair projects to asking me every single time I called during graduate school "So,

how is THE science?". My discussions with you have taught me how to communicate my science in "plain English" and have, hopefully, made me a better scientist for it.

Finally, I'd like to thank Kenny Matreyek, my boyfriend and fellow graduate student, without your support I literally would not have survived this thesis writing process. Thanks for talking science with me, even after long days in lab, bouncing ideas off you is always valuable. Thanks for being my editor-in-chief, and for reading my thesis from start to finish. Also, thanks for keeping me fed and in clean clothing while writing my thesis!

Chapter 1

Introduction

Breaking into cells: Viral entry proteins, host encoded triggering factors, and the mysteries of Ebola virus entry.

Virus entry

As obligate intracellular parasites viruses must deliver their genetic material into the host cell in order to propagate and spread. The first major physical barrier that a virus must bypass in order to productively infect a cell is the plasma membrane. Viruses have evolved highly specialized mechanisms for getting past the protective lipid bilayer that surrounds the host cell. All viruses must enter the cell through a mechanism that leaves the host undamaged so that it may continue to subvert the resources of the host for its own replication and spread. For non-enveloped viruses, which are protected by a proteinaceous shell, entry is facilitated by penetration and disruption of the host membrane by viral coat proteins. Enveloped viruses protect their genetic material by acquiring a lipid bilayer during budding from the parent cell and must facilitate fusion of the virus and host membranes in order to deliver their genome. A high kinetic barrier must be overcome to bring the two membranes in close enough proximity for fusion to occur.

Structural Rearrangements Facilitate Membrane Fusion

Enveloped viruses have evolved a diverse set of specialized surface expressed viral glycoproteins (GPs) that serve to lower the kinetic barrier to membrane fusion (Chernomordik and Kozlov, 2003). These fusion proteins lower this kinetic requirement by providing free energy when they undergo an energetically favorable structural rearrangement as they bring the virus and host membrane in close proximity. Despite a wide range of differences in both fusion

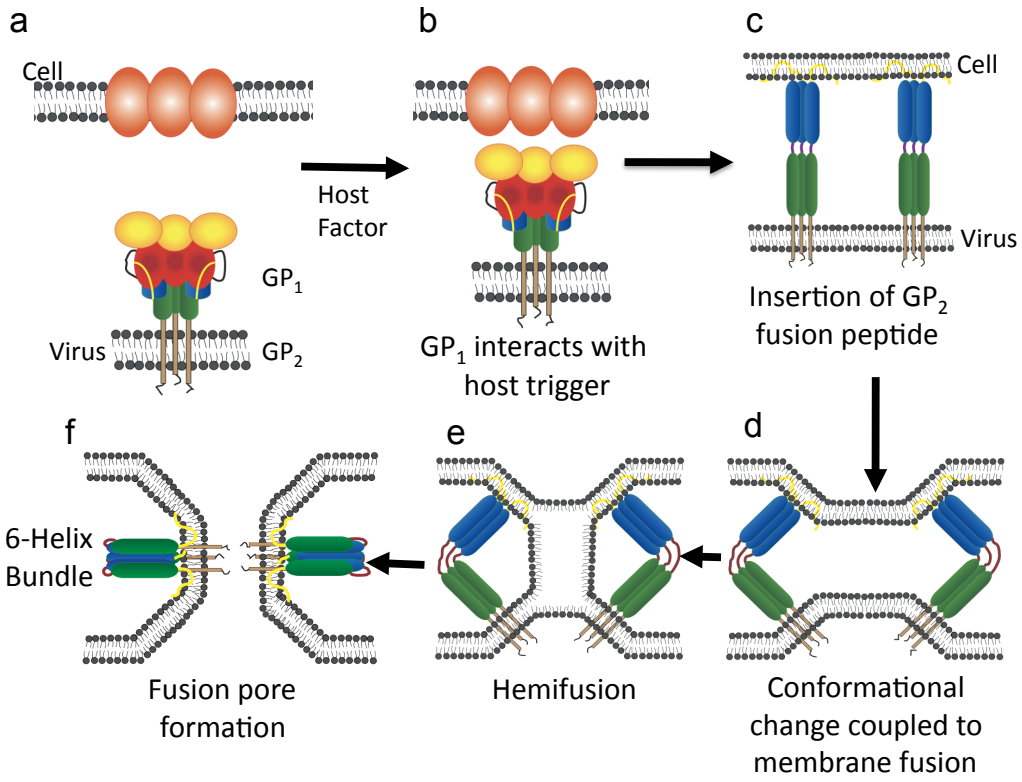

Figure 1-1. ***A generalized mechanism for enveloped virus entry.*** (a-c) As the virus approaches the host cell the attachment domain (GP1), interacts with a triggering factor provided by the target cell. This then causes a structural change that releases GP1 imposed constraints on the fusion subunit (GP2). GP2 extends towards the cellular membrane to facilitate fusion peptide (yellow) insertion into the cellular lipid bilayer, thus, forming what is termed the extended pre-hairpin intermediate. (d) GP2 continues to undergo structural rearrangements as it continues to fold to its lowest energy level conformation, a trimer of hairpin. As GP2 begins to fold back on itself the virus and host membranes begin to deform as they are bought in close proximity to each other. (e) These membrane deformations lower the energetic barrier between the two lipid bilayers and a hemifusion intermediate begins to form where the outer lipid bilayers begin to mix while the inner bilayers remain separate. (f) As GP2 undergoes its final rearrangements which bring the fusion peptide and transmembrane regions of GP2 in close proximity in a trimer of hairpins, a fusion pore beings to form and finally expands allowing for delivery of viral contents into the cell.

protein structure and cellular signals that trigger their conformational changes, all classes of virus fusion proteins share a generalized fusion mechanism. Viral fusion proteins have two membrane interacting domains that facilitate the juxtaposition of the membranes: a hydrophobic patch that ultimately inserts into the host membrane termed the fusion peptide (F) and a trans-membrane (TM) domain at the C-terminus that anchors the protein in the viral membrane. Upon stimulation from the host cell, the GP undergoes a structural rearrangement leading to a homo-trimeric extended pre-hairpin intermediate that connects the two membranes (Figure 1-1a-c). During the formation of this intermediate, the hydrophobic fusion peptide is released from its pre-fusion confirmation and extends to imbed in the target (cellular) membrane (Figure 1-1c). The reaction proceeds as the fusion protein folds back onto itself to form a 'trimer-of-hairpins', which function to bring the fusion peptide (cellular membrane) and the transmembrane domain (viral membrane) together (Figure 1-1d). The two membranes deform as they are brought into close proximity, lowering the energetic barrier between the two bilayers until a hemifusion intermediate forms. During hemifusion, the outer leaflets merge while the inner leaflets of the lipid bilayers remain separate (Figure 1-1e). As the conformational rearrangement is completed, the hemifusion intermediate develops into a fusion pore, which expands to allow delivery of the contents of the virion into the host cell (Figure 1-1f). The structural rearrangements that occur between the prefusion and postfusion confirmations of the viral GP provide the free energy required to catalyze membrane fusion. This generalized model of membrane fusion has

been established over the course of over thirty-years from the accumulation of several pioneering structural and functional studies of virus membrane fusion.

Structural classifications of virus fusion proteins: Class I, II, and III

Viral membrane glycoproteins can be categorized into three classes of proteins based on structural homology between their extracellular domains in their prefusion and postfusion conformations (reviewed in White et al., 2008 and Harrison, 2008). Class I proteins form trimeric oligomers in both the pre- and postfusion conformations that are mostly α-helical in secondary structure. A broad range of viral families have class I fusion proteins including Orthomyxoviridae (with the classical example of influenza HA), Retroviridae, Paramyxoviridae, Coronaviridae, Filoviridae, and Arenaviridae. In contrast, class II fusion proteins are composed primarily of ß-strands and are expressed as flat dimers on mature virions. Triggering of class II fusion proteins converts the dimers into trimerized projections from the viral membrane, which subsequently fold back to form a trimer-of-hairpins composed of β-sheets. Flaviviridae, Togaviridae, and Bunyaviridae all encode class II fusion proteins. Class III viral proteins share structural characteristics with both class I and class II viral proteins and are composed of a mix of β-stands and α-helicies. The fusion proteins from Rhabdoviridae and Herpesviridae are class III fusion proteins. Although the pre- and postfusion confirmations have been solved for all classes of fusion proteins, we know the most about the structure, function, and triggering of class I fusion proteins.

Class I fusion proteins

Class I viral proteins are the most widely studied class of viral fusion proteins and much of our insight into viral fusion proteins, and specifically class I proteins, comes from groundbreaking structural work done by Wiley and Skehel that solved the prefusion conformation of influenza HA (Wilson et al., 1981), the postfusion conformation of HA2 (Bullough et al., 1994) and the conformation of the uncleaved precursor HA0 (Chen et al., 1998). Class I glycoproteins are often synthesized as a polypeptide precursor (GP0) that must be cleaved post-translationally into two domains. This processing step requires the action of a host cell protease late in the biosynthetic process or an extracellular enzyme after budding. This cleavage, which is N-terminal to the fusion peptide, creates two functional domains in the GP: a transmembrane domain that mediates fusion (GP2) and an ectodomain (GP1) that serves as a clamp that maintains GP2 in its pre-fusion confirmation. For most class I fusion proteins the cleavage of the poly-protein is required for infectivity; indeed, viral particles containing only uncleaved influenza HA0 or HIV gp160 are noninfectious (Kawaoka and Webster, 1987; McCune et al., 1988; Bosch and Pawlita, 1990). This trimer of hetero-dimers created by the cleavage takes on a metastable conformation, a state in which GP1 forms an energetic barrier by providing stabilizing contacts that prevent rearrangement of GP2 into the post-fusion conformation. GP2 contains structural domains that are crucial for membrane fusion, including a N-terminal fusion peptide (F), an α-helical heptad repeat region 1 (HR1), a linker region, a second

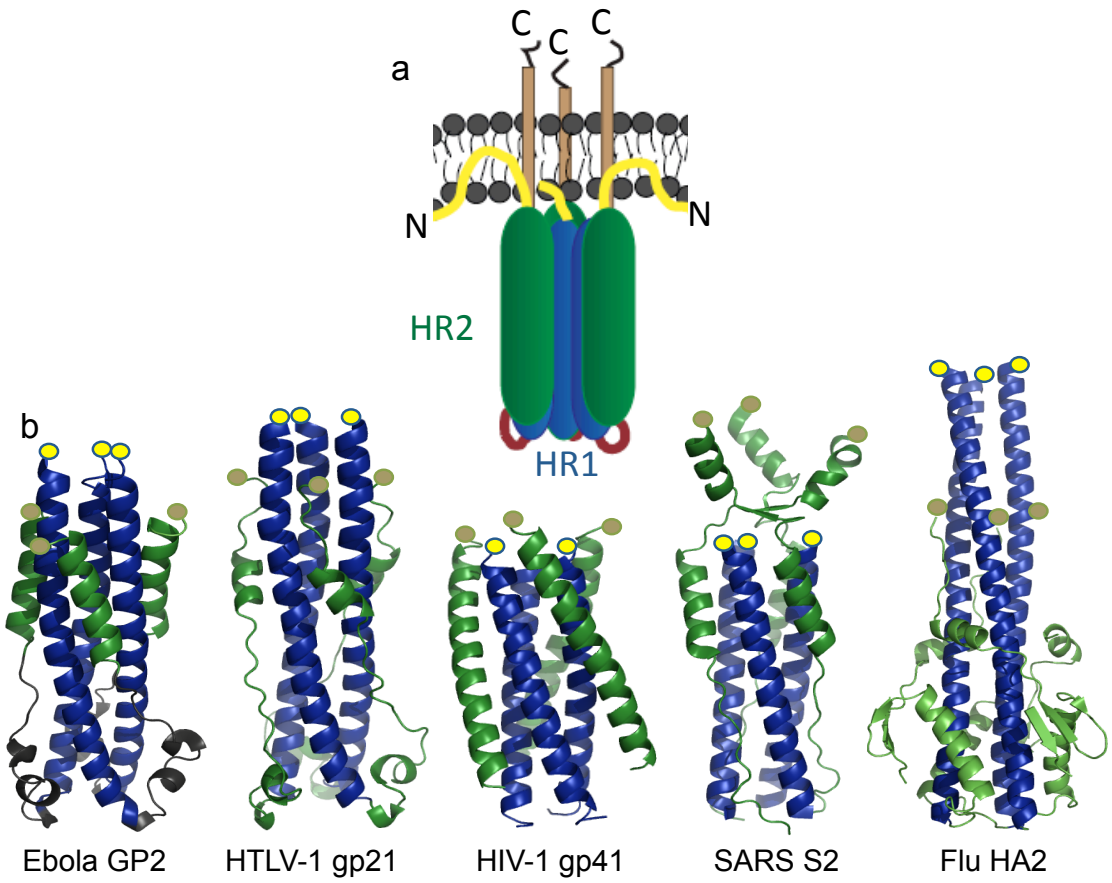

Figure 1-2. ***Class I viral fusion proteins have a trimeric coiled-coil post-fusion conformation.*** **(a)** During fusion the extended pre-hairpin intermediate folds back to form a hairpin in which the C-terminal transmembrane domain of the fusion protein (depicted here in brown, attached to the viral membrane) comes into close proximity to the N-terminal fusion peptide (depicted in yellow, attached to the host membrane). This conformational change facilitates fusion of the two membranes. HR1 (blue) forms the central coiled coil of the hairpin, while HR2 (green) packs into the groves of the HR1 coiled coil to form a trimer of hairpins or a 6-HB. (b) Atomic resolution structures of the post-fusion conformations of several representative class I viral fusion proteins. Only the transmembrane subunit (or GP2) is depicted. The N-terminal fusion loops and the C-terminal transmembrane regions are not resolved. Structures are color coded as in (a). PDB files are as follows: Ebola GP2 (1EBO), HTLV-1 gp21 (1MG1), HIV-1 gp41 (1ENV), SARS S2 (2BEQ), and Flu HA2 (1HTM).

α-helical heptad repeat region (HR2), and a C-terminal transmembrane (TM) region which anchors the domain to the viral envelope. During membrane fusion, GP2 irreversibly converts into a stable postfusion conformation, in which the N-terminal fusion peptide is adjacent to the C-terminal TM. For all class I proteins, this postfusion trimer-of-hairpins conformation is termed the six helix-bundle (6HB) because it is composed of a trimer of HR2 that "zips up" into the grooves of the central α-helical HR1 core (Figure 1-2a). The 6HB form of the fusion protein is the most stable conformation that the GP takes on during the fusion process. Although a broad range of viruses with extremely diverse sequences have class I GPs, the central 6HB of the postfusion conformation remains structurally conserved (Bullough et al., 1994; Kobe et al., 1999; Weissenhorn et al., 1997; Weissenhorn et al., 1998; Supekar et al., 2004) (Figure 1-2b). The transition to 6HB formation is an irreversible rearrangement because the postfusion conformation represents the lowest energy state of the protein. Thus, it is essential that viruses trigger conversion to the postfusion conformation only when they are in close enough proximity to a target membrane to initiate productive fusion. The GP1 of class I fusion proteins have evolved several regulated mechanisms to sense cellular 'triggers' and initiate fusion only when the virus is close enough to the target membrane.

Entry mechanisms

Dissection of the membrane distal subunit of GP have revealed that this protein has two functions: the first is to provide stabilizing contacts with the

prefusion form of GP2, or the so called “clamp” function, and the second is to sense a host provided signal that releases the restraints on GP2, known as the “triggering” function. GP1 must also mediate attachment to the plasma membrane of target cells, which can be mediated by specific or non-specific attachment factors and, occasionally, by a specific receptor-virus interaction. Here, we will make a distinction between virus receptors and attachment factors, a distinction that is not often made in the literature; we will refer to host factors on the cell surface that simply bind to the GP as attachment factors. Attachment factors can form specific interactions such as the binding between sialic acid (SA) and influenza HA (Weis et al., 1988), or can be broader factors that bind non-specifically to the sugars on the surface of the GP, as is the case for the interactions between DC-SIGN and HIV, SARS-CoV, Influenza or EboV (Geijtenbeek et al., 2000; Alvarez et al., 2002; Wang et al., 2008; Yang et al., 2004; Marzi et al., 2004). Attachment factors serve to tether the virus to the plasma membrane, facilitating a subsequent interaction with an entry receptor on the cell surface, or mediating virus uptake into the cell through the endocytic pathway, upon which the virus may then encounter its necessary trigger. In contrast, a virus entry receptor binds to the GP and induces a conformational change that ultimately leads to the fusion of the virus and host membranes. Host factors that trigger this fusion reaction can act in a one-step manner, where a single signal leads to the conformational change needed to trigger fusion, or in a multi-step manner, where two or more host factors are required to induce sequential and step-wise conformational rearrangements necessary for

membrane fusion.

Host factors that trigger: a one-step or multi-step mechanism

Various examples of host factor triggers are known for both one- and multi-step mechanisms of fusion protein activation. To date only two types of host signals trigger single-step fusion mechanisms: either low pH or receptor binding. In the case of influenza HA, the virion is internalized following attachment to sialic acid on the cell surface, and is trafficked through the endocytic pathway until the pH of the endosome drops to a level capable of triggering a pH dependent structural rearrangement responsible for releasing the fusion peptide (Skehel et al., 1982). The interaction of the ecotropic murine leukemia virus (E-MLV) glycoprotein (SU) with its receptor murine cationic amino acid transporter 1 (MCAT-1) provides an example of a receptor-induced one-step fusion mechanism (Albritton et al., 1993). The binding of the receptor binding domain (RBD) on the E-MLV SU with MCAT-1 triggers structural changes that reveal a disulfide bond isomerization CXXC motif in the clamping domain of SU (Davey et al., 1997; Wallin et al., 2006). Exposure of this motif leads to a disulfide bond rearrangement that releases the covalent bond between SU and the fusion subunit (TM), allowing for the subsequent transformation to the 6HB postfusion state (Wallin et al., 2004; Wallin et al, 2005; Li et al., 2007).

By contrast, multi-step fusion mechanisms utilize either a combination of receptors at the cell surface or a combination of receptor binding followed by an endosomal triggering step. One of the best-characterized two-step triggering

mechanism is that of HIV-1. During entry the HIV-1 distal unit of GP (gp120) interacts with its two receptors in a sequential manner. Initially, CD4 binding to gp120 induces a conformational change that moves aside an immunoprotective domain and reveals the co-receptor binding site (Dalgleish et al., 1984; Klatzmann et al., 1984). The revealed binding site is capable of interacting with a co-receptor, either CXCR4 or CCR5, which leads to the release of gp41 (GP2 equivalent) and catalysis of membrane fusion (Choe et al., 1996; Deng et al., 1996; Dragic et al., 1996; Feng et al., 1996). Still, not all two-step receptor interactions simply move aside domains to reveal the final triggering interaction. The interaction between the avian leukosis virus type A (ALV-A) envelope and its receptor, Tva, induces a conformational change into a stable extended pre-hairpin fusion intermediate, in which the fusion peptide is embedded in the target membrane. This intermediate only converts into the postfusion 6HB conformation after subsequent exposure to low pH (Mothes et al., 2000). In yet another permutation of a two-step triggering mechanism, the binding of the S glycoprotein of SARS coronavirus with its cell surface receptor, angiotensin-converting enzyme 2 (ACE2), potentiates the cleavage of the S glycoprotein with the pH dependent endosomal protease cathepsin L, which ultimately triggers membrane fusion (Simmons et al., 2005). Although numerous virus receptors have been identified, the exact manners in which they are able to propagate a binding signal into large structural rearrangements are not fully understood. The regions that constitute the RBD in HIV GP120 and MLV gp70 are distinct from the regions that stabilize GP2 and can, in the case of MLV, remain functional in absence of

covalent linkage to the remainder of Env (Barnett et al., 2001). The findings that domains for attachment, triggering, and stabilization of the transmembrane subunit are distinct is consistent with the suggestion of Wiley and colleagues that viruses acquired multistep regulation of Env function by incorporating functional domains into a basic fusion machine composed of the clamp and transmembrane domains (Rosenthal et al., 1998). Regardless of how many steps an entry mechanism may have, the identification of the key host triggers of virus entry are essential for understanding the ways in which viruses have evolved to use these host factors for productive infection.

Identifying essential host factors

For the cases described above, the host factors and receptors have been identified with a combination of experimental approaches using genetics, biochemistry, and chemical biology. One commonly used genetic method for receptor identification involves the transfer of host genes responsible for virus entry into non-permissive cell lines; a method that was used to identify the receptor for E-MLV, as well as the CXCR4 co-receptor for HIV (Albritton et al., 1989; Feng et al., 1996). This method requires the identification of non-permissive cell lines as well as the construction of cDNA libraries from permissive cells. Another commonly used method involves physically capturing a proteinaceous host factor through biochemical purification of host proteins capable of binding the receptor binding subunits of the viral fusion proteins. The virus receptors for SARS-CoV (ACE2), the paramyxovirus Nipah virus

(ephrinB2), and the New World arenavirus Machupo (transferrin receptor 1) were identified using artificially engineered ligands composed of the receptor binding subunit of GP fused to the Fc domain of human IgG (Li et al., 2003; Radoshitzky et al., 2007; Negrete et al., 2005). After binding to the surface of permissive cells, these engineered proteins were used to co-immunoprecipitate their corresponding receptor proteins, which were then identified through mass-spectrometric analysis. This method is potentially hindered by the cellular location of the receptor, the affinity with which the GP binds to the cellular receptor, and the capability of mass-spectrometric analysis to identify the protein. Indeed, if the host factor is not a proteinaceous binding partner, then neither of these two methods would reveal its identity. In the cases of low pH induced fusion of influenza HA and cathepsin protease-dependent fusion mechanism of SARS-CoV, chemical inhibitors of known function were used to tease out the relevant host factors (Yoshimura et al., 1982; Simmons et al., 2005; Huang et al., 2006). However, these discoveries required significant *in vitro* characterization to confirm that the inhibitors were indeed acting in the manner suspected because of the high probability of off-target effects for small molecules. More often than not, follow-up experiments that confirm the roles of the identified host factors employ a combination of all of these experimental tools. Although the viral receptors and host factors that mediate entry for several major human pathogens with class I fusion proteins have been identified, relatively little is known about the entry mechanism of the highly pathogenic Ebola virus. Recent studies have suggested that Ebola virus has a unique entry mechanism that involves drastic

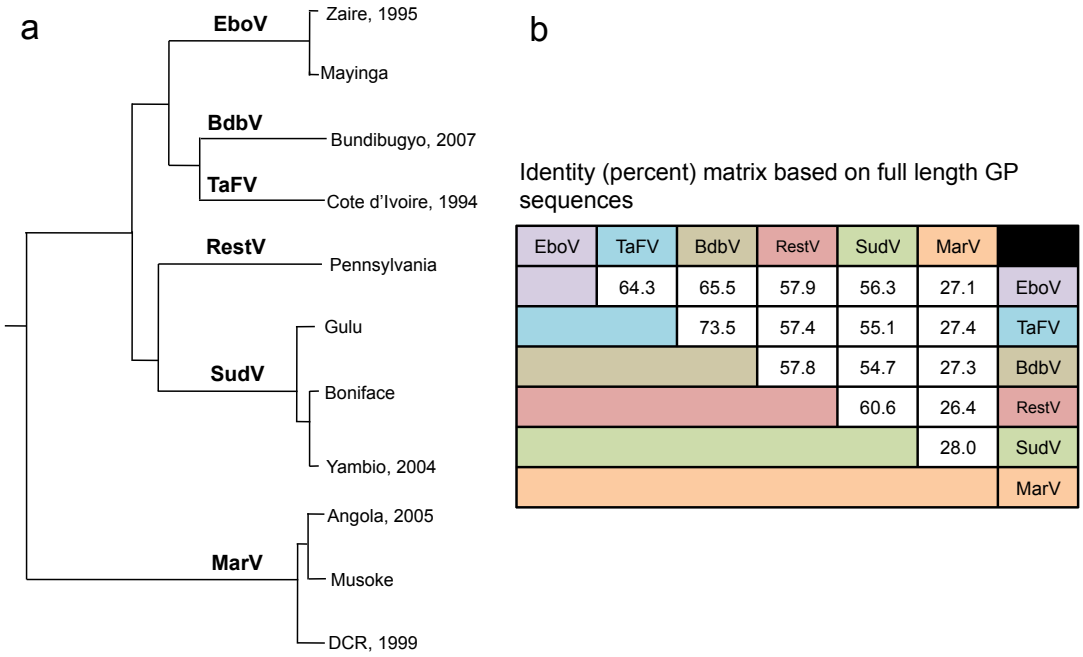

Figure 1-3. ***Phylogenetic analysis reveals six species of filoviruses.*** **(a)** A phylogenetic tree comparing the full length viral genomes of representative strains of ebolavirus and marburgvirus. The two genera can be divided into one marburg species, *Marburg marburgvirus* (MarV), and five ebola species, *Zaire ebolavirus* (EboV)*, Sudan ebolavirus* (SudV)*, Taï Forest ebolavirus* (TaFV), *Reston ebolavirus* (RestV*)* and *Bundibugyo ebolavirus* (BdbV*).* **(b)** A percent identity matrix was produced using amino acid sequences of the full length glycoproteins of the reference strains for all filovirus species.

cleavage of the ectodomain and subsequent unidentified triggering steps.

Ebola virus as a class I envelope virus

Infection by the *Filoviridae* family of viruses, which consists of the two genera *Marburgvirus* and *Ebolavirus*, often causes a highly lethal hemorrhagic fever syndrome in humans and nonhuman primates. The two genera can be divided into a single marburg species, *Marburg marburgvirus* (MarV), and five ebola species, *Zaire ebolavirus* (EboV)*, Sudan ebolavirus* (SudV)*, Taï Forest ebolavirus (*TaFV*,* formerly *Cote d'Ivoire ebolavirus), Reston ebolavirus* (RestV*)* and *Bundibugyo ebolavirus* (BdbV*)* (Figure 1-3a). While the genomes of the ebolavirus species differ from each other by only about 30-40% at the nucleotide level, the differences between the two genera are much greater, at approximately 70% (Towner et al., 2008).

These filamentous viruses have non-segmented negative stranded RNA genomes which are enveloped by a host-derived membrane acquired through virus budding. During Ebola virus infection, fusion of the virus and host membranes is mediated by the viral membrane glycoprotein (GP), a class I viral fusion protein, which forms trimers of hetero-dimers on the surface of virions (Figure 1-4a). The two subunits that make up the mature dimer are GP1 and GP2; GP1 mediates viral adhesion and regulates GP2, the transmembrane subunit that drives viral fusion (Watanabe et al., 2000; Manicassamy et al., 2005). As with other class I proteins, EboV GP is synthesized as a polyprotein that is cleaved during biosynthesis in the Golgi by a furin-like protease into GP1

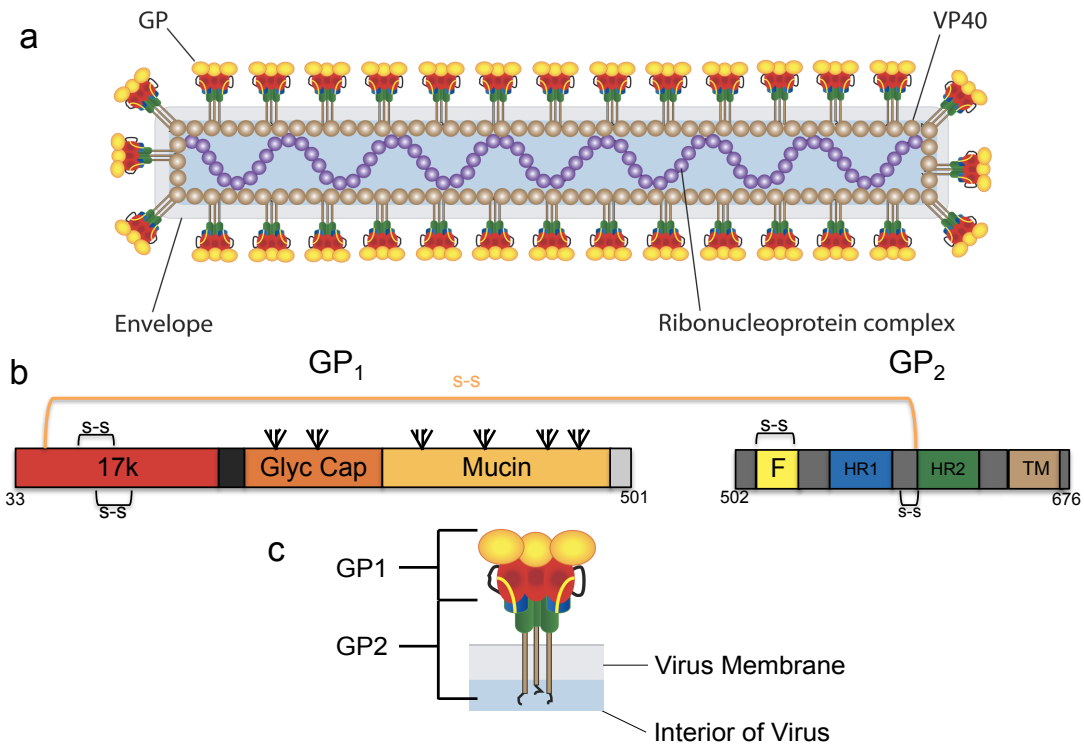

Figure 1-4. ***Schematic of filovirus virions and glycoprotein.*** **(a)** Filovirus virions are long filamentous particles with a negative stranded RNA genome bound to proteins, which together make the ribonucleoprotein complex core. The core is surrounded by the matrix protein VP40 which lies between the core and the envelope. The glycoprotein (GP), the only virus protein that lies on the surface of the virion, forms trimerized spikes. **(b)** GP is a type I viral glycoprotein. The precursor polyprotein is cleaved in the Golgi by furin between amino acids 501 and 502, splitting the protein into GP1 and GP2 domains. GP1, the distal subunit that mediates virus attachment, is divided into two central domains, a N-terminal protease resistant core (17k) and a heavily glycosylated domain composed of the glycan cap (Glyc Cap) and a highly variable mucin-like domain (Mucin). GP2, the membrane proximal domain that mediates fusion, is composed of an internal fusion loop (F), followed by two canonical type I heptad repeat regions (HR1 and HR2), and a transmembrane domain (TM) that anchors the protein into the virus membrane. **(c)** After furin cleavage, GP1 and GP2 remain covalently linked through a disulphide bond (s-s) and trimerize to form spikes on the virion surface.

and GP2 (Volchkov et al., 1998) (Figure 1-4b). However, unlike the previously mentioned examples of class I GPs (such as HIV, E-MLV, and influenza), the furin cleavage site between EboV GP1 and GP2 is dispensable for both entry and pathogenesis (Wool-Lewis and Bates, 1999; Neumann et al., 2007). After furin cleavage, GP1 and GP2 remain disulfide linked and trimerize to form a functional GP (Figure 1-4c) (Ito et al., 1999; Ito et al., 2001; Takada et al., 1997; Watanabe et al., 2000; Wool-Lewis and Bates, 1998). GP, the sole viral protein on the virion surface, drives a multistep entry process that requires attachment, uptake into vesicles via a macropinocytic like mechanism (Saeed et al., 2010; Nanbo et al., 2010), trafficking to the late endosome/ lysosome (LE/LY), and fusion with the limiting membrane of the LE/LY.

EboV attachment factors

Although little is know about the minimal requirements for EboV fusion, the search for host factors that mediate fusion has lead to the identification of several factors that enhance EboV infection. These factors include molecules that bind non-specifically to the sugars present on the heavily glycolyated GP, such as DC-SIGN (dendritic cell-specific ICAM3-grabbing non-integrin) and L-SIGN (liver and lymphnode SIGN), which likely enhance infection by concentrating virions on the cell surface (Alvarez et al., 2002; Marzi et al., 2004). By contrast, other enhancement factors that do not bind directly to the GP, such as β1 integrins and the TYRO3 family tyrosine kinase receptor Axl, act to enhance infection through indirect mechanisms like promotion of downstream protease activity or induction

of macropinocytosis respectively (Shimojima et al., 2006; Shimojima et al., 2007; Schornberg et al., 2009; Hunt et al., 2011). Finally, a recently identified enhancement protein, T cell immunoglobulin and mucin domain-containing 1 (TIM1), appears to bind EboV GP. However, several cells that do not express this protein are still highly susceptible to EboV infection, thus indicating that it is not an essential entry factor (Kondratowicz et al., 2011). Although each of these factors enhance EboV entry by enhancing virion attachment or uptake, they are not essential for infection; cells that lack these proteins are still susceptible to EboV entry. The early search for essential host factors for EboV entry was impeded by two key characteristics of the virus. First, filoviruses are able to infect a vast range of cell types from many different species (Wool-Lewis and Bates, 1998), so the resulting lack of non-permissive cell lines limits the usefulness of gain of function genetic approaches. Secondly, binding of a soluble GP1 ligand to the surface of permissive cells did not reveal a high-affinity binding site on the plasma membrane that could be purified by affinity chromatography and identified by mass spectroscopy. To date, chemical approaches have yielded the few clues we have as to which essential host factors may function in EboV entry.

Low pH and Cathepsins are essential EboV Host Factors

Early studies of Ebola virus entry revealed that entry occurred in a low pH-dependent manner. Lysosomotropic agents such as bafilomycin-A, ammonium chloride (NH_4Cl), and chloroquine, which each prevent the acidification of the endosome, inhibited EboV-GP mediated entry (Wool-Lewis and Bates, 1998;

Takada et al., 1997). However, unlike other low pH dependent viruses such as influenza, *in vitro* exposure of virions to low pH did not inactivate the virus, indicating that low pH alone was not sufficient to trigger entry.

Subsequently, our lab and others have demonstrated that EboV entry requires the acid dependent endosomal proteases cathepsins, a family of related enzymes that function optimally at pH 5.0 in the late endosomes and lysosomes of cells (Chandran et al., 2005; Schornberg et al., 2006). These studies showed that cathepsin B (CatB) is an essential host factor, while CatL serves an accessory role. *In vitro* cleavage with purified cathepsins suggests that proteolysis of the GP by cathepsins is likely a multi-step process involving several cysteine proteases. Digestion of virus with CatB or CatL cleaves the 130kD GP1 molecule down to an 18kD intermediate, which then undergoes further processing by CatB into a stable 17kD intermediate (Chandran et al., 2005 and Schornberg et al., 2006). The protease cleaved virus remains fully infectious and sensitive to the cysteine protease inhibitor E-64 and to the endosomal acidication blocking drug bafilomycin A (Figure 1-5) (Schornberg et al., 2006). Follow-up experiments on the role of cathepsins in entry have mapped the cathepsin cleavage site to amino acid 190 in GP1 and have suggested that *in vitro* protease cleavage increases EboV GP binding and infectivity (Kaletsky et al., 2007; Dube et al., 2009; Hood et al., 2010). Cleavage of GP is necessary but not sufficient for entry, thus, suggesting that additional host factors activate the GP fusion mechanism (Figure 1-5). Although it is possible that another

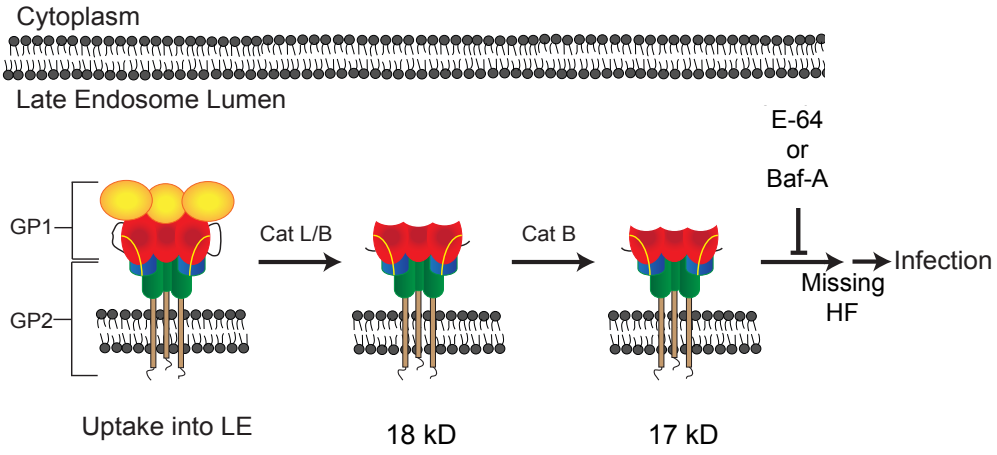

Figure 1-5. ***Role of cathepsins B and L in EboV entry.*** EboV is taken up and trafficked to the late endosomes (LE) of cells. Once in the LE, cathepsins (Cat) B and/or L act on the GP1 domain and cleave off a significant portion of the GP1 protein, leaving an intermediate fragment that is only 18kD in size. This intermediate then undergoes further cathepsin B processing to form a 17kD post-cathepsin intermediate. This intermediate is still fully infectious and is able to overcome specific CatB/L blocks to infections, but remains sensitive to the cysteine protease inhibitor E-64 or the inhibitor of endosomal acidification bafilomycin A (Baf-A), suggesting that there is still a role for another as of yet unidentified LE host factor (HF) in EboV entry.

endosomal protease or other LE/LY factor may mediate the final triggering step for Ebola virus fusion, there is mounting evidence that receptor binding may play a critical role in filovirus entry.

Evidence for a filovirus receptor

There are three lines of evidence that suggest that Ebola virus entry may require an active receptor: (1) mutagenesis and infection studies show that single point mutants in a 150 amino acid region of the highly conserved N-terminal domain of GP1 decrease infectivity (Brindley et al., 2007; Manicassamy et al., 2005; Manicassamy et al., 2007; Mpanju et al., 2006), (2) a putative minimal receptor binding domain (RBD) has been identified in GP1 that binds to permissive cells (Kuhn et al., 2006 and Dube et al., 2009) and (3) the atomic resolution structure of the prefusion Ebola GP suggests that highly variable and heavily glycosylated domains of the protein may have evolved to shield this putative minimal RBD from immune recognition (Lee et al., 2008).

Studies utilizing recombinant proteins that fuse the putative receptor-binding domain (RBD) of GP1 to the Fc domain of human IgG, have given us our first clues into the potential role for a receptor in Ebola virus entry. Kuhn et al. identified a homologous 151-amino acid fragment in MarV GP1 and EboV GP1 (AA 54-201) that bound specifically to permissive cell lines but showed no binding to non-permissive lymphocyte cell lines (2006). In contrast, full-length GP1-Fc did not bind to permissive cells. Both the MarV and EboV GP-Fc

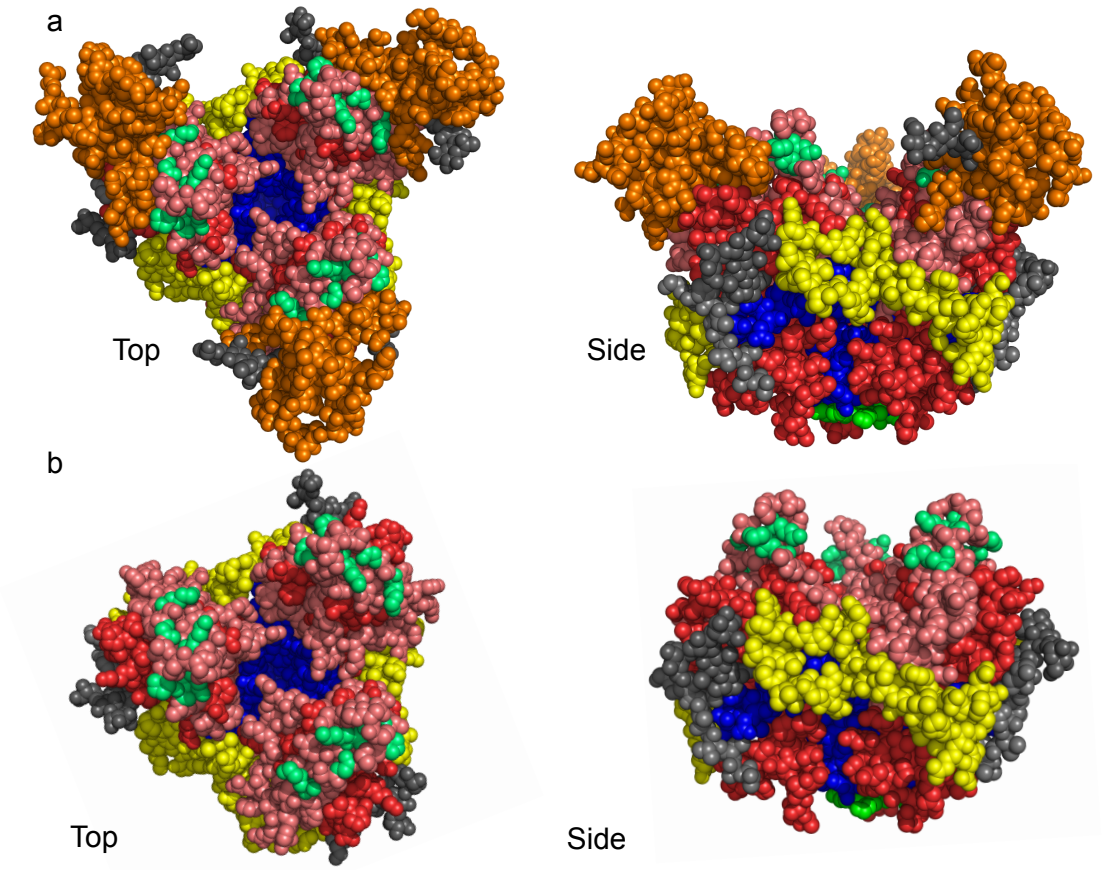

Figure 1-6. ***Structure of the prefusion EboV GP prior to cathepsin cleavage and a modeled post-cleavage GP.*** **(a)** A space fill model of the atomic resolution prefusion trimer structure of EboV GP (PDB 3CSY, left, view from top; right, view from side). Glycans that were resolved in the structure are depicted here in gray. The region of the protein that corresponds to the glycan cap is shown as orange spheres. The "minimal" RBD is depicted here in pink with key residues important for binding highlighted in light green. The remainder of GP1, shown in red, constitutes the base or clamping domain. The fusion loop of GP2, depicted here in yellow, nestles into an adjacent GP1 monomer. The HR1 region of GP2, shown in blue, forms the stalk and cradles the base of the chalice bowl created by GP1. **b)** Predicted model of the GP trimer after cathepsin mediated removal of the glycan cap. The site of cathepsin cleavage has been mapped to amino acid 190 in GP1, which is consistent with complete removal of the glycan cap and subsequent exposure of the RBD.

constructs inhibited the entry of retroviruses pseudotyped with either filovirus envelope, suggesting an overlap in receptor usage between these highly divergent filovirus species (Kuhn et al., 2006). Subsequent experiments narrowed down the minimal RBD to residues 90-149 of GP1, found that the fusion protein bound in a saturable manner at very high concentrations, and indicated that certain cells have an extensive intracellular pool of RBD-Fc binding partners (Dube et al., 2009; Dube et al., 2010). The mapping of the minimal RBD as well as the localization of the cathepsin cleavage site correlates well with structural data from the atomic resolution structure of the prefusion EboV GP.

Structure of EboV GP suggests protease cleavage reveals the RBD

The prefusion GP structure shows that the trimer takes on a chalice like conformation (Figure 1-6a); the three GP1 subunits come together to form the bowl of the chalice with the putative receptor binding sites present on the inside of the bowl, while the GP2 helices cradle the bowl and form the stalk of the chalice (Lee et al., 2008). The inside of the chalice bowl and the RBD are at least partially occluded by both a glycan cap (Figure 1-6a), a domain of the protein that includes several N-linked glycans, and a mucin-like domain, a highly variable domain with several N- and O-linked glycosylation sites that are not present in the crystal structure, but has been modeled to lay on top of the bowl (Lee et al., 2008). Interestingly, the cathepsin cleavage site lies within a disordered loop that bridges the portions of GP1 containing the RBD to the glycan cap, suggesting that cathepsin proteases serve to remove these heavily glycosylated

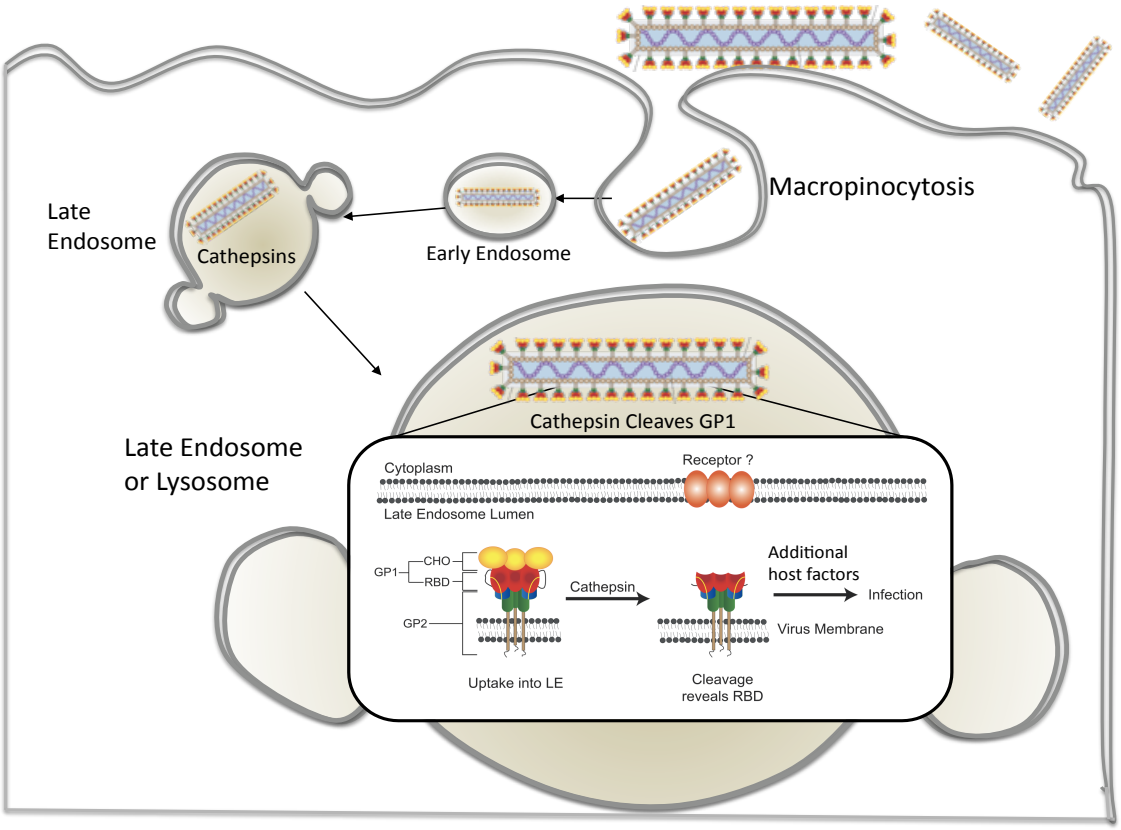

Figure 1-7. ***Model of ebola virus entry circa 2010.*** EboV particles bind to attachment factors on the cell surface and are internalized by macropinocytosis. Cleavage of EboV GP by the endosomal cysteine proteases cathepsins exposes the receptor binding domain. Additional unidentified host factors are required to trigger virus fusion with the host cell membrane. There could be one or more host factors that trigger fusion. Data suggests that binding to an unidentified intracellular receptor may play a key role in entry.

immunoprotective domains to expose a functional receptor binding site (Figure 1-6b) (Lee et al., 2008). The findings of a structurally distinct RBD that is revealed only in the LE/LY compartments after cathepsin cleavage, and the presence of an extensive intracellular pool of RBD binding partners (Dube et al., 2010), provide compelling evidence for the role of an intracellular receptor during EboV entry (Figure 1-7).

Using small molecules to identify a missing intracellular host factor

A central step towards understanding the mechanism of Ebola virus entry is the identification of the putative intracellular receptor. However, as previously mentioned, the nearly ubiquitous nature of permissive cells combined with the fact that the RBD binding site may be in an intracellular compartment, has prevented the productive use of biochemical or gain-of-function genetic tests to identify a GP1 binding partner. Instead, our lab decided to take an unbiased chemical biology approach to take advantage of a key characteristic of small molecule inhibitors: that the size and hydrophobicity of many small molecules allows them to diffuse past the cellular membrane, making them more likely to be capable of targeting a potential intracellular host factor. We employed a vesicular stomatitis virus-pseudotyping (VSV) system to develop an entry assay that could be utilized in BSL2 for a high-throughput screen (HTS) to identify small molecule inhibitors of EboV entry. A single cycle VSV system engineered to express firefly-Luciferase in the place of the VSV glycoprotein (VSV-G) was used for the assay. The viruses were pseudotyped with either VSV-G or EboV-GP. VSV-G was

chosen as a counter screen since it also enters through a low pH dependent mechanism. The entry assay scored a molecule as positive for EboV entry inhibition if the molecule inhibited EboV-GP but not VSV-G, thus eliminating hits that were overly toxic to the cells, affected the post-entry steps of VSV infection, or inhibited viral entry through a mechanism shared by both glycoproteins. In collaboration with the Institute of Chemistry and Cell Biology (ICCB) at Harvard Medical School, our lab screened a chemical library of approximately 50,000 compounds, as well as a pool of known bioactive compounds. Six unique hits specific to EboV-GP were identified, referred to as compounds 3.0, 4.0, 5.0, 6.0, 7.0, and 8.0. These compounds exhibited IC50s of less than 5μM, and no apparent cell cytotoxicity. The bioactive screen yielded a number of cysteine protease inhibitors (including E-64d), as well as specific cathepsin B and L inhibitors, validating the ability of this screen to identify EboV-specific inhibitors. In addition to the inhibitors of the known EboV host factors, the bioactive screen and subsequent confirmatory experiments identified a number of surprising compounds that inhibited EboV entry. These compounds include sertraline, tamoxifen, alverine, and U18666A.

Scope of the Dissertation

A central step towards understanding the mechanism of Ebola virus entry is the identification of the missing host factors that activate fusion, a task that has long eluded those studying EboV entry. In an attempt to use an unbiased chemical biology approach to identify chemical probes that target the suspected

but unidentified host factors involved in EboV entry, our lab performed a HTS. The screen identified several small molecules and bioactives that inhibited EboV entry. The data presented in this dissertation represents the body of work that followed the screen, work that ultimately lead us to the identification of Niemann-Pick C1 as a novel host factor for EboV entry and a target of one of the compounds.

The initial characterization of the inhibitors established that they were specific and reversible, that the target was likely in the cell rather than the virus particles, and that they did not disrupt cathepsin activity. We demonstrated that the compounds were active against protease cleaved virus, suggesting that they possibly inhibited a novel entry step downstream of cathepsin cleavage. In an attempt to further characterize the compounds, we studied the physiochemical properties of the compounds identified in the small molecule and bioactive screen. We noticed that many of the compounds identified in the screen were hydrophobic amines and had physiochemical properties that suggested they act like cationic amphiphilic drugs (CAD). We tested our compounds for the ability to induce cholesterol accumulation in the LE/LY of cells, a common phenotype observed in cells treated with CADs. Compound 3.0 and its potent derivative 3.47 lead to accumulation of cholesterol in the LE/LY of cells. Because 3.0 and 3.47 did not share the physiochemical properties characteristic of CADs, we investigated the possibility that these inhibitors could be targeting components of the cholesterol uptake pathway. Systematic analysis of components of the LE/LY cholesterol uptake pathway, through the use of human fibroblasts from patients

with cholesterol transport disorders and siRNA knockdown of genes, revealed that NPC1 played a critical role in EboV entry. Experiments in knockout cells established that NPC1 expression was strictly required for EboV entry but that cholesterol transport activity was not required. Consistent with a role as a possible receptor, we found that only cathepsin cleaved GP bound to NPC1. Studies conducted with 3.0 and its derivatives confirmed that these compounds directly target NPC1, that they are able to prevent the binding of cleaved GP to NPC1, and that the NPC1-GP interaction is important for virus entry. Finally, the observation that mutations in the RBD of GP1 conferred resistance or sensitivity to the inhibitor strengthens the claim that the interaction between NPC1 and cleaved GP may represent the long-sought-after virus-receptor interaction.

The identification of the NPC1 as the missing intracellular receptor for EboV fills in a substantial gap in the knowledge of the mechanisms that mediate EboV entry. Fortunately, the findings in this dissertation fit nicely into the established model for Ebola virus entry. They reveal an elegant mechanism by which the virus is able to shed its immuno-protective domain using host cathepsin proteases in the LE/LY. Thus, the receptor-binding site is revealed only once it is in the LE/LY of cells where the receptor, NPC1, is located. The implications of these findings are explored in detail in the discussion.

Chapter 2

Identification of NPC1 as an essential host factor for EboV entry

The data presented in this chapter is derived in part from the following published work.

Côté M.*, Misasi J.*, Ren T.*, Bruchez A.*, Lee K., Filone C.M., Hensley L., Li Q., Ory D., Chandran K., Cunningham J. Small molecule inhibitors reveal Niemann–Pick C1 is essential for Ebola virus infection. *Nature.* 447, 344-348 (2011).

*Contributed equally.

Contributions: KC and TR performed the inhibitor screen. KL synthesized and purified inhibitor analogs. AB and TR tested inhibitors in infection assays. AB tested cellular phenotypes of inhibitors. AB performed initial characterization of the inhibitors. TR, AB, JM, and MC carried out infection assays with pseudotyped viruses. AB did infection assays in primary human fibroblasts. AB performed microscopy. TR and MC performed siRNA experiments. JM purified recombinant glycoprotein. MC and JM designed and performed binding assays. MC performed immunoprecipitation. Ebola virus infections were performed in the lab of LH by CF.

Figure contributions: MC produced the data for Figures 2-10b, 2-11b, 2-13, and 2-14b. TR produced the data for Figure 2-10c. CF produced the data for Figure 2-11c. JM produced the data for Table 2-3 and Figure 2-12. AB and JM collaborated to produce the data for Figure 2-14a. AB produced all other Figures.

Abstract:

Ebola virus (EboV) is a highly pathogenic enveloped virus that causes outbreaks of zoonotic infection in Africa. Here we report the identification of several novel and bioactive compounds that inhibit EboV entry. In characterizing the antiviral activities of these compounds, we found that they are reversible and that the target(s) for inhibition are present in cells and not in virus particles. The compounds are not inhibitors of the known EboV host factors cathepsin proteases or low pH. Treatment of cells with one of the compounds, a novel benzylpiperazine adamantane diamide-derived compound, leads to cholesterol accumulation in the late endosome and lysosome (LE/LY) of cells, suggesting that the compounds target one or more proteins involved in regulation of cholesterol uptake in cells. Using mutant cell lines and siRNA knockdown of key proteins in this pathway, we show that the endosomal membrane protein Niemann-Pick C1 (NPC1) is essential for EboV infection. We find that NPC1 expression but not cholesterol transport activity is essential for infection and that it binds to the virus glycoprotein (GP). Combined with the results of previous studies of GP structure and function, our findings support a model of EboV infection in which cleavage of the GP1 subunit by endosomal cathepsin proteases removes heavily glycosylated domains to expose the N-terminal domain, which is a ligand for NPC1 and regulates membrane fusion by the GP2 subunit. Thus, NPC1 is an essential host factor for EboV entry.

Introduction:

Ebola virus (EboV) infection often causes a highly lethal hemorrhagic fever syndrome in humans and nonhuman primates. The clinical symptoms are manifestations of the massive production of pro-inflammatory cytokines in response to infection, and mortality has exceeded 75% in many of the outbreaks (Zampieri et al, 2007). The unpredictable onset, ease of transmission, rapid progression of disease, high mortality and lack of effective vaccine or therapy have created a high level of public concern about EboV (Geisbert and Jahrling, 2004). EboV entry is a multistep process that requires an interaction with multiple host factors, thus making it an attractive target for potential therapeutic interventions.

During Ebola virus infection, fusion of the virus and host membranes is mediated by the viral membrane glycoprotein (GP), a class I viral fusion protein, which forms trimers of hetero-dimers on the surface of virions. The two subunits that make up the mature dimer are GP1 and GP2; GP1 mediates viral adhesion and regulates GP2, the transmembrane subunit that drives viral fusion (Watanabe et al., 2000; Manicassamy et al., 2005). GP drives a multistep entry process that requires attachment, uptake into vesicles, trafficking to the late endosome/ lysosome (LE/LY), and activation of GP fusion activity. Ebola GP mediated entry is dependent on both low pH and the acid dependent endosomal proteases cathepsins. Previous studies have shown that fusion activity is dependent on cleavage of the GP1 subunit by cathepsins (Chandran et al., 2005; Schornberg et al., 2006). Cleavage exposes the N-terminal domain of GP1, which may be a receptor ligand (Kuhn et al., 2006; Lee et al., 2008; Dube et al., 2009; Hood et al.,

2010). Cleavage of GP is necessary but not sufficient for entry, suggesting that additional host factors activate the GP fusion mechanism.

A central step towards understanding the mechanism of Ebola virus entry is the identification of the missing host factors that activate fusion. The lack of known non-permissive cell lines for EboV infection has prevented the use of the same gene-transfer based, gain-of-function approaches that have been successful in identifying receptors for other enveloped viruses (Albritton et al., 1989; Feng et al., 1996). Furthermore, the likely intracellular nature of the host-factor interaction has confounded the use of biochemical co-purification and identification techniques. Thus, our lab has instead taken an unbiased chemical biology approach to identify chemical probes that may target the suspected, but yet unknown host factors involved in EboV entry.

Results:

A. Initial characterization of compounds identified by screening

To identify chemical probes that target EboV entry host factors, we screened a library of small molecules and identified six novel molecules (3.0, 4.0, 5.0, 6.0, 7.0, 8.0) that inhibit infection by vesicular stomatitis virus particles (VSV) pseudotyped with EboV GP, but not VSV particles pseudotyped with native G or Lassa Fever virus (LFV) GP (Table 2-1). The IC50s of these compounds were each less than 5μM and there were no apparent cell cytotoxicities observed.

Table 2-1. EboV GP entry inhibitors identified through HTS

Compound	Structure	IC_{50}†	IC_{90}†
3.0	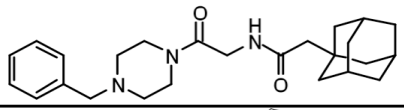	1.8 μM	8.6 μM
3.47*	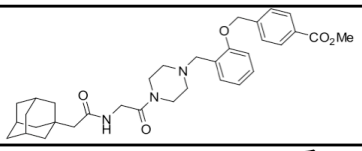	80 nM	1 μM
4.0	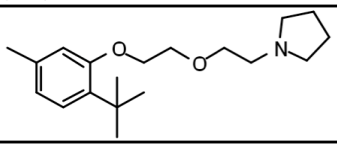	1.6 μM	4.7 μM
5.0	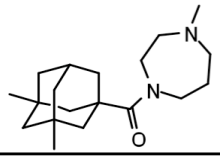	1.3 μM	5.0 μM
5.10*	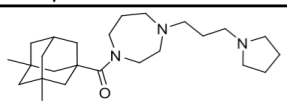	1.2 μM	1.7 μM
6.0	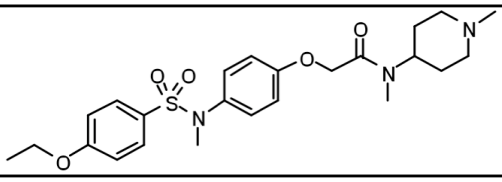	680 nM	2.0 μM
7.0	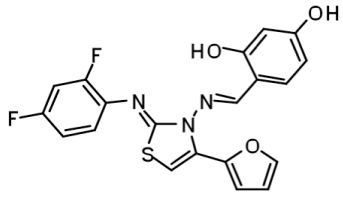	920 nM	2.5 μM
8.0	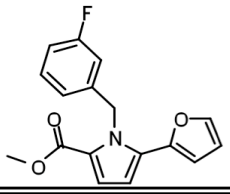	3.0 μM	12.5 μM

† IC_{50} and IC_{90} values were estimated from dose response curves obtained using in the following manner. Vero cells were grown in media containing increasing concentrations of compounds for 90 min before the addition of VSV particles encoding luciferase and pseudotyped with EboV GP (VSV-Luc-GP). Virus infection was graphed as a percent of luminescence units (RLU) relative to cells exposed to DMSO vehicle alone and IC values were estimated from these graphs. Data is representative of three independent experiments. N=6. *Potent derivatives of parent compounds 3.0 and 5.0 that were discovered through structure activity relationship (SAR) studies.

Subsequent studies of structure and (antiviral) activity relationships (SAR) with compounds 3.0 and 5.0 resulted in identification of derivatives 3.47 and 5.10, which exhibited greater anti-EboV activity than their parent compounds. Thus, our screen identified a panel of small molecules specifically capable of inhibiting EboV GP mediated viral entry.

B. Pre-incubation of virus with the compounds is not sufficient to block entry

Virion pre-incubation experiments were performed to determine whether compounds 3.0-8.0 block EboV entry by acting on the viral particle itself. Virus particles were incubated with inhibitors (≤10 μM) at 37°C for two hours (Figure 2-1a). Subsequent addition of the virus-inhibitor mixtures to the medium of susceptible cells reduced the concentration of inhibitor by 100-fold to ≤10 nM, well below the concentrations previously observed to be active during infection. Drug pre-incubation with virus did not inhibit infection under these conditions (Figure 2-1b). In contrast, when cells were exposed to ≤10 μM of the inhibitors during infection, the levels of VSV EboV GP-dependent infection were reduced by ≥80%. These findings suggested that the target(s) of each of the inhibitors were in the cell, rather than associated with the virus particles. It is important to note that these findings do not exclude reversible inhibition of an inhibitor target on virus particles.

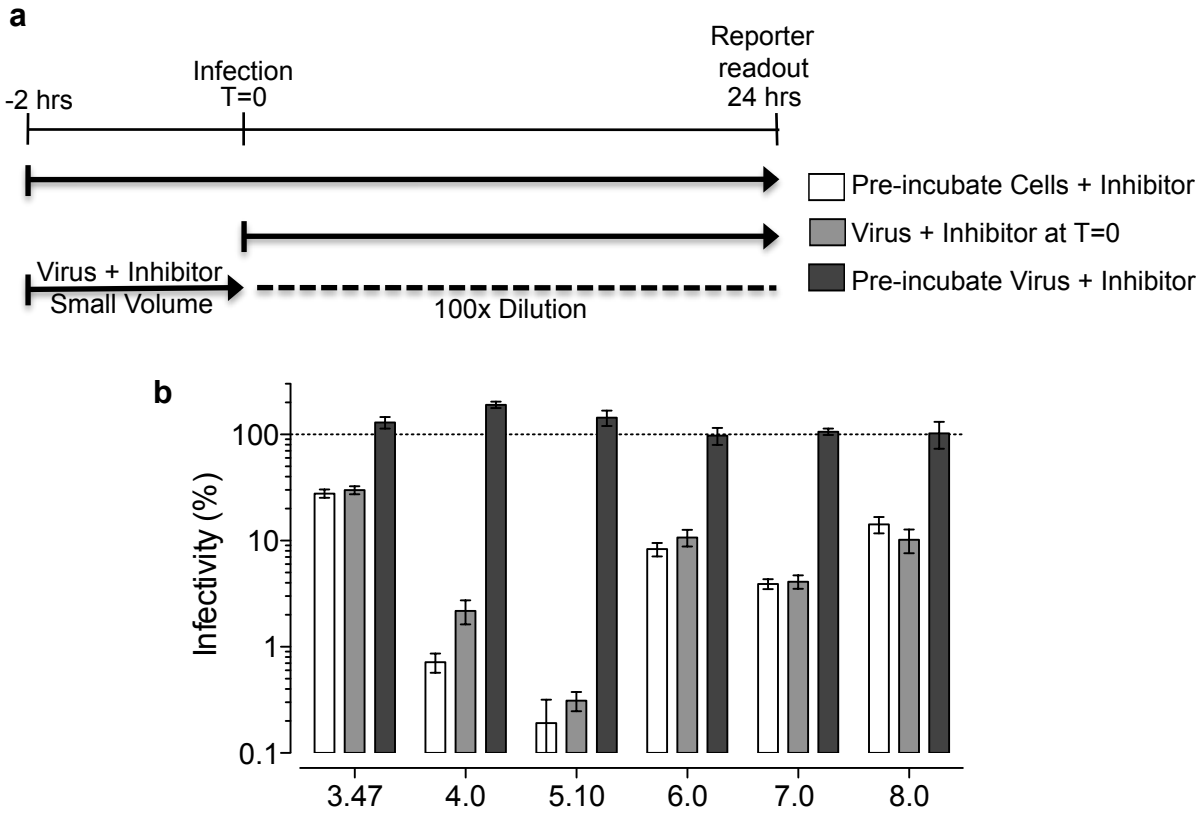

Figure 2-1. ***Pre-incubation of virus with inhibitors does not block entry.*** (a) Schematic of order of addition assays. Vero cells were seeded onto 12-well cell culture plates. Compounds 3.47 (1μM), 4.0 (10μM), 5.10 (2μM), 6.0 (1μM), 7.0 (2μM), 8.0 (10μM) and a vehicle control (DMSO) were added to cells or virus in the following three manners. (1) Cells were pre-incubated with inhibitors (white bars) at 37°C for two hours prior to infection and virus was added to the cells in the presence of the inhibitor. (2) Virus and inhibitors were added to cells simultaneously (gray bars) and inhibitors remained on the cells during infection. (3) Virus was pre-incubated with the inhibitors (black bars) in a small volume at 37°C for two hours before the addition of the mixture to the cells. The mixture was diluted 100x when added to the cells. **(b)** Cells were incubated with VSV particles encoding GFP and pseudotyped with EboV GP. Virus infection is reported as percent GFP-positive cells relative to cells exposed to DMSO vehicle alone. Data are mean ± s.d. (n=3)

C. Order of addition experiments

The temporal relationships between inhibitor action and infection were investigated. We performed a series of washout experiments in order to investigate the reversibility of the inhibitors. Vero cells were incubated for one hour at 37°C with an inhibitory concentration of the antiviral compounds or positive control ammonium chloride (NH_4Cl), which buffers and thus prevents acidification of lysosomes. Subsequently, the cells were cooled down to 25°C, and virus was added to allow the particles to bind in the presence of inhibitors. After 30 minutes, cells were washed to remove unbound virus and fresh media containing inhibitors were added back to the wells. Infection was initiated by raising the temperature to 37°C. At the indicated times post infection, media containing the inhibitors were removed and replaced with fresh media without inhibitor. No inhibition of infection was observed when the antiviral compounds were removed from culture media immediately before infection was initiated (Figure 2-2a). In contrast, incubation with the inhibitors for two hours after exposure to virus particles was sufficient to achieve the same degree of antiviral activity obtained by prolonged inhibitor treatment. These findings indicate that inhibitor action is reversible and occurs within the first two hours of infection.

Time-of-addition experiments were also performed to further characterize the minimal window upon which EboV entry is susceptible to the antiviral activity of inhibitors. Virus was again bound to cells at 25°C for 30 minutes, and infection was allowed to synchronously progress upon shift to 37°C. Either 20μM of EboV inhibitors, or 30mM NH_4Cl were added at various time points post infection.

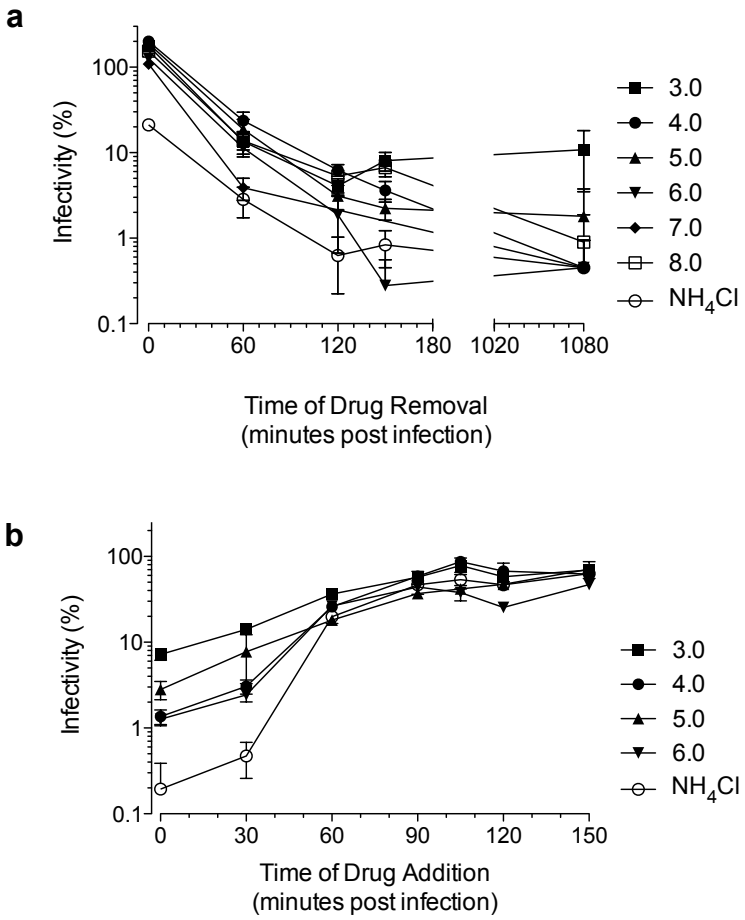

Figure 2-2. ***Kinetic experiments indicate that inhibitors can act up to 30 minutes post-infection.*** **(a)** Vero cells were incubated for one hour at 37°C with compounds 3.0, 4.0 , 5.0, 6.0, 7.0, 8.0 (20 μM), the lysosomatropic agent ammonium chloride (NH_4Cl, 30mM), or vehicle control (DMSO). Cells were then cooled to 25°C and VSV EboV-GP virus was added to allow the particles to bind in the presence of compounds. Wells were washed to remove unbound virus and media containing the inhibitor was added back to the wells. Infection was initiated by raising the temperature to 37°C. At the indicated times post infection, media containing the compounds was replaced with media containing no inhibitors. **(b)** Virus was bound to cells at 25°C, wells were washed to remove unbound virus, and infection was initiated by raising the temperature to 37°C. Media was replaced with inhibitor containing media at the indicated times post-infection. Concentrations of compounds are the same as in (a). Virus infection is reported as percent GFP-positive cells relative to cells exposed to DMSO vehicle alone. Data are mean ± s.d. (n=3)

Similar to NH_4Cl, each of the compounds were effective up through 30 minutes, but much less at 60 minutes following infection (Figure 2-2b). Taken together, these studies indicate that the newly identified compounds are reversible inhibitors of infection, and suggest that the antiviral target(s) exists within cells to mediate EboV trafficking and/or fusion.

D. Compounds do not target known EboV host factors: Low pH or Cathepsins

Previous studies indicate that the acid pH-dependent endosomal cysteine proteases cathepsin B and L are necessary but not sufficient for Ebola virus infection. We thus sought to determine whether the newly identified anti-EboV compounds inhibited cathepsin protease activity. In an initial experiment, we examined whether the antiviral compounds change the pH of the LE/LY where cathepsin B and L reside. This was achieved using LysoTracker Red, a probe that consists of a fluorophore attached to a weak base, which diffuses freely through membranes until it becomes protonated and concentrated in low pH compartments (Lemieux et al., 2004). We found that concentrations of the antiviral compounds corresponding to the IC_{99} had no effect on accumulation of LysoTracker within cells, while the buffering agents NH_4Cl and chloroquine ablated LysoTracker staining (Figure 2-3a). Corroborating this result, we found that the anti-EboV compounds have no effect on the entry of VSV particles pseudotyped with the acid pH-dependent glycoproteins of LCMV or VSV (Figure 2-3b). These findings strongly suggest that the antiviral activities of the newly

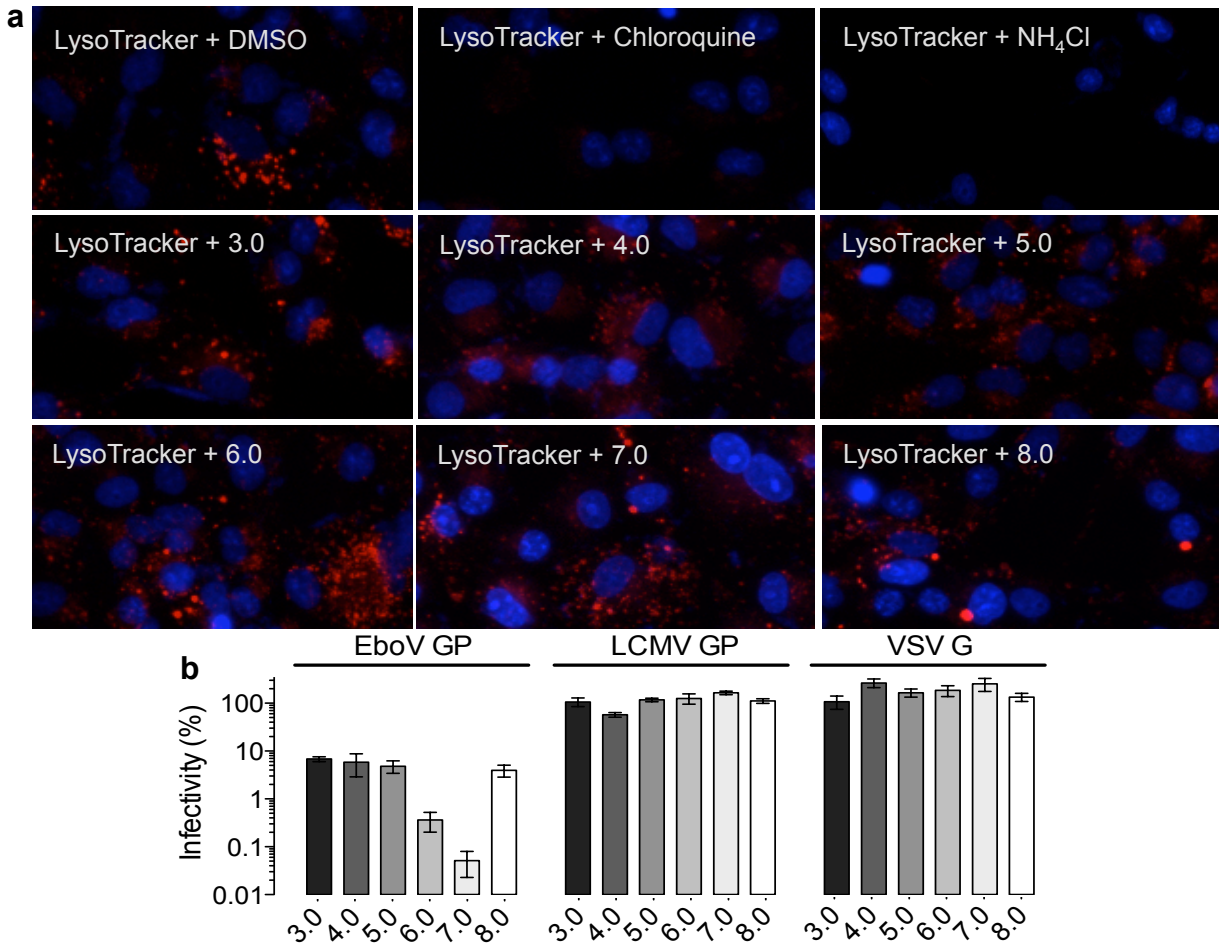

Figure 2-3. ***Inhibitors do not prevent acid dependent accumulation of LysoTracker nor entry of acid dependent viruses VSV and LCMV.*** **(a)** Cells were pre-incubated at 37°C for one hour with media containing the following compounds at their IC99, 3.0 (20μM), 4.0 (10μM), 5.0 (10μM), 6.0 (5μM), 7.0 (5μM), 8.0 (20μM), chloroquine (20μM), NH_4Cl (10mM) or vehicle control (DMSO). The cells were exposed to LysoTracker (red) at 37°C and then imaged ten minutes post-incubation. The presence of low pH compartments is indicated by the concentration of LysoTracker in those compartments (red) and the cell nuclei were counterstained with Hoechst stain (blue). **(b)** Vero cells were grown in media containing 3.0 (20μM), 4.0 (10μM), 5.0 (10μM), 6.0 (10μM), 7.0 (10μM), or 8.0 (20μM) for 90 min before the addition of VSV particles encoding luciferase and pseudotyped with either EboV GP, VSV G or LCMV GP. Virus infection is reported as percent of relative luminescence units (RLU) normalized to cells exposed to DMSO vehicle alone. Data are mean ± s.d. (n=3) and is representative of three experiments.

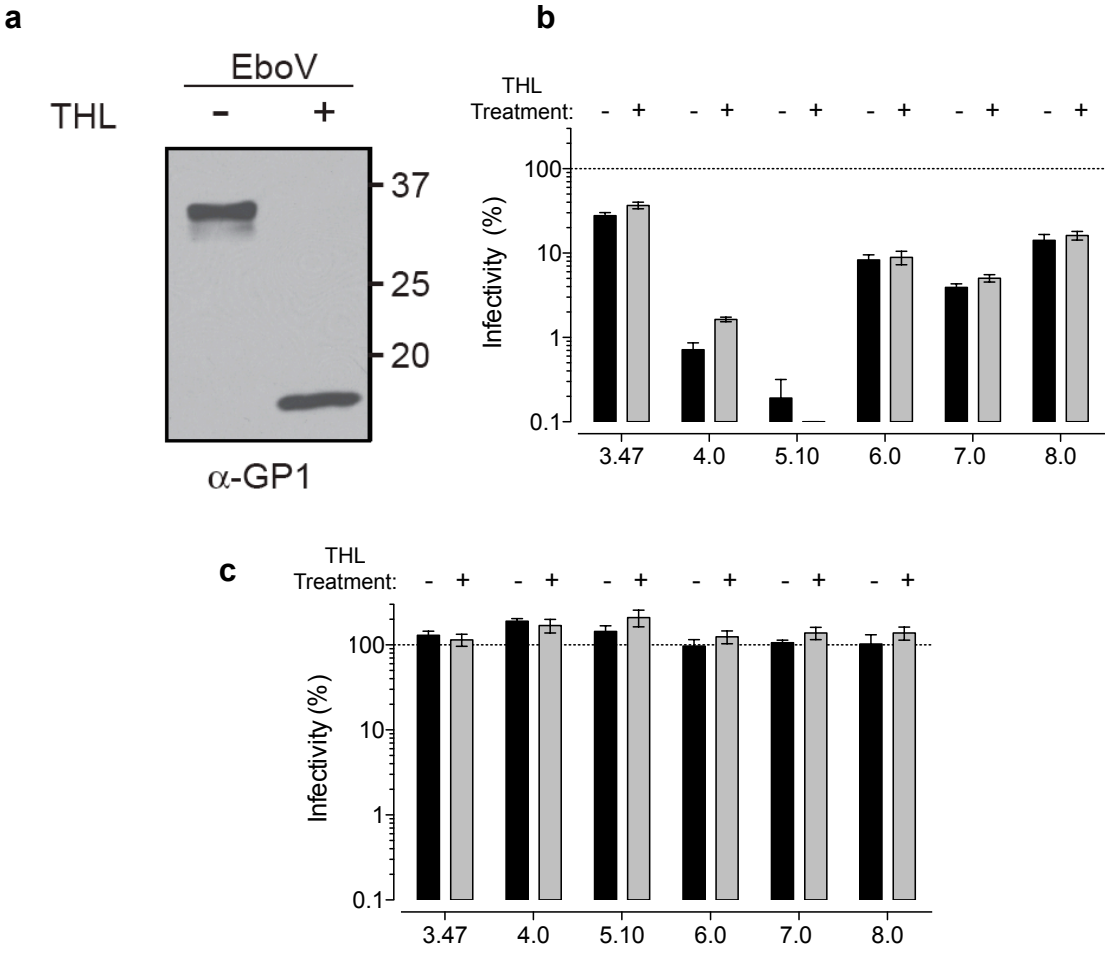

Figure 2-4. ***Compounds inhibit infection by protease-cleaved virus particles.*** **(a)** EboV pseudotyped particles were incubated with thermolysin (THL) and cleavage of GP1 was analyzed by immunoblot following deglycosylation with PNGaseF. **(b)** Vero cells were treated with 3.47 (1μM), 4.0 (10μM), 5.10 (2μM), 6.0 (1μM), 7.0 (2μM), 8.0 (10μM) or DMSO and exposed to native or thermolysin-cleaved VSV EboV GP particles. **(c)** Native or thermolysin-cleaved VSV EboV GP particles were pre-incubated with the inhibitors in a small volume at 37°C for two hours before the addition of the mixture to the cells. The mixture was diluted 100x when added to the cells. Virus infection is reported as percent GFP-positive cells relative to cells exposed to DMSO vehicle alone. Data are mean ± s.d. (n=3)

identified inhibitors are not simply dependent on buffering the endosomal and lysosomal pH.

Previous studies revealed that the endosomal protease cathepsin B is essential for EboV infection because it cleaves the GP1 subunit of GP (Chandran et al., 2005; Schornberg et al., 2006). To address the possibility that our compounds target this step, we measured cathepsin B activity in the presence of the anti-EboV compounds and found no effect *in vitro* or in cells (data not shown). Moreover, all of the compounds tested still inhibited infection by VSV EboV particles pre-cleaved with thermolysin (THL), a metalloprotease that faithfully mimics cathepsin cleavage of the GP1 subunit of GP (Figure 2-4a,b) (Schornberg et al., 2006; Wong et al., 2010). Furthermore, much like untreated virus, pre-incubation of THL-treated virus particles with the anti-EboV compounds did not reduce infectivity (Figure 2-4c). These findings demonstrate that the target of the antiviral compounds is neither cathepsin B nor a CatB-dependent GP intermediate.

E. Chemical properties of EboV inhibitors

In an attempt to identify the potential targets of our compounds, we examined the physiochemical and structural properties of the “hits” from screening libraries of existing drugs and small-molecules. We noticed that many of the hits of the anti-EboV bioactives screen, including alverine, tamoxifen, setraline and U18666A, are cationic amphiphiles (Table 2-2). Although cationic amphiphilic drugs (CADs) are a structurally and functionally diverse group of compounds, they each contain a hydrophobic ring attached

Table 2-2. Bioactive CAD-like compounds that inhibit EboV GP entry

Compound	Structure	IC_{50}	IC_{90}
Tamoxifen	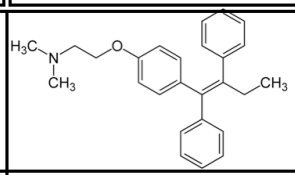	480 nM	2 μM
Alverine	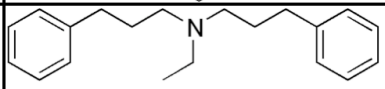	3.8 μM	12.7 μM
Sertraline	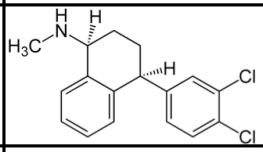	3.1 μM	4.7 μM
U18666A	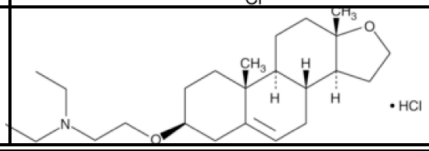	6.1 μM	15.5 μM

† IC_{50} and IC_{90} values were estimated from dose response curves as described for Table 2-1. Virus infection was graphed as a percent relative to cells exposed to DMSO vehicle alone and IC values were estimated from these graphs. Data is representative of three independent experiments. N=6.

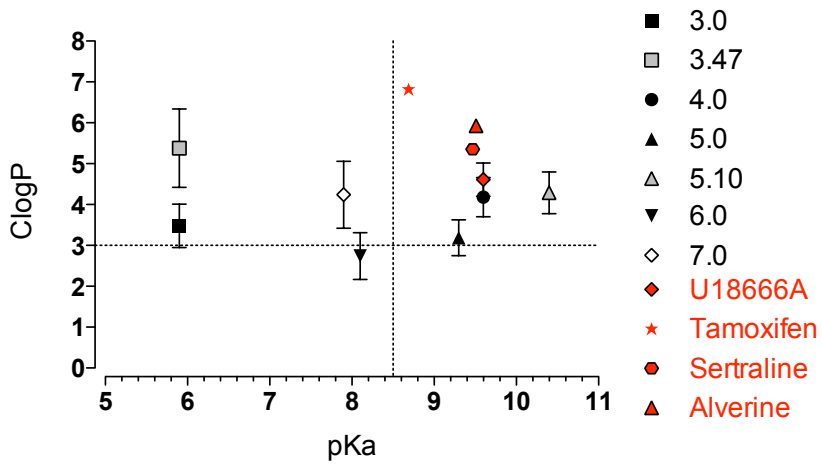

Figure 2-5. ***Predicted physiochemical properties of compounds that inhibit EboV entry.*** A comparison of the calculated relative lipophilicity, represented here as the log of the partition constant (clogP), versus the calculated relative acidity, represented as the log of the acid dissociation constant (pKa) for the EboV entry inhibitors identified through the bioactive (red) and small molecule screens (gray scale). The physiochemical properties were calculated using the Virtual Computational Chemistry Laboratory, VCCLAB (http://www.vcclab.org; Tetko et al., 2005). The clogP values are the average of several different methods of calculating the clogP ± s.d. Where available, experimentally observed logP and pKa were plotted. Dotted lines represent the minimal clogP (>3.0) and pKa (>8.5) values required for CAD like activity.

to a hydrophilic side chain (clog P>3.0) that contains a basic amine (pKa>8.5) (Kodavanti and Mehendale, 1990; Kornhuber et al., 2008; Hanumegowda et al., 2010). To examine the possible relationship between these parameters and antiviral activity, the clogP and pKa of each compound were calculated and plotted (Fig 2-5). We observed that 4.0, 5.0 and 5.10 met the criteria to be classified as cationic amphiphiles while 3.0, 3.47, 6.0 and 7.0 did not.

F. Antiviral compounds *3.0 and 3.47 induce cytoplasmic cholesterol accumulation*

Previous studies of CADs indicate that many accumulate in LE/LYs and inhibit degradation of phospholipids, sphingomyelin and cholesterol (Matsuzawa and Hostetler, 1980; Yoshikawa, 1991; Kobayashi et al., 1999; Makino et al., 2006; Sawada et al., 2005; Sobo et al., 2007). To see whether the antiviral compounds function like CADs, we treated Vero cells with the compounds and after 24 hours, fixed and stained the cells with the cholesterol-avid fluorophore filipin. As expected, we observed that the CADs tamoxifen and U18666A induced accumulation of filipin-positive vesicles in the perinuclear region of cells. Interestingly, we observed accumulation of filipin-positive cytoplasmic vacuoles in cells treated with inhibitors 3.0 and 3.47, although not in cells treated with 4.0, 5.0, 5.10, 6.0, 7.0, 8.0 or E64d (Figure 2-6). Compounds 3.0 and 3.47 also induced cholesterol-positive vacuoles in HeLa (Figure 2-10a) and CHO-K1 cells as well as primary human fibroblasts. These filipin-positive vacuoles were induced by compounds 3.0 and 3.47 in a dose-dependent manner, which correlated with their antiviral activities. Notably, 3.0 and 3.47 are significantly less basic and hydrophobic than the other anti-EboV compounds, as well as the well-characterized CADs,

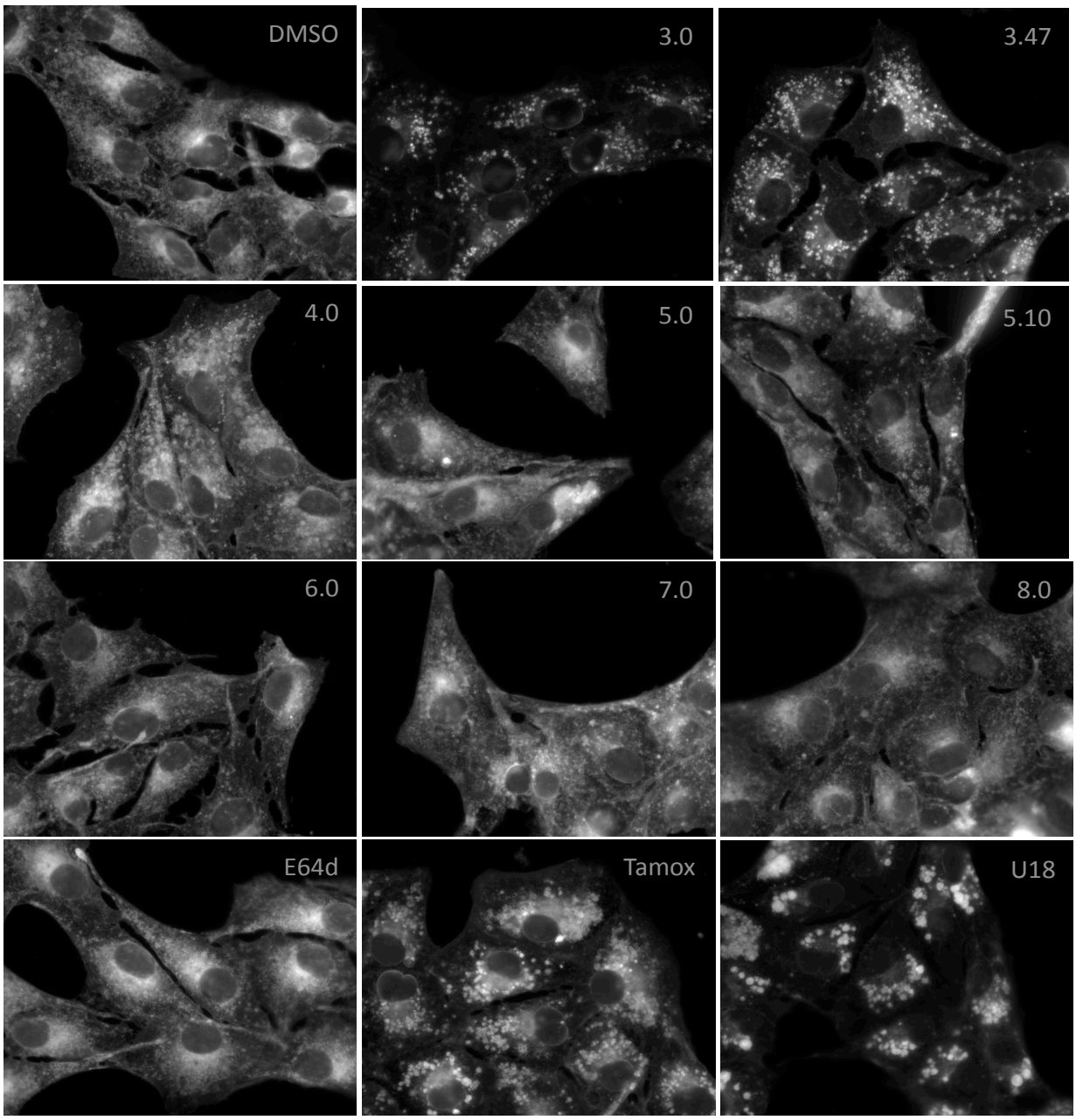

Figure 2-6. ***Compounds 3.0 and 3.47 lead to cholesterol accumulation in cells.*** Vero cells were treated with vehicle (DMSO), 3.0 (20 μM), 3.47 (10 μM), 4.0 (20 μM), 5.0 (20 μM), 5.10 (10 μM), 6.0 (20 μM), 7.0 (20 μM), 8.0 (20 μM), the cystine protease inhibitor E64d (30μM), tamoxifen (Tamox, 10μM), or U18666A (U18, 20μM) for 18 h. then fixed and incubated with the cholesterol-avid fluorophore filipin. The cationic amphiphilic drugs tamoxifen and U18666A served as positive controls for cholesterol accumulation in these experiments.

suggesting these properties are not strict predictors of cholesterol accumulating activity.

G. Cholesterol uptake pathway

To determine the origin of the filipin stained vacuoles, cells treated with 3.0 and 3.47 were analyzed using membrane-compartment specific antibodies. We observed that filipin-positive vacuoles were also positive for the LE/LY-specific lipid bis(monoacylglycerol)phosphate (BMP) and also for LysoTracker (data not shown). The induction of filipin-stained LE/LY membranes by 3.0 and 3.47 suggested that they might target one or more proteins involved in regulation of cholesterol uptake in the LE/LY of cells. Dietary cholesterol is normally taken up by the cell in low-density lipoproteins (LDL) through binding and endocytosis of LDL receptors (LDLR). The lipoproteins are then cleaved within the LE/LY, and the released cholesterol esters are hydrolyzed and transported across the limiting membrane into the cytoplasm (Brown and Goldstein, 1986). This transport of cholesterol from LDL to the cytoplasm is dependent on a complex mechanism involving carrier protein Niemann-Pick C2 and formation of specific lipid microdomains mediated by ALG-2-interacting protein X (Alix), acid sphingomyelinase (ASM), and BMP (Chevallier et al., 2008; Devlin et al., 2010). NPC2 then transfers the cholesterol to NPC1, a multi-pass cholesterol transport protein in the limiting membrane of the LE/LY (Kwon et al., 2009), which facilitates cholesterol export from the late endosome through an intracellular interaction with oxysterol binding protein-like 5 (ORP5), which may help transport cholesterol from NPC1 to the ER (Du et al, 2011). Disruption of any of the components in this highly regulated pathway results in accumulation of LDL cholesterol and other lipids in the LE/LY (Reaves et al., 2000;

Leventhal et al., 2001; Chevallier et al., 2008).

H. NPC1 is an essential host factor for EboV entry

To test the hypothesis that the target of 3.0 and 3.47 might be a protein essential for the uptake of cholesterol in the late endosome compartment, we studied EboV GP infection of primary human fibroblasts from patients with genetic lysosomal storage disorders affecting the cholesterol uptake pathway. We tested primary human fibroblasts from Niemann-Pick disease patients with mutations in the cholesterol transport proteins Niemann–Pick C1 (NPC1-(A)), Niemann–Pick C2 (NPC2-), and acid sphingomyelinase (ASM-) (Kolter and Sandhoff, 2010). As expected, all three of these cell lines contained filipin-positive cytoplasmic vacuoles (Figure 2-7a and 2-8a). Remarkably, we found that only the fibroblasts from the patient with mutations in NPC1, but not those in NPC2 or ASM, were highly resistant to EboV GP infection (Figure 2-7b, Figure 2-8b). Interestingly, in contrast to the two-log decrease in EboV GP-dependent infection in NPC1-(A) cells, we only observed a two-fold defect in EboV GP mediated infection upon infection of a second source of NPC1 mutant cells from a different patient (NPC1-(B)) (Figure 2-8 a,b). This difference was likely explained by the specific effects caused by the mutations in each sample; NPC-(A) cells expressed low levels of NPC1 in the LE/LY (Gelsthorpe et al., 2008), while NPC-(B) cells abundantly expressed a gene product with a single missense mutation disrupting its cholesterol transport activity (Blom et al., 2003).

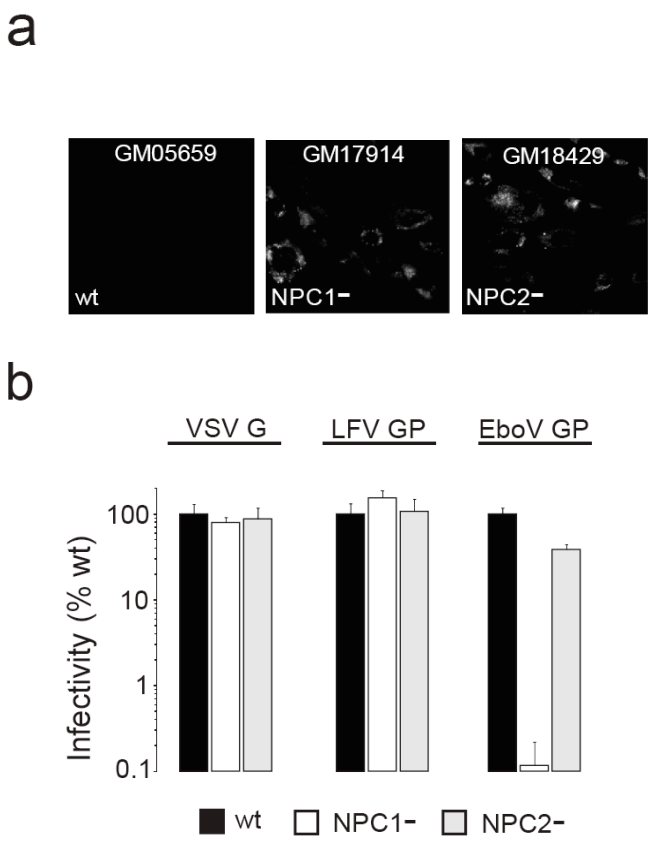

Figure 2-7. ***Cells from patients with Niemann-Pick type C1 are resistant to EboV GP infection.*** **(a)** Human fibroblast cell lines derived from patients with Niemann-Pick type C1 or C2 disease were analyzed for cytoplasmic cholesterol deposits using filipin staining. (Coreill, GM17914) (NPC1-) is a compound heterozygote with a frameshift and a missense mutation (I106T) that results in a misfolding; GM18429 (NPC2-) is homozygous for a substitution that results in defective splicing of NPC2 RNA; and GM05659 (wt) fibroblasts are from a healthy human donor. Representative images are shown. **(b)** Wt, NPC1-, and NPC2- fibroblasts were exposed to VSV particles pseudotyped with VSV G, LFV GP or EboV GP. Virus infection is reported as percent of luminescence units (RLU) on wt cells. Data is mean ± s.d. (n=3) and is representative of 3 experiments.

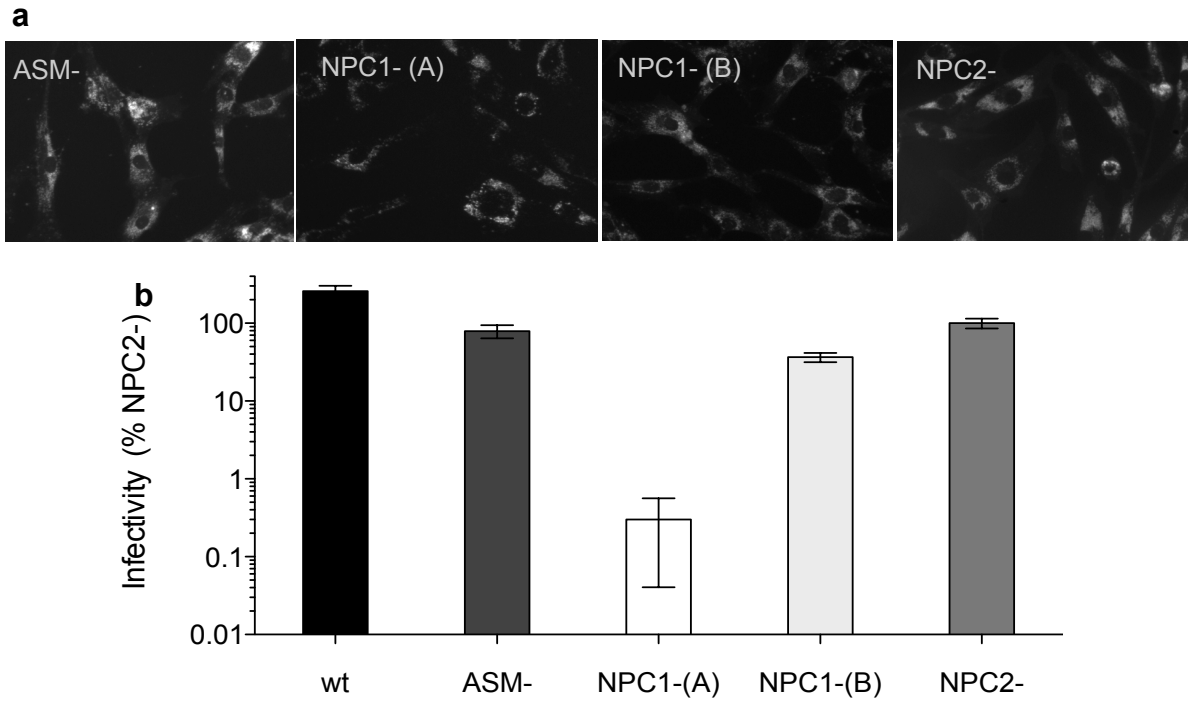

Figure 2-8. ***Comparison of EboV GP infection on two different NPC1- mutant fibroblasts.*** **(a)** Human fibroblast cell lines derived from patients with Niemann-Pick disease caused by mutations in acid sphingomyelinase (ASM-), Niemann–Pick C2 (NPC2-), and two different mutations in Niemann-Pick C1 (NPC1-(A) or NPC-1(B)) were analyzed for cholesterol accumulation using filipin staining. Both NPC1- cells are compound heterozygotes with one allele that has a missense mutation (I106T) that results in a misfolding and degradation of NPC1. In NPC1-(A) (GM17914, Coreill) the second allele has a 2bp insertion that leads to a premature stop codon. In NPC1-(B) (GM03123, Coreill) the second allele has a missense mutation (P237S) in which NPC1 traffics to late endosomes, but is defective in cholesterol transport function. NPC2- (GM18429, Coreill) is described in Figure 2-7. ASM- (GM16195, Coreill) is homozygous for a missense mutation (L302P) that results in defective enzyme function. Representative images are shown. **(b)** Fibroblasts were exposed to VSV GFP particles pseudotyped with EboV GP. Virus infection is reported as percent GFP-positive cells relative to NPC2- control. Data are mean ± s.d. (n=3)

These findings suggest that NPC1 protein is specifically required for infection. We further tested this conclusion by infecting cells systematically disrupted in the other cellular factors involved in the LDL derived cholesterol uptake pathway (Kolter and Sandhoff, 2010; Ko et al., 2001; Du et al., 2011; Chevallier et al., 2008). To determine if BMP is required, infectivity was assessed in cells treated with a well-characterized antibody to BMP (Kobayashi et al., 1999; Le Blanc et al., 2005). Vero cells incubated overnight with 5 or 50 μg/ml of either α-BMP or mouse IgG isotype control (mIgG) antibody showed little appreciable difference in EboV GP mediated infectivity under conditions that lead to more than a two-fold reduction in VSV G infectivity (Figure 2-9). We further studied the roles of the known host proteins involved in cholesterol uptake by assessing the effects of siRNA knockdown of their expression on EboV GP-dependent infection. We confirmed that EboV GP-dependent infection required expression of NPC1, but did not observe a comparable effect upon knockdown of NPC2, ASM, Alix, or ORP5 under these conditions (Figure 2-10 b,c).

In order to more rigorously test the role of NPC1 during EboV infection, we studied a set of Chinese hamster ovary (CHO)-derived cell lines in which expression of endogenous NPC1 had been knocked out. We found that the titer of a murine leukemia virus (MLV) vector pseudotyped with EboV GP on wild-type CHO cells (CHO_{wt}) exceeded 10^6 infectious units per ml (Fig. 2-11 a,b), while CHO cells lacking NPC1 (CHO_{null}) were completely resistant to infection. Importantly, infection of these cells was fully restored when NPC1 was exogenously expressed (CHO_{NPC1}), indicating that NPC1 expression is indeed essential for EboV infection.

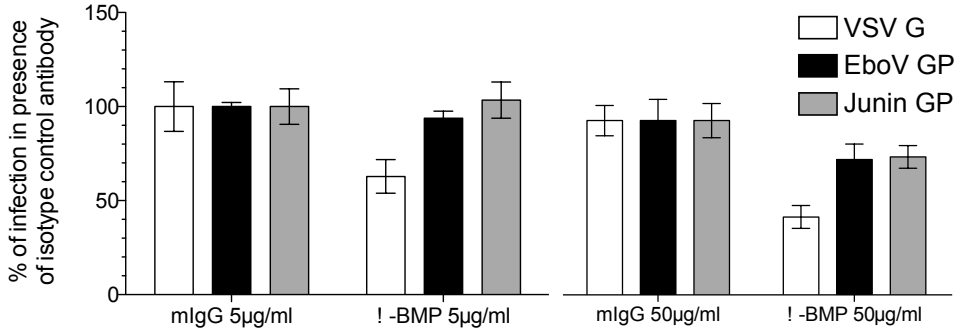

Figure 2-9. ***A BMP antibody does not inhibit EboV GP entry.*** Vero cells were plated in a 96-well plate and incubated with 5 or 50 µg/ml of an antibody directed against BMP or a mouse monoclonal IgG isotype control (mIgG). After 24 hours, the cells were infected VSV particles encoding GFP pseudotyped with either EboV GP (black bars), VSV G (white open bars) or Junin GP (gray bars). Virus infection is reported as percent of GFP-positive cells relative to cells exposed to the isotype control antibody. Data are mean ± s.d. (n=3).

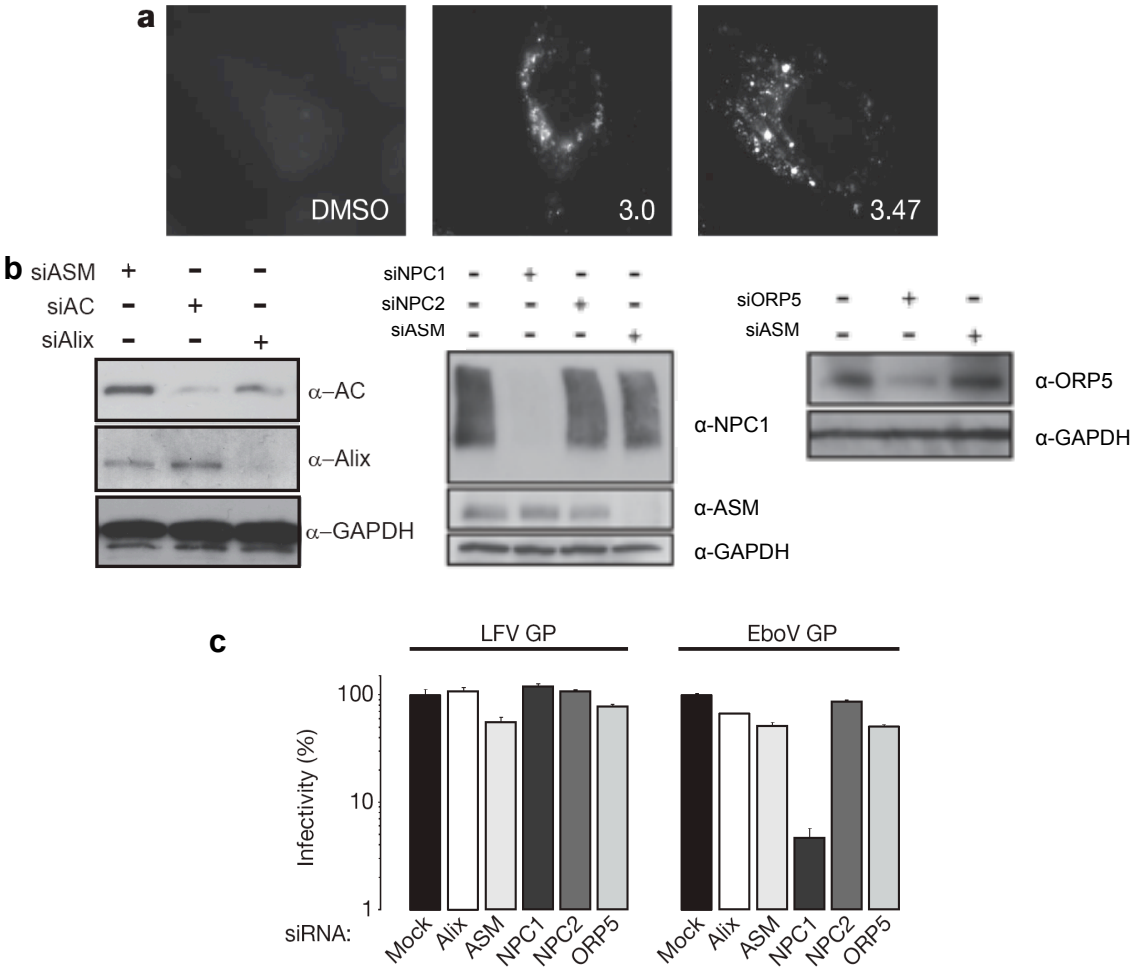

Figure 2-10. ***NPC1 is essential for Ebola virus infection.*** **(a)** HeLa cells were treated with 3.0 (20 μM), 3.47 (1.25 μM) or vehicle for 18 h, then fixed and incubated with the cholesterol-avid fluorophore filipin. **(b,c)** Expression of NPC1, NPC2, ASM, Alix, acid ceramidase (AC) and ORP5 was knocked-down in HeLa cells using SMARTpool siRNA (20 nM, Dharmacon). After 72 hours, cells were assessed for infection or protein expression. **(b)** Protein expression was measured by immunoblot of cell lysates using anti-ASM 1H7 (Genzyme), anti-NPC1 (Abcam), anti-AC (BD Biosciences), anti-Alix (Biolegend), and anti-ORP5 (Abcam). **(c)** HeLa cells were transfected with siRNAs targeting Alix, ASM, NPC1, NPC2 and ORP5. After 72 h, VSV-EboV-GP or LFV-GP infection of these cells was measured as in Fig. 2-7b. Data are mean ± s.d. (n=3) and is representative of three experiments.

CHO_{null} cells have enlarged LE/LY that contain excess cholesterol and sphingolipids (Millard et al., 2005). To determine if EboV infection is inhibited by endosome dysfunction secondary to the absence of NPC1, we studied a well-characterized sterol-sensing domain mutant P692S that is defective in cholesterol uptake and NPC1-dependent membrane trafficking but not expression or localization (Ko et al., 2001; Millard et al., 2005; Ohgami et al., 2004). We found that expression of NPC1 P692S fully supports infection of CHO_{null} cells (Fig. 2-11 a,b). Conversely, mutants NPC1 L657F and NPC1 D787N, which exhibit increased rates of cholesterol transport (Millard et al., 2005), did not enhance EboV GP infection. Thus, consistent with what we previously observed with human NPC1-(A) and NPC1-(B) cells, EboV entry is strictly dependent on NPC1 expression, but not on NPC1-dependent cholesterol transport activity. Consistent with the conclusion that NPC1 expression is essential for EboV GP-dependent entry, we found that replication competent Ebola virus could not grow on CHO_{null} cells (Fig. 2-11c). The requirement for NPC1 was found to exist for all known filoviruses, as single-round infection by MLV particles bearing GPs from the filovirus species *Marburg marburgvirus* (MarV), *Sudan ebolavirus* (SudV)*, Taï Forest ebolavirus (*TaFV*), Reston ebolavirus* (RestV*)* and *Bundibugyo ebolavirus* (BdbV*)* were all strictly dependent on NPC1 expression (Table 2-3). As these viruses are not closely related (Towner et al., 2008), these findings suggest that the requirement for NPC1 as an entry factor has been conserved through evolution of the *Filoviridae* family.

a

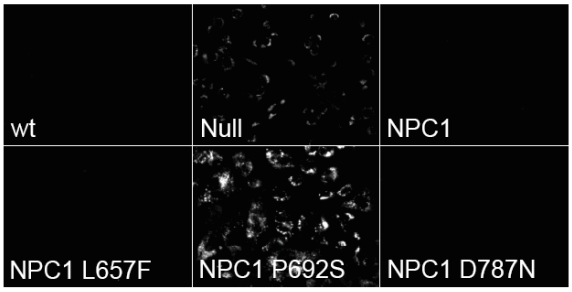

b

CHO cell line	Retroviral titre (FFU ml^{-1})	
	EboV GP	VSV G
Wild type	(5.7 ± 1.7) x 10^6	(2.9 ± 0.6) x 10^7
Null	< 2.0	(1.6 ± 0.9) x 10^7
NPC1	(2.2 ± 1.6) x 10^6	(1.1 ± 0.6) x 10^7
L657F	(1.3 ± 0.8) x 10^6	(6.7 ± 2.2) x 10^6
P692S	(3.1 ± 1.5) x 10^6	(2.2 ± 0.2) x 10^7
D787N	(1.9 ± 1.0) x 10^6	(1.1 ± 0.4) x 10^7

c

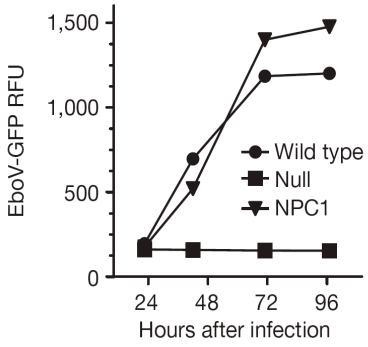

Figure 2-11. ***Presence of NPC1 protein but not cholesterol transport function is essential for Ebola virus infection.*** **(a)** Phenotype of cells expressing NPC1 mutant proteins. CHO_{wt}, $CHO_{null,}$ and CHO_{null} cells stably expressing wild type mouse NPC1 or NPC1 mutants L657F, P692S, D787N were fixed and stained with filipin, and representative images are shown. **(b)** These CHO cell lines were exposed to MLV particles encoding LacZ and pseudotyped with either EboV GP or VSV G. Results are the mean ± s.d. (n=4) and is representative of three experiments. FFU, focus forming units. **(c)** CHO_{wt}, CHO_{null}, and CHO_{NPC1} cells were infected with replication competent Ebola virus Zaire-Mayinga encoding GFP (m.o.i.=1). Results are mean relative fluorescence units ± s.d. (n=3).

Table 2-3. Infection of CHO cells by filovirus GP pseudotyped retrovirus particles

CHO Cell Line	Retroviral Titer* (FFU/ml)						
	EboV GP	TaFV GP	BdbV GP	SudV GP	RestV GP	MarV GP	LFV GP
Wt	(4.3±0.4)x 10^6	(1.1±0.1)x 10^6	(1.1±0.8)x 10^7	(4.2±0.1)x 10^6	(3.0±0.4)x 10^5	(1.2±0.4)x 10^6	(2.6±0.6)x 10^5
Null	< 4.0	< 4.0	4 ± 0	< 4.0	< 4.0	2.7 ± 2.3	(2.2±0.9)x 10^6
NPC1	(1.6±0.6)x 10^6	(7.3±0.2)x 10^5	(2.7±0.3)x 10^6	(2.5±0.6)x 10^6	(5.0±0.9)x 10^4	(2.1±0.3)x 10^5	(1.2±0.3)x 10^6

* CHO wt, CHO cells lacking NPC1 (Null) and CHO_{null} cells stably expressing mouse NPC1 (NPC1) were exposed to MLV particles encoding LacZ and pseudotyped with GPs from the filovirus species *Marburg marburgvirus* (MarV), *Zaire ebolavirus* (EboV), *Sudan ebolavirus* (SudV), *Taï Forest ebolavirus (*TaFV*), Reston ebolavirus* (RestV*)* and *Bundibugyo ebolavirus* (BdbV*)* or Lassa fever virus (LFV). Results are the mean ± s.d. (n=12). FFU, focus forming units.

I. Cathepsin B and NPC1 mediate distinct steps during EboV entry

Since NPC1 and cathepsin B are both essential host factors, we analyzed their relationship during infection. We found that treatment of cells with the cathepsin inhibitor E64d at concentrations that blocked infection did not induce cholesterol accumulation (Figure 2-6, bottom left). Additionally, we tested the possibility that disruption of NPC1 could interfere with the protease activity of cathepsin B. In our initial experiment, we measured cathepsin B activity in CHO_{null} cells and found that it was not significantly different from CHO_{wt} cells (Figure 2-12a). To determine if NPC1 is required for virus processing by cathepsin B, we tested whether thermolysin-cleaved particles were dependent on NPC1. As expected, we found that thermolysin-cleaved particles are infectious and resistant to inactivation of cathepsin B when NPC1 is present (Figure 2-12b). However, thermolysin cleavage did not bypass the barrier to virus infection in NPC1 deficient cells. Taken together, these findings indicate that cathepsin B and NPC1 mediate distinct steps in infection.

J. Protease-cleaved EboV GP binds NPC1

Previous studies suggest that the product of cathepsin B cleavage of the GP1 subunit of EboV GP is a ligand for a host factor (Kuhn et al., 2006; Kaletsky et al., 2007; Brindley et al., 2007; and Dube et al., 2009 and 2010). To determine if NPC1 is this host factor, we performed a series of experiments measuring binding of EboV GP to LE/LY membranes from CHO_{null}, CHO_{NPC1} and CHO_{P692S} cells (Figure 2-13 a, b left panel). EboV GP was prepared in the form of a purified recombinant protein that is truncated

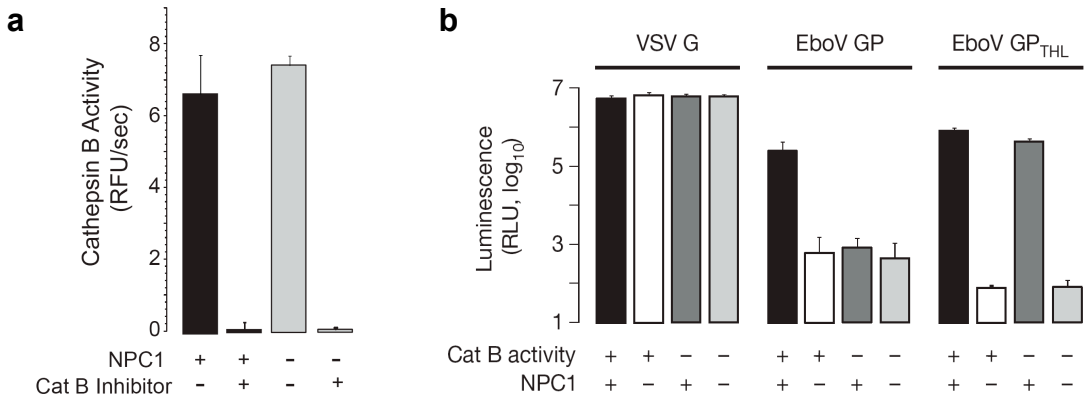

Figure 2-12. ***Cathepsin B and NPC1 mediate distinct steps during EboV entry.*** **(a)** The relationship between NPC1 expression and cathepsin B activity in CHO cells. CHO_{wt} and CHO_{null} cells were incubated in medium containing the Cat B inhibitor CA074 (80 μM) or vehicle (1% DMSO) for 4 hours, and Cat B protease activity was measured in cell lysates using a fluorogenic substrate. Cat B activity (V0, relative fluorescence units (RFU)/sec) is plotted. Results are mean ± s.d. (n=9). **(b)** CHO_{wt} and CHO_{null} cells were treated with the cathepsin B inhibitor CA074 (80 μM) or vehicle. These cells were challenged with VSV G particles or VSV EboV GP particles treated with thermolysin (EboV GP_{THL}) or untreated control (EboV GP). Infection was measured as in Fig. 2-9. Data are mean ± s.d. (n=9).

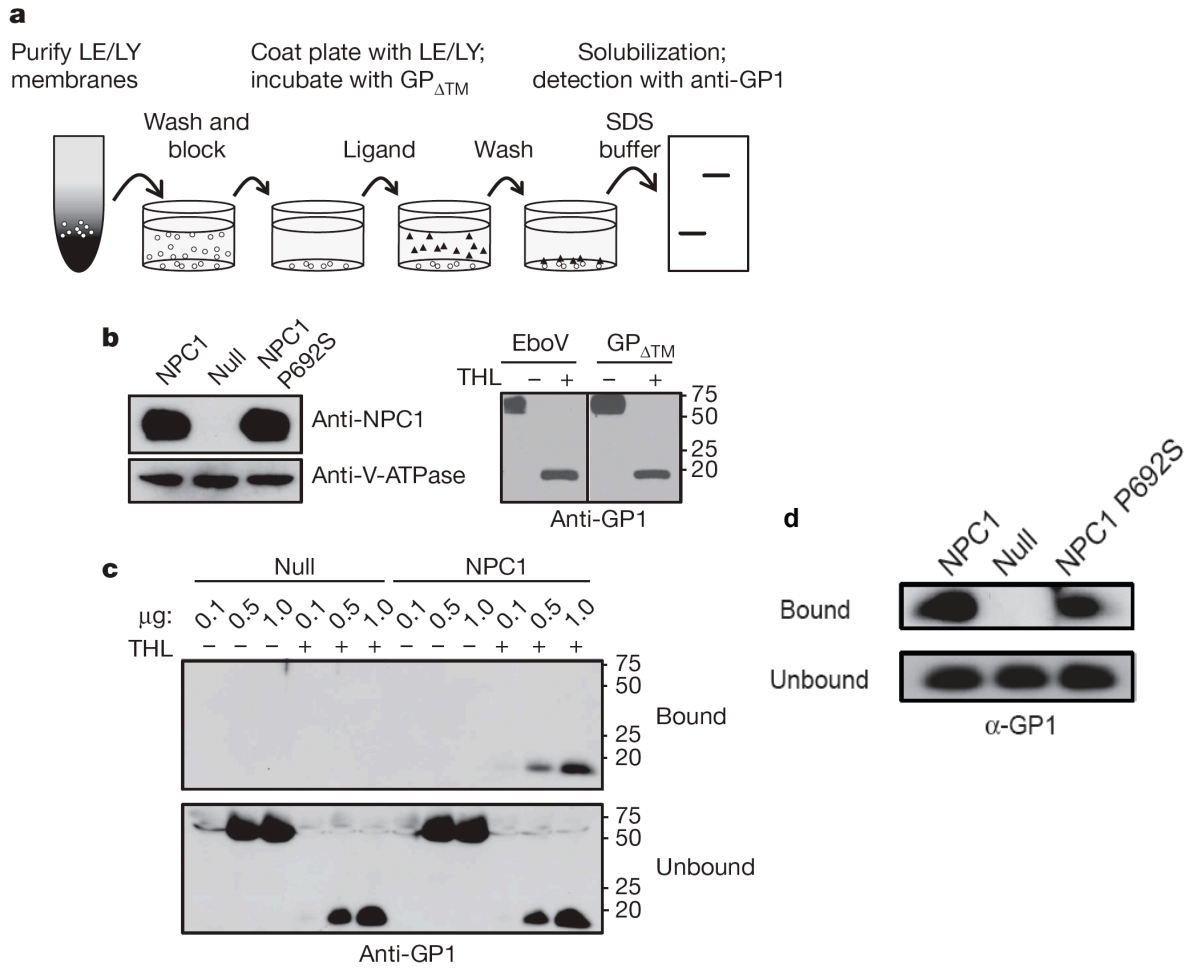

Figure 2-13. ***Protease-cleaved EboV GP binds to NPC1 containing membranes.*** **(a)** Schematic diagram of EboV GP1 binding assay used in panel (c and d). **(b)** Left, LE/LY membranes from CHO_{NPC1},CHO_{null} and CHO NPC1 P692S cells were analyzed by immunoblot using antibodies to NPC1 or V-ATPase B1/2. Right, VSV EboV GP particles and EboV $GP_{\Delta TM}$ protein were incubated in the presence or absence of thermolysin (THL) and analyzed by immunoblot for GP1. **(c)** EboV $GP_{\Delta TM}$ or thermolysin-cleaved EboV $GP_{\Delta TM}$ (0.1, 0.5, or 1.0 µg) was added to LE/LY membranes purified from CHO_{null} or CHO_{NPC1} cells. Membrane bound and unbound GP1 were analyzed by immunoblot. **(d)** Thermolysin-cleaved EboV $GP_{\Delta TM}$ binds to membranes containing the NPC1 mutant P692S. Thermolysin-cleaved EboV $GP_{\Delta TM}$ protein (1 µg) was added to LE/LY membranes from CHO_{null}, CHO_{NPC1}, or CHO NPC1 P692S cells and analyzed as in (c).

just before the transmembrane domain (EboV $GP_{\Delta TM}$). EboV $GP_{\Delta TM}$ is a trimer that is faithfully cleaved by thermolysin (Figure 2-13 b right panel). We found that binding of EboV $GP_{\Delta TM}$ to LE/LY membranes is concentration dependent, saturable, and strictly dependent on both thermolysin cleavage of GP1 and membrane expression of NPC1 or NPC1 P692S (Figure 2-13 c,d; 2-14a). We performed a co-immunoprecipitation experiment to determine whether cleaved GP binds to NPC1. LE/LY membranes were incubated with EboV $GP_{\Delta TM}$ and then solubilized in detergent. NPC1 was recovered from the lysate by immunoprecipitation and the immune complexes were fractionated on a polyacrylamide gel, and analyzed for the presence of GP1. We found cleaved EboV $GP_{\Delta TM}$, but not uncleaved EboV $GP_{\Delta TM}$ bound to and co-immunoprecipitated with NPC1 (Figure 2-14b). These results suggest that cathepsins act upstream of the NPC1 binding step, and may serve to unmask a NPC1 binding domain present within EboV GP.

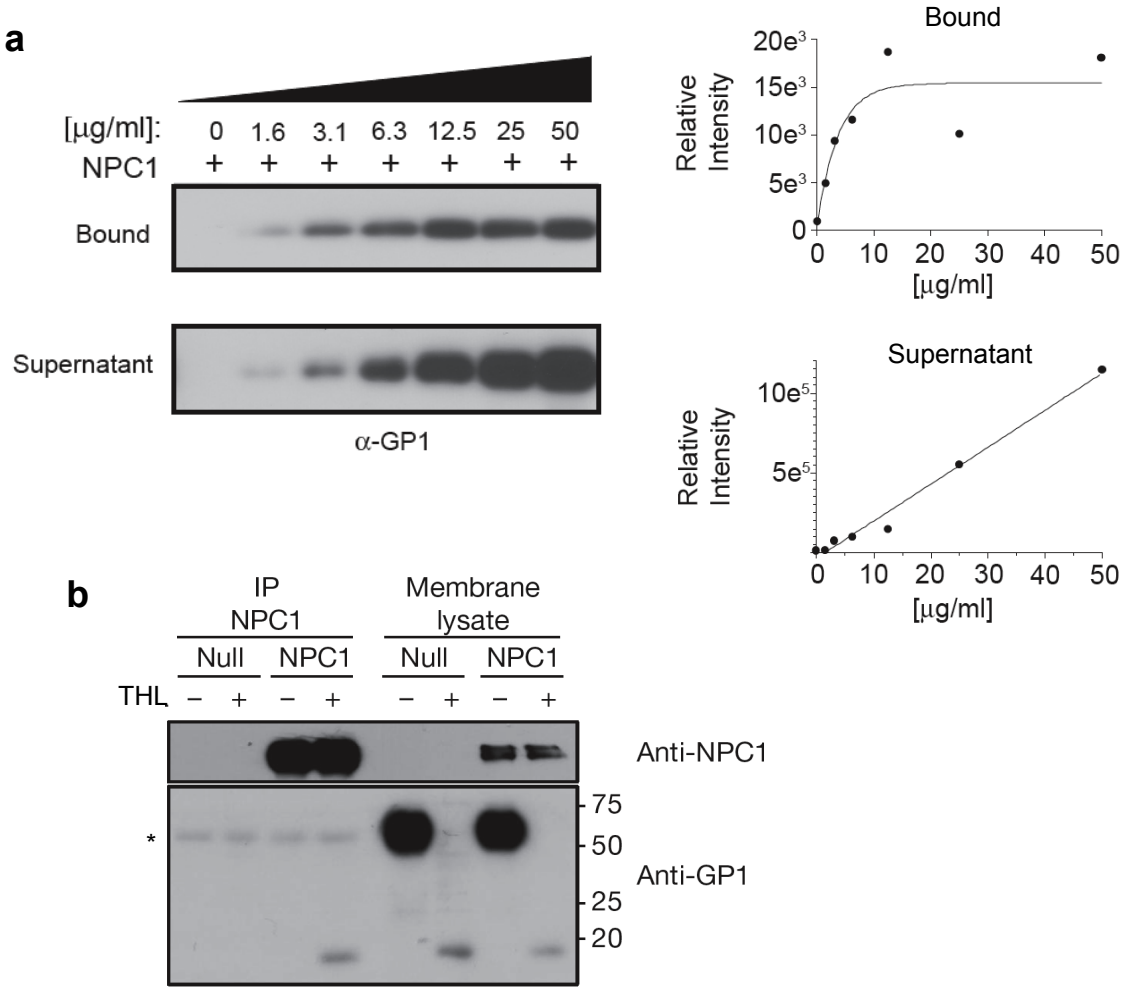

Figure 2-14. ***Protease-cleaved EboV GP binds to NPC1.*** **(a)** LE/LY membranes from CHO_{NPC1} were incubated with increasing concentrations of thermolysin cleaved EboV $GP_{\Delta TM}$ as in Figure 2-13. GP1 was analyzed in membrane bound and supernatant fractions using immunoblot (top). Densitometry was performed and the relative intensity of each GP1 band was measured using Quantity One Software (Bio-Rad). The data was used to plot the amount of GP1 in the supernatant and the amount bound to LE/LY membranes as a function of the input concentration of EboV $GP_{\Delta TM}$. **(b)** LE/LY membranes from CHO_{null} or CHO_{hNPC1} cells were incubated with EboV $GP_{\Delta TM}$ or thermolysin cleaved EboV $GP_{\Delta TM}$. Following binding, membranes were dissolved in the detergent CHAPSO, NPC1 was precipitated using an NPC1-specific antibody, and the immunoprecipitate and the input membrane lysate were analyzed by immunoblot for NPC1 (top) or GP1 (bottom). * IgG heavy chain.

Discussion:

Although numerous host factors responsible for the initial steps of EboV entry have been proposed, including attachment, uptake, and priming through GP proteolysis, the identities of the host-factors responsible for the later steps that are directly responsible for triggering fusion within the LE/LY have remained a major unknown facet of the EboV entry mechanism. Indeed, the latest understood step, that of endosomal cathepsin-mediated proteolysis of GP1, has demonstrated that EboV particles are not infectious until the heavily glycosylated exterior subdomains are removed. The domain of GP1 exposed by cathepsin cleavage has been previously proposed to be a binding site for an unidentified host factor required for, or immediately preceding triggering of the fusion protein. Unfortunately, repeated biochemical attempts have not been able to fish out the hypothesized binding partner for this ligand.

Experiments investigating the antiviral mechanisms of a series of small molecule EboV entry inhibitors lead us to investigate the possible role for components of the LE/LY cholesterol processing pathway in EboV entry. One of the integral components of this pathway, the multi-spanning protein NPC1, was found to be an essential factor in EboV infection as well. Although drug-induced defects originally informed our investigations into the potential roles of NPC1 and the other cholesterol transport components, our subsequent experiments showed that the requirement for NPC1 in EboV entry was actually quite distinct from this process; neither disruption of the other essential components of the cholesterol transport pathway, such as NPC2 or ORP5, nor infection of cells encoding missense mutations of NPC1 specifically perturbing the rate of cholesterol transport, had a significant effect on the outcome of EboV GP-dependent

infection. Instead, the physical availability of NPC1 within LE/LY appeared critical, as neither hamster cells with complete deletions of NPC1, nor human cells containing misfolded and thus prematurely degraded NPC1, were able to support EboV GP-dependent infection.

Critically, our experiments returned to where the aforementioned *in vitro* biochemical experiments had left off (Chandran et al., 2005; Schornberg et al., 2006; Dube et al., 2009), as we were able to demonstrate that EboV GP is capable of binding NPC1, using either an NPC1-containing membrane binding ELISA, or a more specific co-immunoprecipitation assay. Furthermore, our data supported a post-cathepsin cleavage binding event, as soluble EboV GP trimers processed *in vitro* using thermolysin were capable of binding NPC1, while unprocessed GP was not. These results support a model wherein cathepsin proteases, active in the low pH environment of the LE/LY, serve to unmask the RBDs present on the EboV GP timers extending from the viral particles. Binding of the exposed RBDs to NPC1 present on the limiting membrane of the LE/LY is able to provide a crucial step for triggering EboV GP to fuse.

Though yet to be proven, it is quite possible that GP1 binding to NPC1 may be sufficient to trigger the conformational changes in the EboV GP that essentially begin the membrane fusion cascade. Analysis of the EboV GP structure reveals that the residues in the N-terminal domain of GP1 that likely mediate binding to NPC1 are interspersed with the residues that make stabilizing contacts with GP2 (Lee et al, 2008). Thus, binding of cleaved GP1 to NPC1 may relieve the GP1-imposed constraints on GP2 and that prevent fusion peptide insertion into the limiting membrane of the LE/LY (Figure 2-15). According to this model, the role of to expose the NPC1 binding site

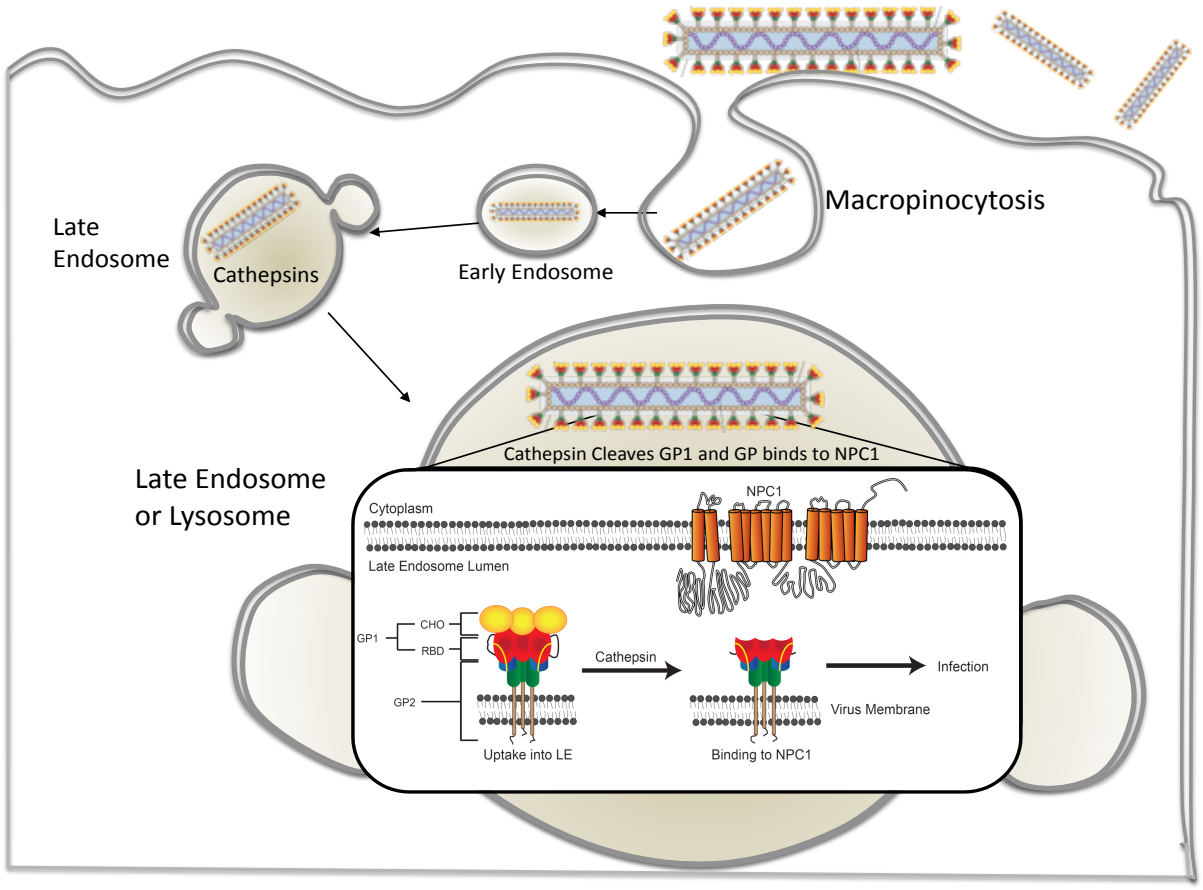

Figure 2-15. ***Revised model of EBOV entry.*** EBOV particles bind to attachment factors on the cell surface and are internalized by macropinocytosis. EBOV GP is cleaved by endosomal cysteine proteases exposing the receptor binding domain, which is a ligand for NPC1.

during EboV infection would be analogous to the role of CD4 in inducing a conformational change in gp120 to expose the co-receptor binding site during HIV infection, while NPC1 would serve as the CCR5 or CXCR4 co-receptor triggers (Harrison, 2008). An alternative possibility is that binding of protease-cleaved GP1 to NPC1 is an essential step in infection, but virus membrane fusion is not triggered until an additional signal is received. This may include further cleavage of GP by cathepsin proteases, as has been previously proposed based on the yet explained existence of a post-cathepsin B E64 sensitive step (Chandran et al, 2005; Schornberg et al, 2006; Wong et al, 2010), or a yet unidentified step, which may or may not require the low pH of the LE/LY. Lastly, these studies provide a successful example of how small molecules identified by screening and optimized by medicinal chemistry, can be used to identify novel virus-host interactions.

Chapter 3

Using small molecule inhibitors to probe the role of NPC1 in Ebola virus entry

The data presented in this chapter is derived in part from the following published work.

Côté M.*, Misasi J.*, Ren T.*, Bruchez A.*, Lee K., Filone C.M., Hensley L., Li Q., Ory D., Chandran K., Cunningham J. Small molecule inhibitors reveal Niemann–Pick C1 is essential for Ebola virus infection. *Nature.* 447, 344-348 (2011).

*Contributed equally.

Author Contributions: KL synthesized and purified 3.0 analogs and AB tested them. AB carried out infection assays with pseudotyped viruses, performed microscopy, and executed NPC1 overexpression studies. AB designed and performed resistant virus studies. JM purified recombinant glycoprotein. MC and JM designed and performed binding assays. MC performed crosslinking and click chemsitry. Ebola virus infections were performed in the lab of LH by CF.

Figure contributions: MC produced the data for Figures 3-1d, 3-2, and 3-3. CF produced the data for Figure 3-1c. JM produced the data for Figure 3-6. AB produced all other Figures.

Abstract

Filoviruses, including Ebola virus (EboV) and Marburg virus, are a family of enveloped negative stranded RNA viruses that are known to cause highly lethal haemorrhagic fever in primates. Despite the fact that these viruses are considered an emerging health risk, due in large part to the increasing frequency of outbreaks and the high morbidity and mortality rates of these infections, currently no effective vaccine or antiviral therapeutics exist and patient care is limited to palliative measures. We have recently reported that a small molecule inhibitor of EboV entry, 3.0, lead us to the discovery of an essential host factor for filovirus entry, the cholesterol transporter Niemann-Pick C1 (NPC1). Here we describe the follow-up inhibitor based studies that probe how 3.0 and its derivatives prevent EboV entry into host cells by interacting with NPC1. A derivative of 3.0 that lacked the tertiary amine, which is unable to become protonated in the late endosome of cells, remained as active as the 3.0 parent compound. This suggests that the compounds do not rely on a charge base mechanism for activity. A photo-affinity labeled derivative of 3.0 cross-linked to NPC1 and active derivatives blocked binding of post-cathepsin cleaved EboV-GP to NPC1 containing membranes. Overexpression of NPC1 rendered cells resistant to EboV inhibition by 3.0 and its potent derivative 3.47. These findings indicate that the 3.0 series of compounds bind to NPC1 and, as a result, interfere with a functionally significant interaction between GP1 and NPC1. Furthermore, mutations that confer sensitivity or resistance to the inhibitors lay within the previously identified receptor binding domain (RBD) of GP1 and are exposed only after cathepsin mediated cleavage. This is consistent with previous findings that GP binds to NPC1 only after protease cleavage. Taken together,

this data suggests that the small molecule inhibitors interact directly with NPC1 in a way that interferes with the virus-receptor interaction of the post-cathepsin cleaved GP1 to NPC1.

Introduction

In Chapter 2 we established that NPC1 was an essential host factor for EboV entry. This finding was corroborated by a publication from another group that identified NPC1 through the use of a haploid genetic screen (Carette et al., 2011). Both studies found that NPC1 was essential for EboV GP mediated entry as well as infection with replication competent EboV, and that differences in NPC1 expression did not affect the entry of other viruses, including other low pH dependent viruses. Carette et al. saw that in NPC1 null cells, entry of VSV pseudotyped with EboV-GP was arrested at a late stage in virus entry, and that virions seemed to accumulate in the late endosome/ lysosome (LE/LY) of these cells (2011). Consistent with this finding, we found that only post-cathepsin cleaved GP could bind to NPC1 containing membranes, suggesting that binding takes place only after cathepsin cleavage has occurred in the late endosome and lysosome of cells. Furthermore, both studies found that disruption of NPC2 expression did not impact EboV infectivity, indicating that cholesterol misregulation itself is not the root cause of defective EboV entry in NPC1 null cells. Additionally, we found that knockdown of additional factors involved in the cholesterol uptake pathway had no appreciable negative effects upon EboV entry. Indeed, the eventual discrepancy between cholesterol transport and EboV entry phenotype became most obvious upon testing cells harboring various NPC1 missense mutations, which exhibited either

enhanced or greatly reduced cholesterol transport activity, but supported levels of EboV entry comparable to WT cells. These results supported the interpretation that the physical presence of the NPC1 protein in the LE/LY was the requirement for EboV entry. Subsequent experiments found that NPC1 is capable of binding the post-cathepsin EboV GP, suggesting that it may provide a receptor-like role in entry. Still, additional structural and functional studies are required to more rigorously characterize the manner in which NPC1 functions during EboV entry. We decided to take advantage of our newly identified EboV inhibitor 3.0, along with its informative derivatives, by incorporating them in additional biochemical, functional, and genetic assays to further understand the interaction between EboV GP and NPC1.

Results

A. Informative derivatives of EboV inhibitor 3.0

In Chapter 2 we described the identification of 3.0, a novel benzylpiperazine adamantane diamide-derived compound, by a high-throughput screen of a small molecule library for EboV entry inhibitors. We subsequently developed a subset of 3.0 derivatives through a series of structure activity relationship (SAR) studies, which carried a distinct set of structural and functional characteristics that could be utilized in additional biochemical and functional assays. Of the greater than 50 analogs of 3.0 that were synthesized and tested, we selected a set of four derivatives with varying potency and physiochemical properties that could serve as particularly informative probes in our assays. A number of derivatives were less potent against EboV GP-dependent infection; in the case of compound 3.18, which has an additional carbon

Figure 3-1.

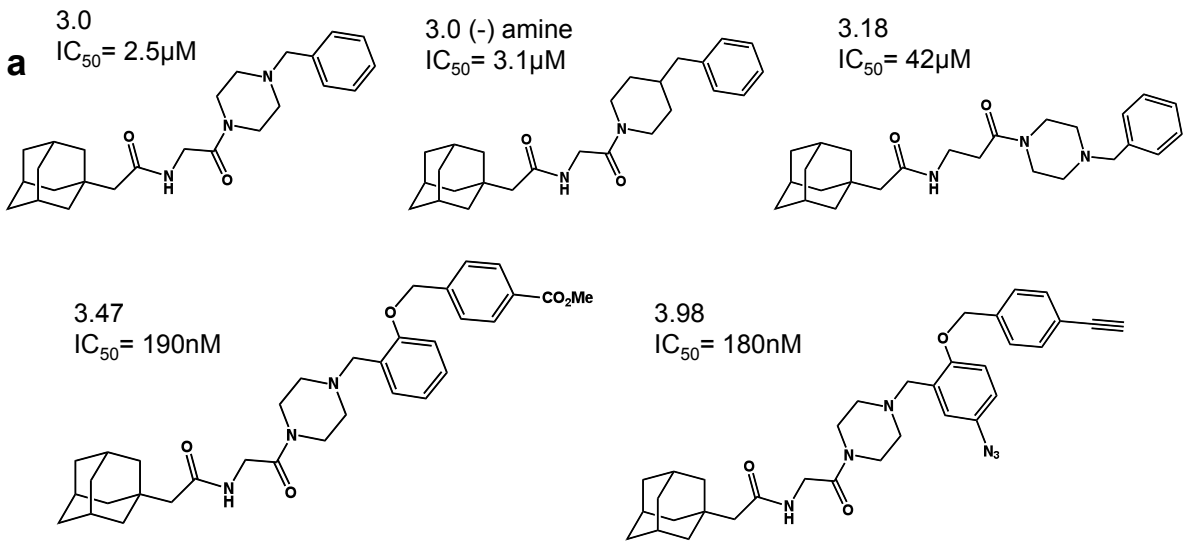
a
3.0
IC50= 2.5μM
3.0 (-) amine
IC50= 3.1μM
3.18
IC50= 42μM
3.47
IC50= 190nM
CO2Me
3.98
IC50= 180nM
N3

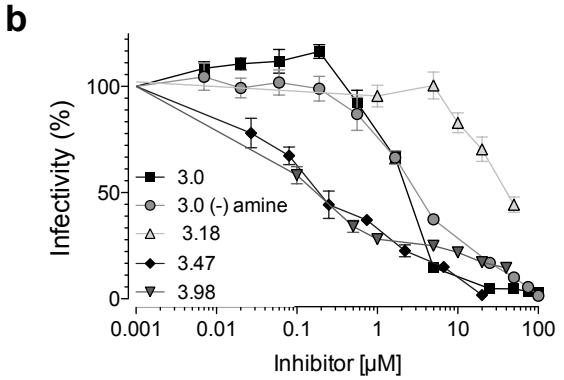
b
Infectivity (%)
100
50
0
3.0
3.0 (-) amine
3.18
3.47
3.98
0.001
0.01
0.1
1
10
100
Inhibitor [μM]

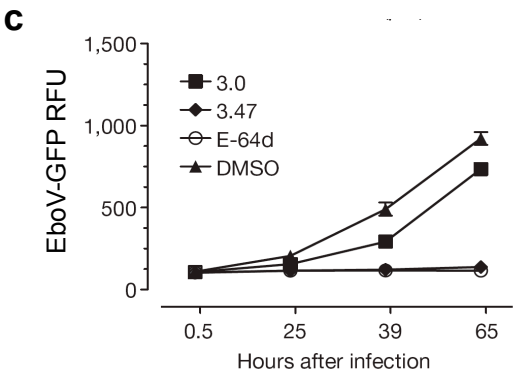
c
EboV-GFP RFU
1,500
1,000
500
0
3.0
3.47
E-64d
DMSO
0.5
25
39
65
Hours after infection

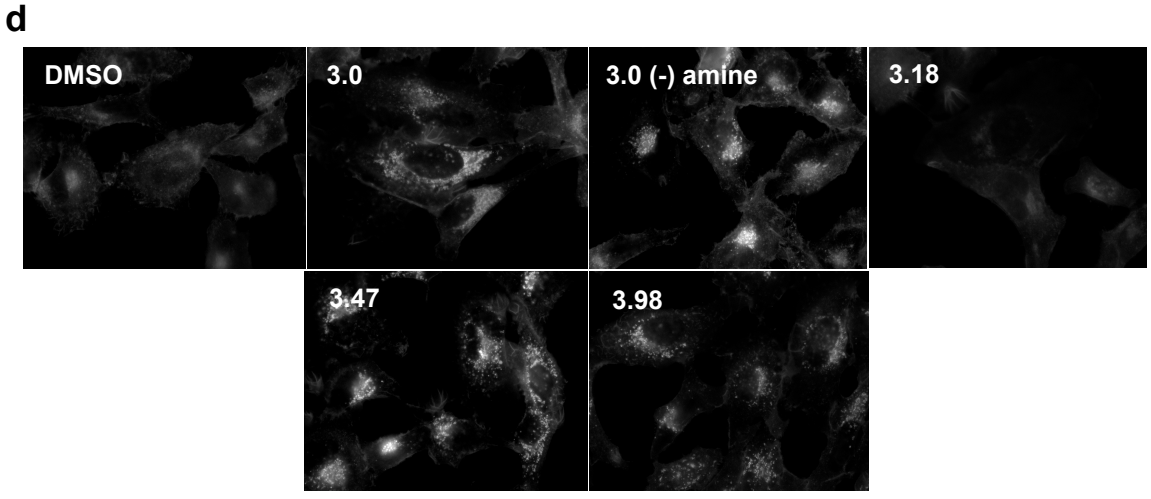
d
DMSO
3.0
3.0 (-) amine
3.18
3.47
3.98

Figure 3-1 (Continued)***. Structure and function of 3.0 derived EboV entry inhibitors.*** **(a)** Compounds 3.0 and informative derivatives 3.0 (-) amine, 3.18, 3.47, and 3.98 . **(b)** Vero cells were grown in media containing increasing concentrations of 3.0, 3.0 (-) amine, 3.18, 3.47, or 3.98 for 90 min before the addition of VSV particles encoding luciferase (3.18, 3.47, 3.98) or GFP (3.0, 3.0 (-) amine) and pseudotyped with EboV GP. Virus infection is reported as percent of luminescence units (RLU) or GFP-positive cells relative to cells exposed to DMSO vehicle alone. Data are mean ± s.d. (n=4) and is representative of three experiments. **(c)** Vero cells were grown in media containing 3.0 (40 μM), 3.47 (40 μM), vehicle (1% DMSO) or the cysteine cathepsin protease inhibitor E-64d (150 μM) 90 min before the addition of replication competent Ebola virus Zaire-Mayinga encoding GFP (multiplicity of infection (m.o.i.)=0.1). Results are mean relative fluorescence units (RFU) ± s.e.m. (n=3). **(d)** Cells treated with 3.0 derived EboV inhibitors develop cholesterol filled intracellular vesicles characteristic of NPC phenotype. HeLa cells treated overnight with 2.5μM of the indicated inhibitor were stained with the cholesterol-avid dye filipin.

inserted into the diamide backbone, the IC_{50} was more than 10-fold higher than parent compound 3.0 (Figure 3-1 a,b). More potent derivatives were identified as well; as described in chapter 2, the addition of a (methoxycarbonyl) benzyl group at the ortho position of the benzene ring yielded compound 3.47, which exhibited a greater than 10-fold decrease in the IC_{50} as compared to parent compound 3.0 (Figure 3-1 a,b). The increased potency of 3.47 was particularly evident in experiments measuring the growth of replication competent EboV on Vero cells, where 3.47 was able to reduce infection to the level of the cathepsin inhibitor E64d, a well characterized inhibitor of EboV replication (Chandran et al., 2005). In contrast, an equal concentration of 3.0 reduced infection less than 2-fold from the vehicle negative control (Figure 3-1 c). These findings suggest that subtle changes in the structure of 3.0 can have a profound impact on the antiviral activity of the compound.

Given that changes to the structure of 3.0 can impact the antiviral activity of the compound, we sought to investigate whether changes to the physiochemical properties of 3.0 could have similar impacts on antiviral activity. In Chapter 2, we initially tested whether our compounds could induce cellular cholesterol accumulation since several of them had CAD like physiochemical properties. A central component of drug-induced phospholipidosis is protonation of the compounds within the lysosomes, which results in the trapping and subsequent accumulation of compound-phospholipid complexes in the lumenal membranes of the late endosome and lysosome (Kodavanti and Mehendale, 1990; Anderson and Borlak, 2006; Alakoskela et al., 2009; Hanumegowda et al., 2010). This accumulation results in the eventual disruption of lipid, cholesterol, and protein regulation in the late endosome

(Kobayashi et al., 1999; Alpy et al., 2001; Kobayashi et al., 2001; Makino et al., 2006; Sobo et al., 2007; Chevallier et al., 2008). As noted in Chapter 2, both 3.0 and 3.47 have relatively low pKa values (~6.0) when compared to known CAD compounds, which traditionally have pKa values of >8.5 (Kornhuber et al., 2008). Thus, both 3.0 and 3.47 would remain uncharged at neutral pH, unlike CADs whose major species at this pH would have a positive charge. However, in the low pH environment of the LE/LY (~pH 5.0) (Schmid et al., 1989), the majority of 3.0 and 3.47 would be protonated and would carry a positive charge. Thus, we used SAR to experimentally test whether 3.0 may act through a protonation induced lysosomal accumulation mechanism similar to well characterized CADs. In order to test if protonation in the LE/LY is required for 3.0 function, we tested the antiviral activity of a non-protonatable derivative, referred to as 3.0 (-) amine. In this derivative the tertiary amine, which carries a charge at low pH, is replaced with a carbon. The 3.0 (-) amine compound was just as potent as the parent compound (Figure 3-1 a, b), indicating that protonation of the tertiary amine is not required for antiviral activity.

Since a non-specific, charged based mechanism was not responsible for the antiviral activity of 3.0 and because subtle changes in the structure could produce large changes in the antiviral activity of the compound, we suspected that the compound may have a specific interaction with its target molecule. In order to identify the proteins that these compounds may target, we used the information gathered from extensive SAR studies to synthesize a tagged 3.47 derivative, 3.98. Compound 3.98 has anti-EboV activity comparable to 3.47 but contains two additional functional moieties: an aryl-azide for photoaffinity labeling of target proteins and an alkyne

group for specific labeling by click chemistry to allow for detection of the cross-linked target (Figure 3-1 a,b).

Considering that we were first led to investigate NPC1 because of the build-up of LE/LY cholesterol in cells treated with 3.0 or 3.47, we sought to test if the informative derivatives of 3.0 retained the ability to induce cholesterol accumulation. To test for cholesterol build-up, we treated HeLa cells overnight with each of the 3.0 derivatives (2.5 μM) and stained the cells with filipin. Interestingly, the antiviral activities of these compounds corresponded with their abilities to induce cholesterol accumulation. When cells were treated with 3.18, we observed a level of cholesterol accumulation that was comparable to the vehicle-treated negative control (Figure 3-1 d). On the other hand, the similar levels of cholesterol accumulation exhibited by cells treated with 3.0 or the 3.0 (-) amine derivative further suggested that cholesterol accumulation was not dependent on a positive charge of the molecule in the LE/LY. Lastly, 3.47 and 3.98 also exhibited similar levels of cholesterol accumulation, further indicating that the addition of the functional aryl-azide and alkyne groups had little effect on the behavior of 3.47 in both infectivity and cell phenotype assays. These results suggested that inhibition of cholesterol transport by 3.0 derived compounds may be coincident with the antiviral activity of the compounds. Given that NPC1 is the only component of the LE/LY cholesterol uptake pathway that mediates infection, we hypothesized that the compounds directly target NPC1.

B. Compound 3.98 covalently cross-links with NPC1

Studies of 3.0 derivatives with different antiviral potencies revealed a correlation between the antiviral activity of the compound and the effect of the compound on cholesterol uptake, suggesting that NPC1 is a direct target of the 3.0 derivatives. As 3.0 and 3.47 lack the functional moieties necessary for biochemical purification, we relied upon the added versatility conferred to derivative 3.98. As described above, compound 3.98 possesses an aryl-azide for photoaffinity labeling of target proteins and an alkyne group for specific labeling by click chemistry for identification of the UV adducts (Ban et al., 2010), while retaining full anti-EboV and cholesterol-inducing activities, thus proving its validity for study. To analyze the direct binding of 3.98 to targets in membrane lysates, membrane extracts were incubated with 3.98 (25μM), exposed to UV light, and proteins were solubilized in detergent (Figure 3-2a). UV adducts were covalently bound to azide-AlexaFluor488 using click chemistry. Membrane lysates or immunoprecipitated NPC1 were analyzed by immunoblot using an antibody to AlexaFlour488 to detect proteins crosslinked to the inhibitor and membranes were re-blotted to detect NPC1. A number of cellular proteins that covalently linked to 3.98 were observed in both CHO_{null} and CHO_{NPC1} membranes (Figure 3-2b, left). The marked increase in labeling of proteins greater than 150 kDa in CHO_{NPC1} correlated with expression of NPC1 (Figure 3-2b, right). Direct probing of NPC1 recovered by immunoprecipitation (Figure 3-2b, bottom right) with AlexaFlour488 antibodies confirmed cross-linking to 3.98 (Figure 3-2b, bottom left). Taken together, the direct labeling of NPC1 by 3.98 and the ability of the 3.0-derived compounds to inhibit EboV GP dependent entry, suggests that NPC1 binding with the these compounds may disrupt the ability of NPC1 to bind cleaved GP1.

Figure 3-2.

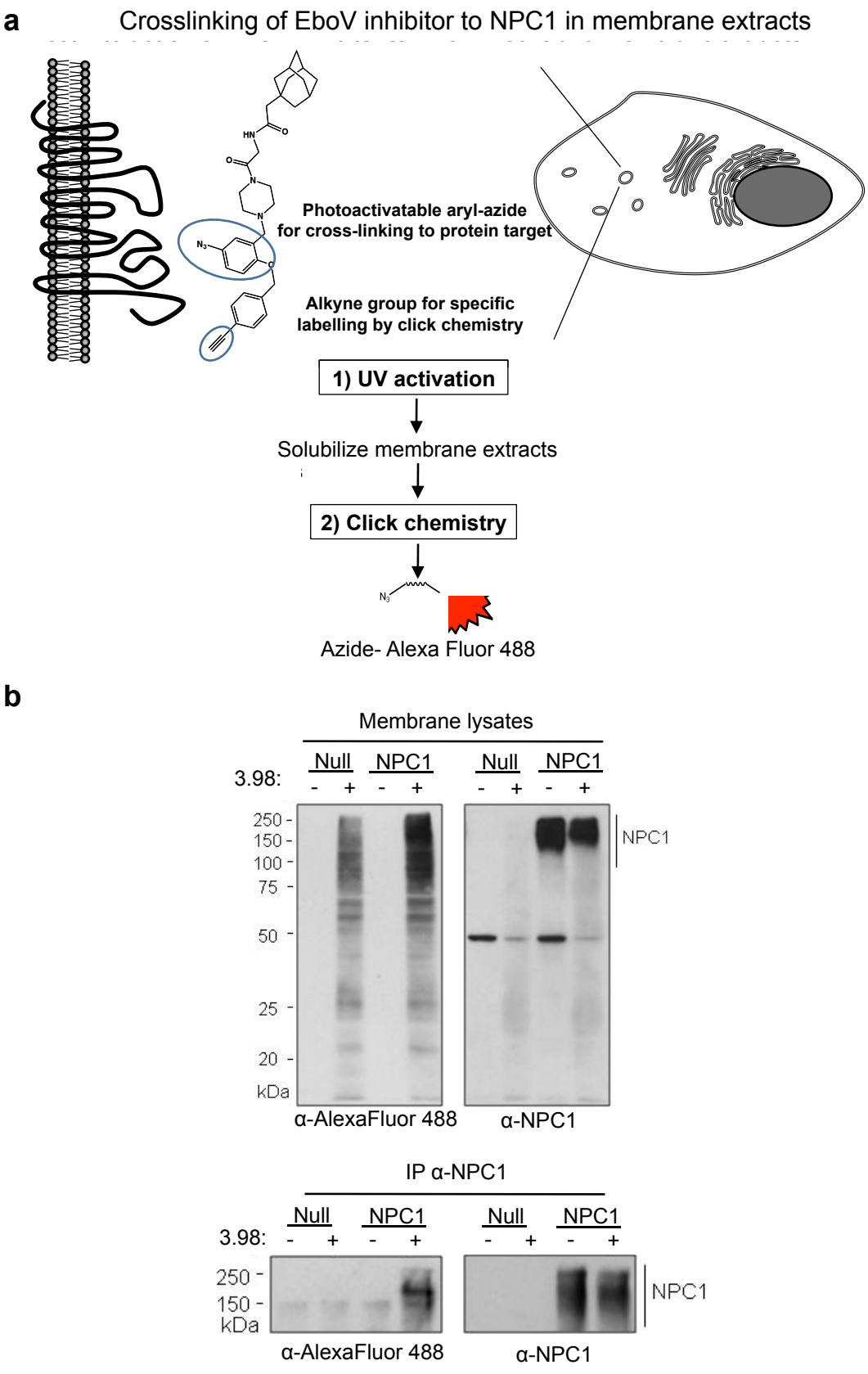
a
Crosslinking of EboV inhibitor to NPC1 in membrane extracts
Photoactivatable aryl-azide
for cross-linking to protein target
Alkyne group for specific
labelling by click chemistry
1) UV activation
Solubilize membrane extracts
2) Click chemistry
Azide- Alexa Fluor 488
b
Membrane lysates
3.98:
Null
NPC1
Null
NPC1
- + - + - + - +
250 -
150 -
100 -
75 -
50 -
25 -
20 -
kDa
NPC1
α-AlexaFluor 488
α-NPC1
IP α-NPC1
3.98:
Null
NPC1
Null
NPC1
- + - + - + - +
250 -
150 -
kDa
NPC1
α-AlexaFluor 488
α-NPC1

Figure 3-2 (Continued). ***NPC1 is a direct target of EboV inhibitor 3.98 .*** **(a)** Compound 3.98 is a derivative of the EboV inhibitor 3.47 that contains a photoactivatable aryl azide to induce the covalent linkage of the compound to its targets and an alkyne group for specific labeling by click chemistry using azide-AlexaFluor488 for protein analysis of UV-adducts. **(b)** For analysis of the direct binding of the EboV compound to NPC1, membrane extracts were incubated with 3.98, exposed to UV light and proteins were solubilized in detergent. Cross-linked compound was labeled with azide-AlexaFluor488. Total lysates (upper panel) or immunoprecipitated NPC1 from these membrane lysates (lower panel) were resolved by SDS-PAGE, transferred to PVDF membranes and proteins cross-linked to compound were detected using immunoblot with anti-AlexaFluor488. PVDF membranes were reblotted for NPC1.

C. Small molecules inhibit binding of EboV GP to NPC1 containing membranes

Since 3.98, and likely the entire series of 3.0-derived compounds directly bind to NPC1, we hypothesized that compound binding to NPC1 may disrupt the ability of NPC1 to also bind cleaved EboV GP1. We tested this hypothesis by performing the GP1 membrane binding assay described in Chapter 2 (Figure 2-13a) in the presence of increasing concentrations of our informative 3.0 derivatives. We first tested the relationship between inhibition of binding and antiviral activity by investigating the ability of 3.0 derivatives of variable potency to inhibit binding of GP to NPC1 containing membranes. We found that 3.0 and 3.47 inhibited binding of cleaved EboV $GP_{\Delta TM}$ to NPC1 membranes in a concentration-dependent manner (Figure 3-3a). Importantly, we observed a direct correlation between the potency of 3.47, 3.0, and 3.18 in inhibiting binding (Figure 3-3a, left panel) and inhibiting infection (Figure 3-1b); 3.47, which is a more potent antiviral than 3.0, was capable of disrupting GP1 binding with NPC1 at a lower concentration than 3.0, while 3.18, which is vastly less potent than 3.0, was not able to disrupt GP1 binding with NPC1 under any of the conditions tested. Notably, the 3.0 (-) amine derivative also blocked GP1 binding to NPC1 containing membranes in a dose dependent manner (Figure 3-3b), confirming that the tertiary amine is dispensable for all relevant antiviral activity. We also tested U18666A, a small molecule inhibitor of LE/LY cholesterol transport and membrane trafficking (Sobo et al., 2007; Huynh et al., 2008) and found that it does not inhibit binding of cleaved EboV GP to NPC1 membranes (Figure 3-3a, right panel). In a third experiment, we compared the ability of 3.47 and its derivative 3.98, to block binding of GP to NPC1 membranes, and

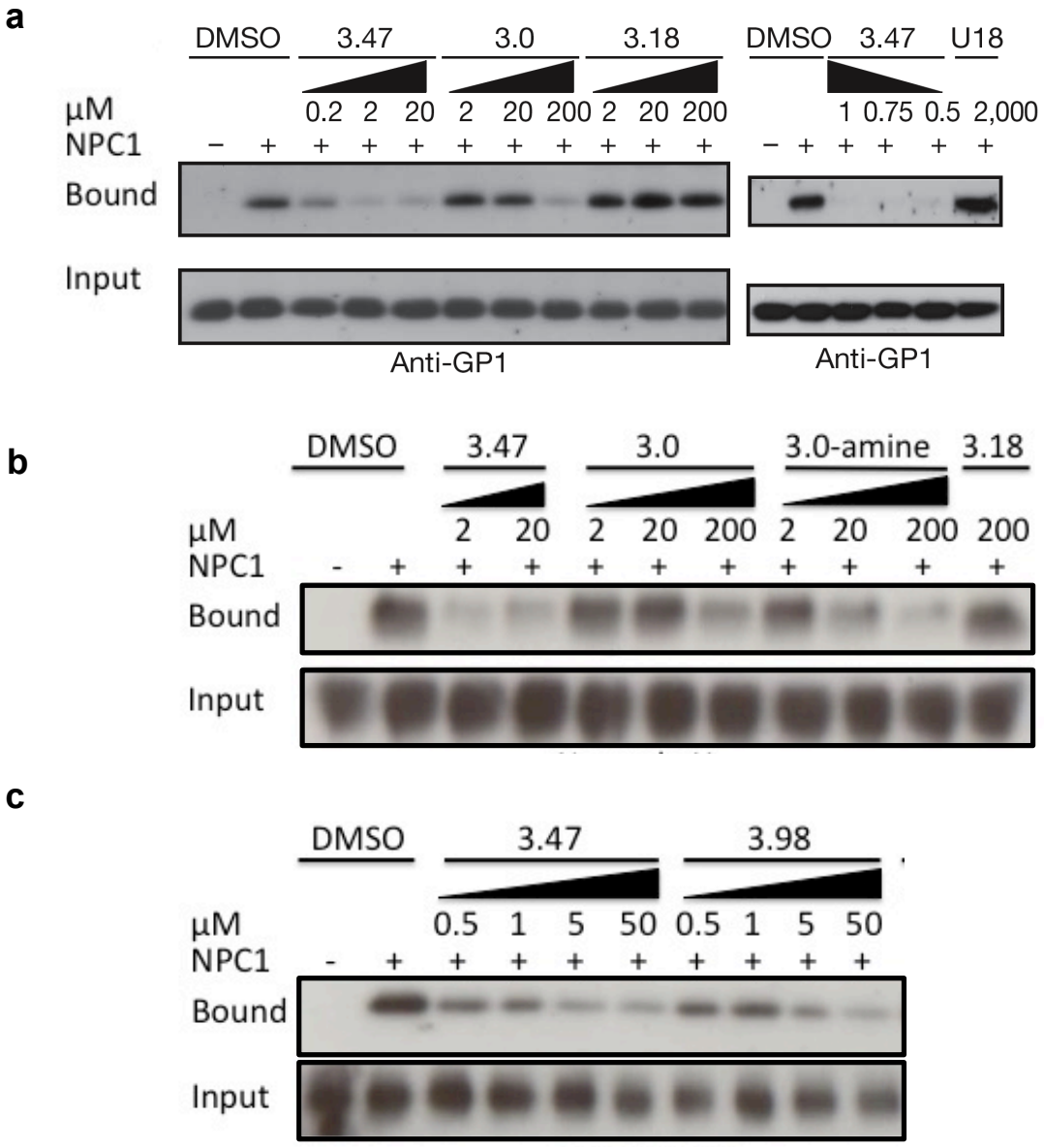

Figure 3-3. ***Inhibitors act by disrupting GP binding to NPC1 containing membranes.*** **(a)** Thermolysin-cleaved EboV $GP_{\Delta TM}$ protein (1μg) was added to LE/LY membranes from CHO_{null} or CHO_{NPC1} cells in the presence of DMSO (10%) or the indicated concentrations of 3.47, 3.0, or 3.18 (left panel), and 3.47 or U18666A (U18, right panel). Membrane-bound and unbound GP1 were analyzed by immunoblot. **(b,c)** Binding assays were done as in part (a) in the presence of 3.0 derived inhibitors (b) or 3.47 and the derivative 3.98 (c).

compound 3.98 was capable of blocking GP binding to NPC1 containing membranes to similar levels as 3.47 (Figure 3-3c). Taken together, the binding studies establish a correlation between the antiviral activity of the compounds and the ability of the compounds to inhibit binding of cleaved GP to NPC1 containing membranes. These experiments are consistent with a mode of antiviral action for the 3.0 series of compounds wherein the drugs bind NPC1 and disrupt its ability to engage cleaved EboV GP1 within the LE/LY, preventing the receptor-engagement steps needed for EboV GP triggering. We next sought to support this model through additional structural and functional studies further detailing the relationships between antiviral activity of the compounds and EboV GP1 function.

D. Overexpression of NPC1 confers resistance to inhibitors

If EboV GP1 binding to NPC1 is an essential step in virus entry, and 3.0-derived antiviral compounds are able to limit the proportion of cellular NPC1 capable of mediating EboV GP binding, then overexpression of NPC1 could increase the overall numbers of inhibitor-free NPC1, and thus the likelihood of an unhindered EboV GP entry event in the presence of inhibitors. In order to address this possibility, we compared the relationship between inhibitor concentration and relative infectivity on CHO cells overexpressing NPC1 (Millard et al., 2000) as compared to cells expressing endogenous levels of NPC1 (wt) (Figure 3-4a). Overexpression of NPC1 conferred resistance to the antiviral activity of 3.0 and 3.47, with cells overexpressing NPC1 showing a greater than 30-fold (3.0) or 50-fold (3.47) increase in the IC_{50} as compared to wt cells (Figure 3-4 b). Furthermore, to eliminate the possibility that this

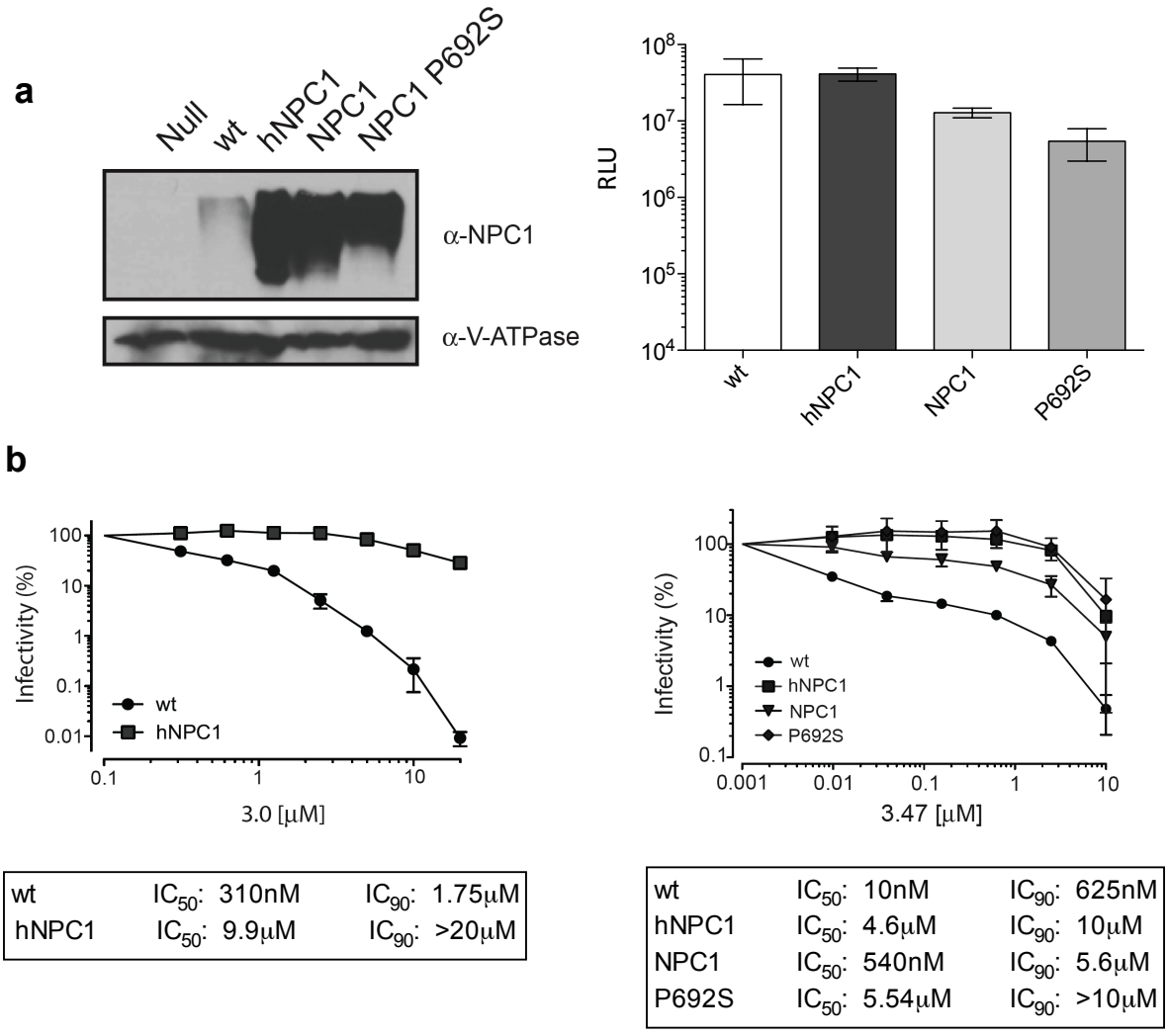

wt	IC_{50}: 310nM	IC_{90}: 1.75μM
hNPC1	IC_{50}: 9.9μM	IC_{90}: >20μM

wt	IC_{50}: 10nM	IC_{90}: 625nM
hNPC1	IC_{50}: 4.6μM	IC_{90}: 10μM
NPC1	IC_{50}: 540nM	IC_{90}: 5.6μM
P692S	IC_{50}: 5.54μM	IC_{90}: >10μM

Figure 3-4. ***NPC1 overexpression confers resistance to inhibitors .*** **(a)** Left panel. CHO_{null}, CHO_{wt}, CHO_{NPC1}, CHO_{hNPC1} and CHO P692S cells were homogenized, and membranes in the post-nuclear supernatant were pelleted at 15000 x *g*. NPC1 and V-ATPase B1/2 in the pelleted membranes were detected by immunoblot. Right panel. CHO cells were infected with VSV-Luc particles pseudotyped with EboV GP. Virus infection is reported as relative luminescence units (RLU) **(b)** CHO_{wt}, CHO_{hNPC1}, CHO_{NPC1}, and CHO NPC1 P692S cells were incubated in the presence of increasing concentrations of 3.0 (left), 3.47 (right) or vehicle prior to the addition of VSV particles pseudotyped with EboV GP. Infection was calculated as a percent of the vehicle control. Data is mean ± s.d. (n=4) and is representative of 3 experiments.

shift in inhibitor sensitivity is due to cell line variability rather than NPC1 expression, we tested several different cell lines stably overexpressing hNPC1, mNPC1 or mNPC1 P692S (Millard et al., 2000; Millard et al., 2005). We found that all of the overexpression cell lines tested exhibited resistance to 3.47, thus minimizing the likelihood that the inhibitor shift is due to variability between the cell lines. Importantly, in the absence of inhibitor, CHO cells overexpressing hNPC1 exhibited a comparable level of overall infectivity when compared to wt CHO cells, while cells overexpressing murine NPC1 or NPC1 mutant P692S exhibited mild decreases in infectivity (Figure 3-3a), showing that these differences were not caused by inherent increases to EboV GP-mediated infectivity in these cells. Additionally, the finding that wt CHO and overexpressing hNPC1 CHO cells exhibited no appreciable difference in infectivity suggested that endogenous levels of NPC1 expression in CHO cells were not a limiting factor in virus entry. These results lend functional support for a model in which binding of 3.0-series compounds to NPC1 disrupts EboV GP1 binding to NPC1, making this binding event a rate limiting step in the presence of inhibitor, which can be counteracted through greatly increased levels of overall NPC1.

E. Inhibitor-resistant viruses suggest target is a receptor-virus interaction

In Chapter 2, we found that only protease cleaved EboV GP was able to bind NPC1 in membrane-binding and co-immunoprecipitation assays, while uncleaved EboV GP was not. This finding is consistent with an entry model wherein protease cleavage of the GP1 subunit reveals a receptor binding domain (RBD) (Kuhn et al., 2006; Kaletsky et al., 2007; Brindley et al., 2007; and Dube et al., 2009 and 2010) that in turn interacts

with a host receptor, which we propose is NPC1. Indeed, the actions of the 3.0 derived EboV inhibitors, which bind directly to NPC1 and disrupt GP binding to NPC1, suggest that they target such a virus-receptor interaction. A classical experiment following small-molecule inhibition of virus replication is the selection of resistance mutations that circumvent the inhibition, and such experiments have previously been used to identify mutations that map to the RBD of viral fusion proteins in cases where the small molecule inhibitor specifically targets the host receptor to disrupt fusion protein interaction (Westby et al., 2007; Tsibris et al., 2008; Ogert et al., 2009). Rather than develop an assay where we would passage and hopefully select for virus encoding EboV GP mutations capable of circumventing the antiviral effects of the compound, we instead decided to look to the naturally occurring sequence variations within various filoviridae GPs to identify viruses, and eventually specific coding mutations, that may confer resistance to the compounds. Thus, we expanded the studies of the EboV inhibitors to include GPs from all known species of filoviruses, which up until this point had only been done with GPs from Ebola Zaire. Since all species of filoviruses strictly require NPC1 expression for infection (Table 2-3), any resistance to 3.47 would likely be due to changes in the way in which GP1 engages NPC1, rather than overall changes in NPC1 utilization.

F. Filoviruses Sudan and Marburg are resistant to inhibitors

We tested the ability of 3.47 to inhibit entry mediated by the GP from each of the five species of ebolavirus as well as marburgvirus. We found that *Reston ebolavirus* (R), *Tai Forest ebolavirus* (T), *Bundibugyo ebolavirus* (B) and *Zaire ebolavirus* (Z or EboV)

a

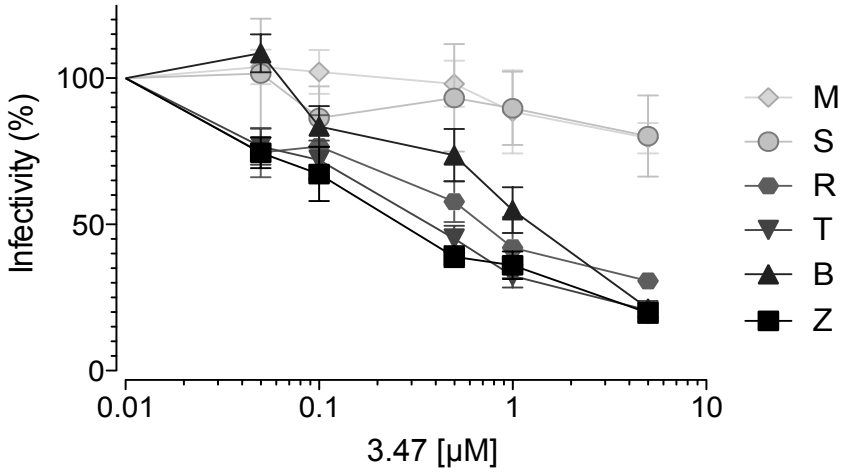

b

Identity (percent) matrix based on mucin domain deleted GP sequences used in this study.

EboV	TaFV	BdbV	RestV	SudV	MarV	
	80.1	81.7	71.5	69.7	32.5	EboV
		89.1	71.9	69.1	33.5	TaFV
			73.0	69.4	32.6	BdbV
				74.3	31.9	RestV
					32.3	SudV
						MarV

Figure 3-5. ***Filoviruses Sudan and Marburg are resistant to 3.47.*** **(a)** The effect of increasing concentrations of inhibitor 3.47 on infection by VSV luciferase particles pseudotyped with glycoproteins from: *Marburg marburgvirus* (M), *Sudan ebolavirus* (S), *Reston ebolavirus* (R), *Tai Forest ebolavirus* (T), *Bundibugyo ebolavirus* (B) and *Zaire ebolavirus* (Z). Infectivity was calculated as in Figure 3-1b. Data are mean ± s.d. (n=6) and is representative of three experiments. **(b))** A percent identity matrix was produced using amino acid sequences of the glycoproteins used in these experiments. For all of the Ebola virus species, GPs were used in which the highly variable mucin-like domains were deleted and these sequences are compared here. For Marburg virus the full-length GP was used in the experiment and is compared to the mucin deleted viruses here.

GPs all exhibited a similar level of sensitivity to 3.47 with an IC_{50} of <1.25 μM. By contrast, *Sudan ebolavirus* (S or SudV) and *Marburg marburgvirus* (M) GPs were resistant to inhibition by 3.47 with an IC_{50} of >20 μM (Figure 3-5a). Since Zaire and Sudan show more sequence conservation (70% identical) in GP than Zaire and Marburg (32% identical) (Figure 3-5b), we decided to exploit the differences in phenotype between Zaire (EboV) and Sudan (SudV) to map the amino acid determinates of inhibitor sensitivity.

G. Compound 3.47 does not inhibit binding of SudV-GP1 to NPC1 membranes

Recent binding studies from our lab have confirmed that, like EboV GP, binding of soluble SudV GP is dependent on both protease cleavage and expression of NPC1 (Misasi et al., 2012). This finding provided a means by which to further test our interpretation that 3.47 antiviral activity is directly related to its ability to disrupt an interaction between GP1 and NPC1; since SudV GP is resistant to the antiviral effects of 3.47, it may also be capable of binding NPC1 in the presence of high concentrations of 3.47 as well. Indeed, when we titrated 3.47 into the membrane-binding assay with soluble SudV GP, we found SudV GP1 binding to NPC1-containing membranes was not significantly reduced under the same conditions in which EboV GP1 binding was reduced by >90% (Figure 3-6). Thus, these results support the interpretation that the antiviral activity of 3.0-series of compounds on GP mediated infection directly correlates with the abilities of the compounds to inhibit GP binding to NPC1 containing membranes.

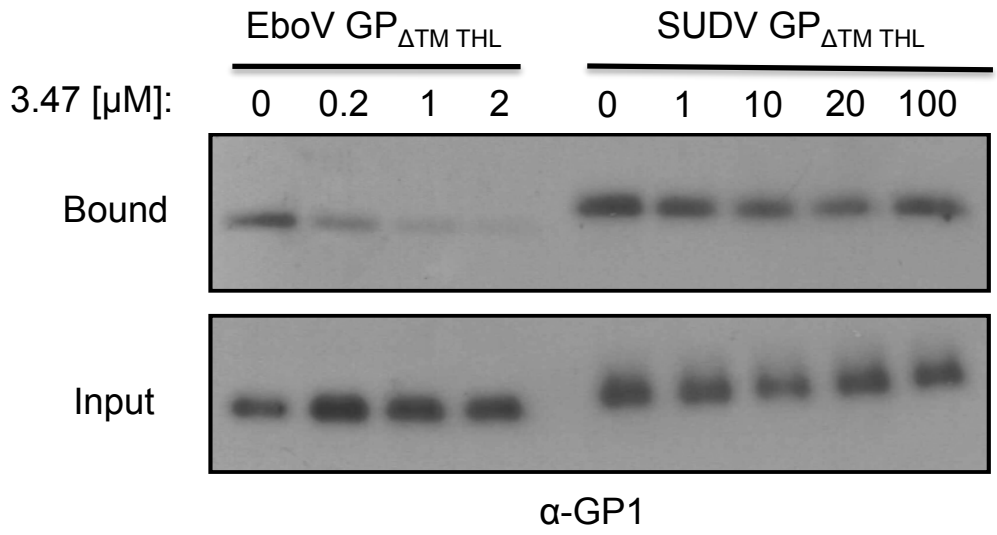

Figure 3-6. ***Sudan GP1 binding to NPC1 is resistant to EboV Zaire inhibitors***. Late endosomal/ lysosomal membranes from cells expressing NPC1 were purified, osmotically lysed and coated on ELISA plates. Membranes were treated with indicated concentrations of EboV inhibitor 3.47 prior to incubation with a soluble form of EboV GP or SudV GP trimer that had been cleaved with thermolysin protease, which faithfully mimics cleavage by endosomal cathepsins to expose the receptor binding domain in GP1. After incubation and washing, membranes were solubilized in SDS buffer and the presence of bound GP was determined by immunoblot using GP1 antibodies.

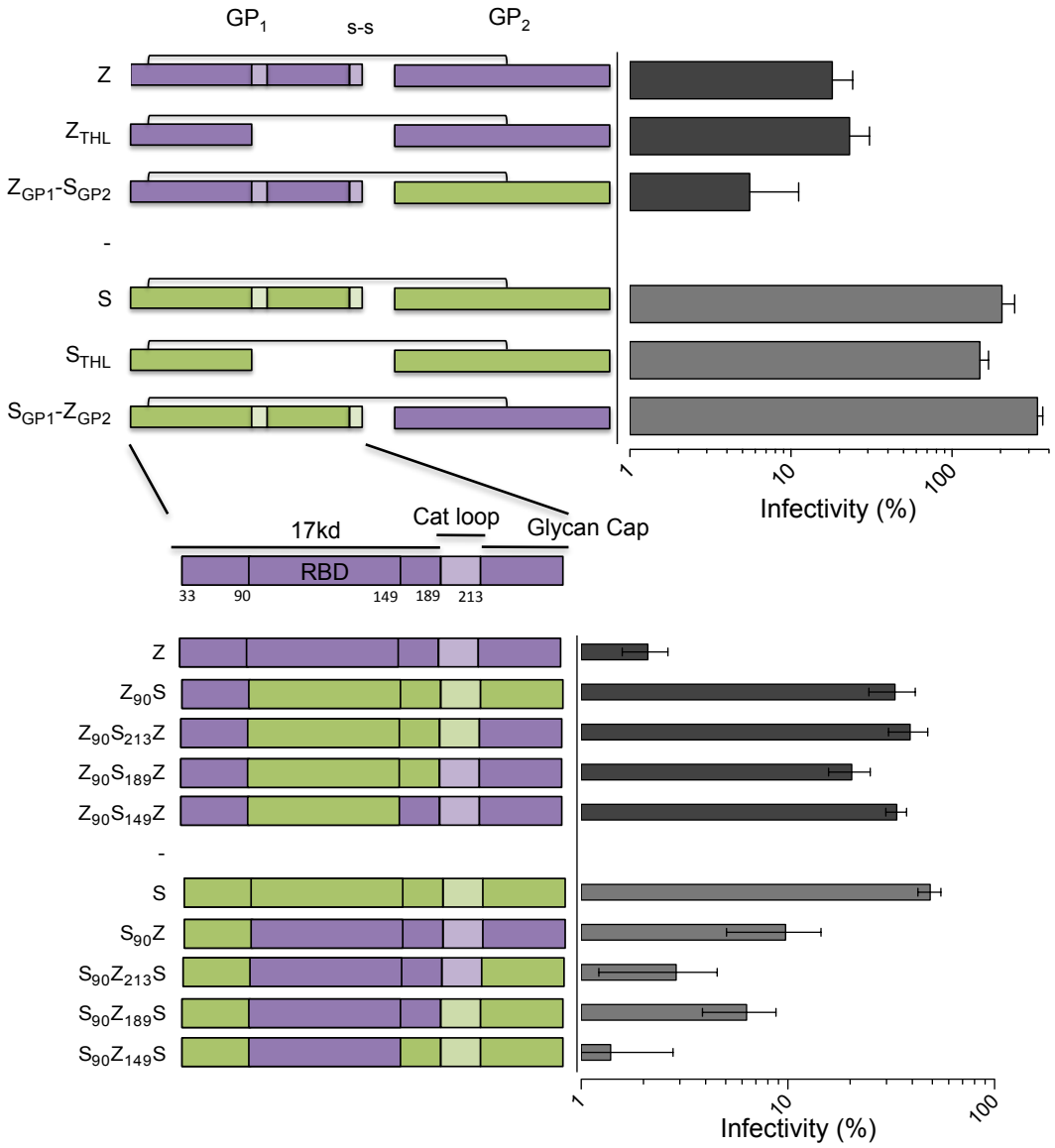

Figure 3-7. ***Reciprocal exchanges between SudV and EboV GP revealed that the receptor binding domain of GP1 conferred sensitivity to 3.47.*** Virus particles (VSV-eGFP, top panel, or MLV-LacZ, bottom panels) were pseudotyped with GPs from Sudan and Zaire in which the entirety of GP1 or GP2 were swapped, and used to infect Vero cells outright or pre-cleaved by thermolysin (top). Once susceptibility was mapped to GP1, additional chimeras were tested to narrow down the determinants of drug sensitivity within various GP1 subdomains (bottom). Cells were treated with 20 μM of compound 3.0 (top) or 10μM of 3.47 (bottom). Reporter positive cells were counted after infection. Results are represented as a percentage of the vehicle control (DMSO).

H. Resistance to 3.47 maps to amino acids 141 and 142 within the RBD of SudV-GP

Although the SudV and EboV GP proteins are divergent enough to harbor contrasting phenotypes to drug sensitivity, they are still conserved enough to be easily aligned, providing us the opportunity to further dissect the amino acid requirements responsible for inhibitor sensitivity. We began to map the molecular basis for resistance by producing viruses pseudotyped with chimeric GPs, in which distinct subdomains of the protein were swapped between the Zaire and Sudan sequences, and the subsequent viruses were tested for sensitivity to compound 3.47. Initial studies revealed that resistance to 3.47 lies within the post-cathepsin cleaved region of SudV-GP1 (Figure 3-7, top panel). GP1 was further divided into smaller subdomains based on existing structural and functional data, including the glycan cap, a cathepsin sensitive loop, and the putative minimal RBD (Lee et al., 2010; Dube et al., 2009). Chimeras of these functional GP1 domains mapped SudV GP resistance down to the minimal RBD of GP1 (Figure 3-7, bottom panel, top half), as the chimeric GPs were resistant to 3.47 only when the minimal RBD of SudV GP1 was present. Conversely, the minimal RBD of EboV GP1 conferred sensitivity to 3.47 when placed in the context of full length SudV GP (Figure 3-7, bottom panel, bottom half). The reciprocal nature of this phenotype suggested that there was a discrete set of amino acids within the minimal RBD of SudV that accounted for resistance to the inhibitor.

The minimal RBDs of SudV and EboV are highly conserved at the amino acid level (88%) and differ at only eight residues (Figure 3-8a). We compared the atomic resolution structures of SudV and EboV GP1 (Lee et al., 2008; Dias et al., 2011; Bale et

Figure 3-8.

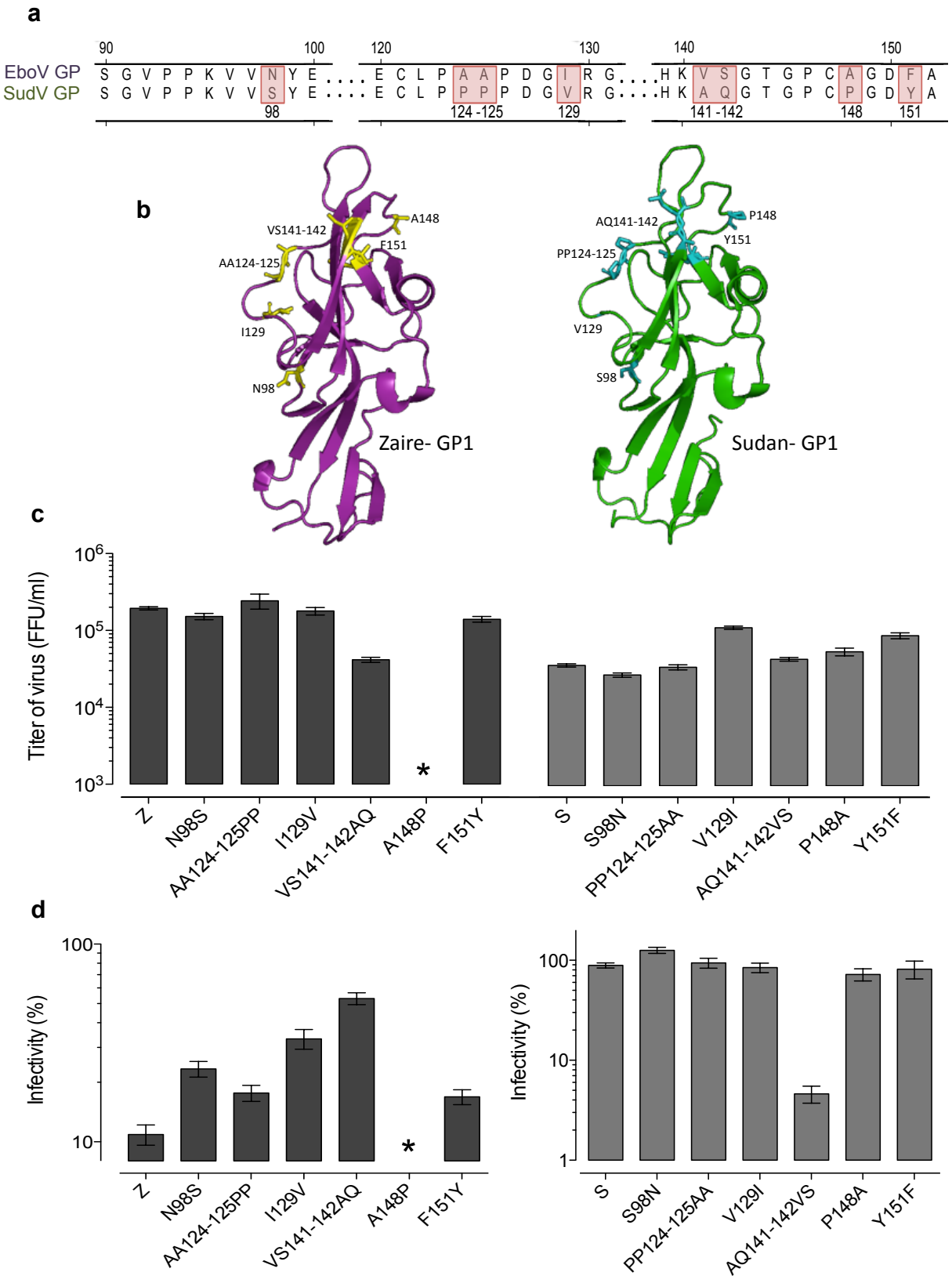
a
EboV GP
SudV GP
b
VS141-142
A148
F151
AA124-125
I129
N98
Zaire- GP1
AQ141-142
P148
Y151
PP124-125
V129
S98
Sudan- GP1
c
Titer of virus (FFU/ml)
Z
N98S
AA124-125PP
I129V
VS141-142AQ
A148P
F151Y
S
S98N
PP124-125AA
V129I
AQ141-142VS
P148A
Y151F
d
Infectivity (%)

Figure 3-8 (Continued). ***Reciprocal exchanges at residues 141-142 within the receptor binding domain of GP1 conferred sensitivity to 3.47.*** **(a)** Sequence alignment for the RBD of EboV GP1 and SudV GP1. **(b)** Location of differences between the RBD of SudV GP1 and EboV GP1 on the post cathepsin cleaved atomic resolution structures of EboV (left, purple, PDB:3CSY) and SudV (right, green, PDB:3S88) GP. **(c)** MLV particles pseudotyped with chimeric glycoproteins obtained by reciprocal exchange of Zaire and Sudan GP sequences were titered on Vero cells. Cells were exposed to MLV pseudotypes encoding β-galactosidase. 48 hours post infection, cells were fixed and exposed to X-gal to assay for reporter expression. Results are represented as focus forming units (FFU) per ml. **(d)** Vero cells were grown in media containing 3.47 (10μM) for 90 min before the addition of MLV-LacZ virus particles pseudotyped with the chimeric glycoproteins. Cells were maintained in the presence of 3.47 until reporter positive cells were counted 48 hours after infection. Results are represented as a percentage of the vehicle control (DMSO). Data are mean ± s.d. (n=3) and is representative of three experiments. "*": not determined (ND)

al., 2012) and identified six clusters of amino acid changes in the RBD (Figure 3-8b). In order to test if any of these sequence variations account for the differential inhibition phenotypes, we continued to refine our chimeric GPs by performing reciprocal swaps of amino acids 98, 124-125, 129, 141-142, 148 and 151 between the two GPs. These reciprocal swaps did not significantly change the overall titer of the pseudotyped virus particles on Vero cells, thus making it unlikely that any change in sensitivity would be due to a secondary effect on virus production (Figure 3-8c). We found that when the residues from EboV were placed within the context of the SudV GP, only residues 141-142 were able to confer sensitivity to 3.47 (Figure 3-8d, right). By contrast, substitutions of the other amino acid clusters showed no increase in sensitivity to the inhibitor. When the converse exchanges were made in the EboV GP background, a swap at residues 141-142 made the GP more resistant to 3.47 inhibition (Figure 3-8d, left). Unlike the exchange of the other residues in the SudV GP, swapping the remaining residues in EboV GP lead to chimeric GPs with intermediate levels of resistance to 3.47, although exchange of residues 141-142 still conferred the most pronounced resistance phenotype in the EboV GP background.

These final chimeric GPs, the minimal RBD chimeras, and the parent GPs, were subject to a titration of compound 3.47 to further quantitate the extent to which the drug sensitivity phenotypes associate with the coding mutations (Figure 3-9). The dose response curve for chimeric SudV $GP_{Z141-142}$ moved to the left, with the IC_{50} shifting from >10μM for SudV GP to <100 nM for SudV $GP_{Z141-142}$, to a level essentially overlapping the IC_{50} of EboV GP-dependent infection. By contrast, the dose response curve for the chimeric EboV $GP_{S141-142}$ moved to the right, as the IC_{50} shifted from <100 nM for EboV

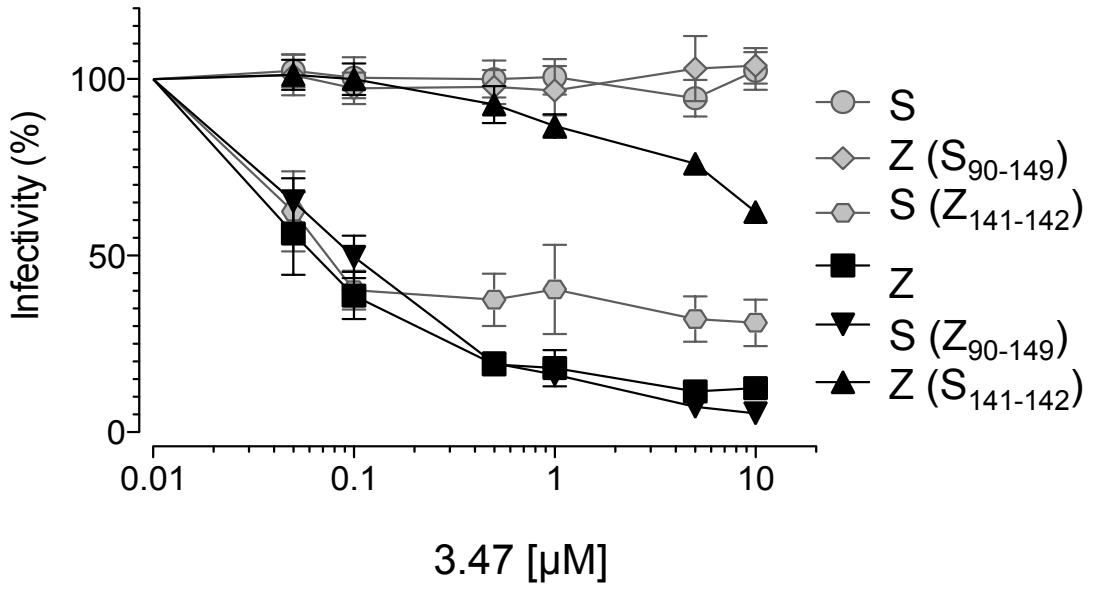

Figure 3-9. ***Zaire GP1 RBD Val141/Ser142 confer sensitivity to 3.47.*** VSV particles pseudotyped with chimeric glycoproteins obtained by reciprocal exchange of Zaire and Sudan GP sequences were incubated with Vero cells in the presence of increasing concentrations of inhibitor 3.47. Vero cells were treated with inhibitors and exposed to VSV encoding luciferase and pseudotyped with the indicated chimeric GPs. Results are represented as % of vehicle (DMSO) control.

GP to >10 μM for EboV $GP_{S141-142}$, exhibiting a dose response curve that more closely resembled the resistance of SudV GP to inhibition by 3.47 (Figure 3-9). These results show that alanine 141 and glutamine 142, found within the RBD of the SudV GP, are the major determinants that naturally render SudV GP resistant to compound 3.47, a phenotype which is dominantly conferred when encoded into the backdrop of the naturally drug- sensitive EboV GP.

Discussion

Recently, studies by our lab and others have identified NPC1 as an essential host factor for Ebola virus entry (Carette et al., 2011). In Chapter 2, we found that EboV entry was strictly dependent on NPC1 expression and that EboV GP bound to NPC1 only after it had been protease cleaved. In this chapter, we expand on these findings by utilizing 3.0, the compound that originally lead us the discovery of NPC1. Extensive SAR studies allowed us to select a set of informative derivatives of 3.0 with a broad set of potencies and chemical characteristics, that could be used in a set of biochemical, functional, and genetic assays designed to probe the NPC1-GP1 interaction.

A. Inhibitors prevent GP-NPC1 interaction in a dose dependent manner

Several compounds that have a tertiary amine are sequestered in the LE/LY of treated cells, depending on where the inhibitor target resides, this can have a deleterious or advantageous effect on the ability of the compound to reach its target. In the case of inhibiting a late step in the EboV entry, accumulation of inhibitors in the LE/LY could be a particularly desirable characteristic given that this is the compartment that contains the host-factors for virus entry (low pH, cathepsins, and NPC1) and that

microscopy experiments reveal co-localization of virions to Rab7 containing LE (Nanbo et al., 2010; Saeed et al., 2010). One of the factors that can affect how efficiently a drug sequesters into these compartments is the pKa. One study that studied the compartmentalization of compounds that were essentially identical, except for their pKa values, showed that a pKa as low as 6.0 could lead to a greater than 20-fold increase in the concentration of compound in the lysosome (Duvvuri et al., 2005). Given that 3.0 had a tertiary amine whose pKa was 6.0, it was formally possible that the compound could be accumulating in the LE/LY of cells, thus, changing the effective concentration of the compound in its target compartment. However, testing of the 3.0 (-) amine derivative proved that the tertiary amine was dispensable for antiviral activity, the ability of the compound to block binding, and the induction of cholesterol build-up. Furthermore, tests of 3.0 derivatives with different potencies revealed that their abilities to inhibit EboV GP1 binding with NPC1-containing membranes closely correlated with the antiviral activity of the compounds in cells, thus, suggesting that the ability to inhibit binding of GP to NPC1 membranes *in vitro* is a manifestation of the antiviral activity.

Interestingly, the antiviral activity also correlated with the ability of the compound to inhibit cholesterol uptake. This result was surprising, as it seems to be at odds with the data from Chapter 2, which indicates that the cholesterol transport function of NPC1 is not required for productive EboV entry. This apparent discrepancy could be due to an allosteric interaction of the compound with NPC1 that locks the protein into a conformation that is incompetent for both GP binding and cholesterol transport. Alternatively, our compounds could be competing directly with a binding site in NPC1 that interacts with GP, but also overlaps directly with a cholesterol binding site or the

binding site of a second cellular factor involved in the cholesterol transport pathway. Recently published work suggesting that the luminal loop 2 (LL2) of NPC1 may be important for GP binding adds support to the later hypothesis, because this loop has also been implicated in the binding of NPC2, a soluble LE/LY protein that transfers cholesterol from the intraluminal membranes to NPC1 (Miller et al., 2012; Deffieu and Pfeffer, 2011). However, more structural and functional work needs to be done to identify the residues on NPC1 important for both GP and inhibitor binding. Identifying the exact sites on NPC1 that are involved in these interactions will provide insight into the mechanism by which the inhibitors are able to inhibit both cholesterol uptake and GP-NPC1 binding.

B. EboV inhibitors bind directly to NPC1

A derivative of 3.47 that could be used for functional crosslinking studies, 3.98, directly labeled NPC1, providing further evidence that the compounds inhibit entry by interacting with NPC1. However, it is crucial to note that 3.98 crosslinks several other cellular proteins, including many proteins found in CHO_{null} cells, thus indicating that the compound targets numerous proteins, most of which are not likely to be involved in EboV entry. Critically, we observed that overexpression of NPC1 reduced the sensitivity of the virus to inhibitors, consistent with the hypothesis that NPC1 is a direct target for 3.0 derived compounds and that the NPC1-GP interaction disrupted by these compounds is functionally important for virus entry. The direct interaction between NPC1 and the inhibitors must be structurally mapped in order to determine exactly the manner in which the inhibitors disrupt binding of GP to its receptor.

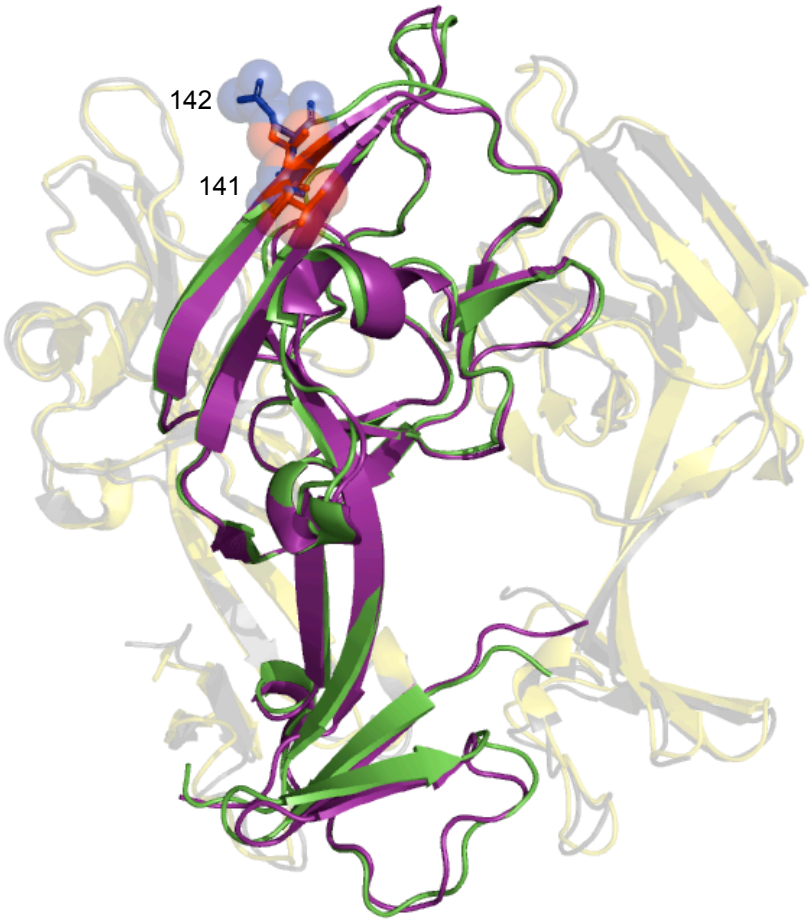

Figure 3-10. ***Inhibitor sensitive mutations 141-142 are solvent exposed on top outer edge of GP1 in the post-cathepsin cleaved trimer.*** The atomic resolution structures of the GP trimer for SudV-GP1 (green and yellow, PDB:3S88) and EboV-GP1 (purple and gray, PDB:3CSY) other domains of GP1 that are cleaved off during cathepsin digestion are excluded from this diagram. Residues 141-142 are represented here as sticks and spheres. SudV residues AQ141-142 that are associated with the resistance phenotype are shown in blue and EboV residues VS141-142 that are associated with sensitivity to the inhibitors are shown in red.

C. Genetic assay for viral determinates of inhibitor sensitivity

In order to gain mechanistic insight into the way in which the virus engages NPC1, we again used the inhibitor 3.47 as a probe, this time in genetic assays that identified mutations in GP1 capable of conferring resistance to the inhibitors. Experiments that explored the relative sensitivity of GPs from naturally occurring filovirus species revealed that SudV GP was resistant to the antiviral activity of the compounds. Consistent with the hypothesis that NPC1-GP binding is like that of a receptor-virus interaction, we found that resistance mutations mapped to the previously identified RBD (Kuhn et al., 2006; Dube et al; 2009). Since the atomic resolution structures of the pre-fusion forms of both EboV GP and SudV GP had previously been solved (Lee et al., 2008; Dias et al., 2011; Bale et al., 2012), we were able to directly compare the impacts that residues 141 and 142 may have on the overall structure of the GPs. Residues 141 and 142 are located near the top outer edge of the GP1 RBD and are surface exposed after protease cleavage (Figure 3-10). Speculations regarding the impact that the mutations may have on GP are discussed below.

D. Structural analysis of resistance residues 141-142 in the GP1 RBD of EboV GP and SudV GP

Although the GPs of SudV and EboV have very similar structures overall, the region immediately after residues 141 and 142 exhibit a change in secondary structure. After these residues, Zaire GP continues to have a β-strand secondary structure that shares multiple hydrogen bonds with another strand in close proximity, which together form a continued parallel β-sheet. By contrast, after residues 141-142 in Sudan, both β-strands that form the β-sheet in Zaire become a random coil that no longer form

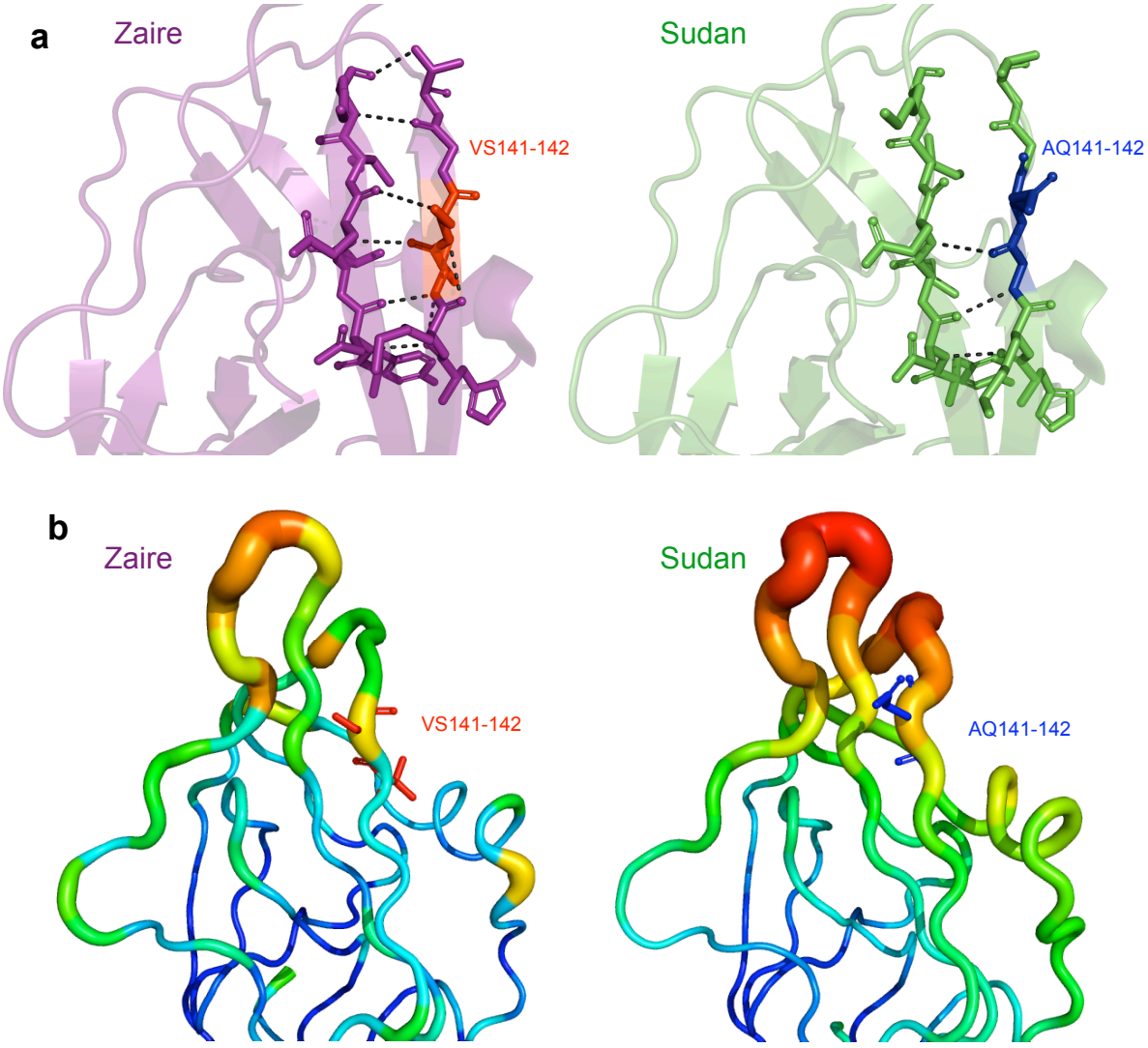

Figure 3-11. ***Sudan GP1 has fewer polar contacts between β7 and β8 after residues 141-142 and exhibits more thermodynamic mobility in these regions.*** **(a)** A model of the polar contacts between EboV-GP1 β7 and β9 (purple, left, PDB:3CSY) and SudV-GP1 β7 and β8 (green, right, PDB:3S88). SudV residues AQ141-142 that are associated with resistance are in blue and EboV residues VS141-142 that are associated with sensitivity are in red. Residues 109-114 and 139-144 are represented as sticks to illustrate polar contacts. **(b)** Comparison of thermal parameter distributions for the regions of SudV and EboV GP1s that are adjacent to residues 141-142. This is illustrated as a B-factor "putty" depicted on the structure from dark blue (lowest B-factor) to red (highest B-factor), with radius of the ribbon increasing from low to high B-factor.

hydrogen bonds with the adjacent strand (Figure 3-11a). The side-chain characteristics of the mutated residues appear to potentially have a direct consequence on the change in secondary structure, as replacement of Ser-142 in Zaire results in the loss of a side-chain hydrogen bond with the backbone carbonyl group of Glu-112, a bond unable to be formed by the rotamers of Gln-142 found in Sudan (Figure 3-11a). This loss of secondary structure in Sudan could account for the increase in flexibility of this region in SudV GP when compared to the relatively rigid structure of EboV GP, as seen in the relative B-factor values (or temperature factor), a measure of the thermal vibration of atoms in the protein crystal, for this portion of GP1 (Figure 3-11b). Indeed, recently published studies involving peptide amide hydrogen-deuterium exchange mass spectrometry, which measures the flexibility and solvent exposure of a peptide by quantifying of the exchange of deuterium in solvent water with the hydrogen bound to peptide amides, have indicated that some regions of SudV-GP1 show increased exchange of ions as compared to EboV-GP1, consistent with the observed B-factor values (Bale et al., 2011 and 2012). It is possible that the flexibility that is observed when AQ141-142 is present allows for the virus to overcome any steric hindrance that is provided by interaction of 3.47 with NPC1. Interestingly, residues 141 and 142 are located between two residues (K140 and G143) that are conserved amongst filoviruses and have been suggested to have an impact on GP binding (Brindley et al., 2007; Lee et al., 2008; Dube et al., 2009). However, the impact that these residues have on GP-NPC1 affinity must be interrogated for a full understanding of the resistance mechanism.

E. Revision of entry model based on inhibitor studies

Analysis of the EboV GP structure shows that the residues in the N-terminal domain of GP1 that mediate binding to the receptor (NPC1) are interspersed with the residues that make stabilizing contacts with GP2 (Lee et al., 2011). This structural feature is consistent with the possibility that binding of cleaved GP1 to NPC1 relieves the GP1-imposed constraints on GP2 and promotes virus fusion to the limiting membrane. The findings that NPC1 is directly labeled with the cross-linkable derivative of 3.47, that 3.47 disrupts binding of GP to NPC1 containing membranes, and that overexpression of NPC1 confers resistance to 3.47, suggests that EboV inhibitors target NPC1 in a manner that prevents the essential interaction between GP and NPC1. Additionally, chimeric analysis of GPs that are resistant to 3.47 inhibition localized resistance to two residues on the top of RBD that are exposed only after cathepsin cleavage, thus indicating that 3.47 directly targets this virus-receptor interaction (Figure 3-12). The role of cathepsin proteases in cleavage of GP1 to expose the NPC1 binding site during EboV infection is analogous to the role of CD4 in inducing a conformational change in gp120 to expose the co-receptor binding site during human immunodeficiency virus infection (Harrison, 2008). Additionally, the mode of action of compound 3.47 is analogous the CCR5 antagonist maraviroc, as 3.47 binding to NPC1 blocks association of the GP with the host-receptor (Dorr et al., 2005). These studies provide an example of how small molecules identified by screening and medicinal chemistry optimization can be used as molecular probes to analyze virus–host interactions.

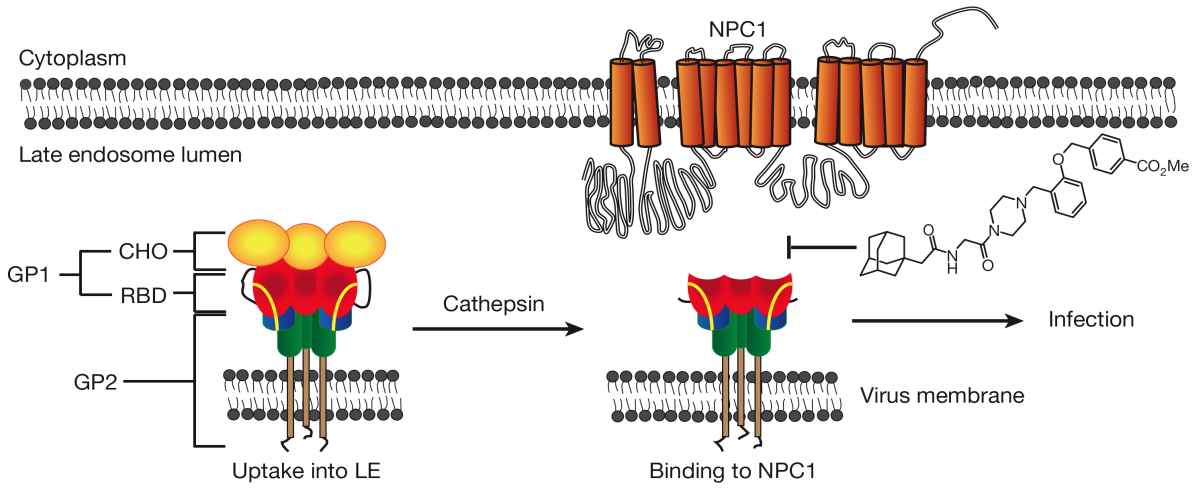

Figure 3-12. ***Revised model of EboV entry and action of 3.47.*** Following EboV uptake and trafficking to late endosomes, EboV GP is cleaved by cathepsin protease to remove heavily glycosylated domains (CHO) and expose the putative receptor binding domain (RBD) of GP1. Binding of cleaved GP1 to NPC1 is necessary for infection and is blocked by the EboV inhibitor 3.47.

Chapter 4

Discussion, Future Directions, and Conclusions

Discussion and Future Directions

A. State of the Ebola virus entry field

In the last seven years several important contributions have been made to the Ebola virus entry field that have begun to fill in long standing gaps in the knowledge of the EboV entry pathway. These contributions include the report of the atomic resolution structure of a pre-fusion EboV and SudV GP (Lee et al., 2008; Dias et al., 2011), live cell microscopy studies of EboV uptake and entry (Nanbo et al., 2010; Saeed et al., 2010), and the identification of essential host factors that function in the late endosome and/or lysosome (LE/LY) of cells to facilitate filovirus entry (Chandran et al., 2005; Schornberg et al., 2006; Carette et al., 2011; Cote et al., 2011). These studies have revealed a complicated multistep process that has continued to reveal new paradigms for how enveloped viruses utilize host factors to mediate productive entry events.

B. Ebola virus entry pathway

The Ebola virus glycoprotein, GP, is the only viral protein that is expressed on the surface of mature filovirus particles and is both necessary and sufficient for mediating viral entry into host cells (Takada et al., 1997; Wool-Lewis and Bates; 1998). GP mediates attachment to target cells, virus internalization, trafficking to an endosomal compartment, and fusion with the LE/LY of cells. Recent advances have provided clues as to how GP mediates the steps required for productive infection of target cells. The first step in entry is viral attachment, which is likely to occur through many redundant interactions, as no single factor has been identified that mediates this step in all

permissive cell types. Several different C-type lectins have been suggested to play a role in the initial attachment step and are believed to interact with the N- and O-linked glycans present on GP (Alvarez et al., 2002; Marzi et al., 2004; Lin et al., 2003; Matsuno et al.; 2010). These C-type lectins are expressed on macrophages and dendritic cells (DCs), key cell types for *in vivo* pathogensis (Geisbert et al., 2003), but not in other susceptible cell types; thus, suggesting a role for redundant attachment factors. Recently, the T-cell costimulatory molecule and phosphatidylserine receptor, TIM-1, was identified as a candidate cell surface receptor for EboV and MarV (Kondratowicz et al., 2011). This protein was shown to interact with EboV GP, enhance infection on weakly permissive cell lines, and may be important for infection of epithelial cells but not DCs or macrophages (Kondratowicz et al., 2011). The redundant nature of the interactions that mediate attachment leave a possibility for the identification of yet other proteins that mediate cell surface attachment, an important first step in virus entry.

After the initial step of virus attachment, EboV virions must be internalized and undergo trafficking through the endosomal pathway to the late endosomes and lysosomes (LE/LYs) of cells. Recent microscopy studies have reveled that particles are internalized through a macropinocytosis-like process that is strictly dependent on GP induced membrane ruffling (Nanbo et al., 2010; Saeed et al., 2010; Mulherkar et al., 2011). Following internalization, the virus is trafficked through the endosomal pathway to the late endosomal compartment where they colocalize with Rab7/LAMP-1 positive late endosomes, a trafficking event that is important for productive entry, as expression of a dominant-negative form of Rab7 is able to reduce viral infection (Saeed et al., 2010). Furthermore a number of other host factors and signaling networks involved in

maturation of the late endosome have been implicated in virus entry, including the phosphatidylinositol-3-kinase and the calcium-calmodulin signaling pathways, and the homotypic fusion and vacuole protein sorting (HOPS) complex (Saeed et al., 2008; Kolokoltsov et al., 2009; Carette et al., 2011).

In the LE/LY compartment, the EboV GP undergoes a series of structural changes mediated by host factors that are essential for viral fusion. Previous studies identified endosomal cysteine proteases, specifically cathepsin B, as essential host factors for EboV entry; these proteases mediate a GP cleavage event that both primes the trimer for fusion and reveals a receptor binding domain (RBD) that is believed to bind to an unknown receptor within the LE/LY of cells (Chandran et al., 2005; Schornberg et al., 2006; Kuhn et al., 2006; Dube et al., 2009; Kaletsky et al., 2007; Hood et al., 2010; Dube et al., 2010). In this thesis, we describe work that has contributed to the EboV entry model through the identification of the membrane protein Niemann-Pick C1 (NPC1) as the previously unidentified LE/LY receptor, and the finding that binding of protease cleaved GP to NPC1 is an essential step for virus entry.

C. The role of NPC1 as an essential host factor for Ebola virus entry

We identified NPC1 as an essential host factor for filovirus entry after following up on a cellular cholesterol accumulation phenotype that was induced by treatment of cells with small molecule inhibitors of EboV entry. The finding that NPC1 is essential for EboV entry has been corroborated by an independent genetic screen that was co-published with our paper (Carette et al., 2011) and by a recently published paper that isolated CHO cells resistant to EboV infection and identified a defective NPC1 as the

mediator of this phenotype (Haines et al., 2012). NPC1 is a large polytopic membrane protein that resides in the limiting membrane of the LE/LY where it functions as a cholesterol transport protein that facilitates the movement of LDL-derived cholesterol out of the LE/LY compartment (Kolter and Sandhoff, 2010; Ko et al., 2001). Through the use of a combination of cell lines defective in other aspects of the cholesterol transport pathway, siRNA knock down of the important components of this pathway, and cell lines that express the cholesterol transport defunct NPC1 point mutant P692S, we were able to demonstrate that EboV GP mediated infection requires NPC1 expression but does not require the cholesterol transport activity of NPC1.

By probing GP binding to NPC1 through a series of membrane binding and co-immunoprecipitation experiments, we show that GP associates with NPC1 only after it has undergone protease cleavage. Both unpublished data from our own lab and a recent study published by Miller et al. has confirmed these findings *in vitro* with a soluble version of the second luminal loop of NPC1, which they suggest is the key mediator of NPC1 dependent binding and entry, thus indicting that the interaction between NPC1 and EboV GP is a direct interaction (Miller et al., 2012). These findings support the hypothesis that cathepsin cleavage functions to remove a heavily glycosylated domain that masks the receptor binding site, as indicated by both atomic resolution structures of the mucin deleted GP, and cryo-electron microscopy of VLPs containing full length GP (Lee et al., 2008; Dias et al., 2011; Beniac et al., 2012).

The location of NPC1 in the limiting membrane of the late endosome makes it tempting to speculate that the NPC1-GP interaction may lead to productive fusion of the viral envelope with the limiting membrane of the LE/LY, thus, leading to delivery of the

nucleocapsid to the site of viral replication. Indeed, this model is supported by the atomic resolution structure of the pre-fusion conformation of the EboV-GP trimer, as the residues that have been suggested to make up the RBD appear to be interspersed with residues that stabilize the pre-fusion conformation of GP2 (Lee et al., 2008). By analogy to other class I fusion proteins, such as MLV and HIV, it is possible that the role of NPC1 during infection is like that of a “classic” receptor like the HIV co-receptor (Futura et al., 1998; Mkrtchyan et al., 2005) or like M-CAT for MLV (Albritton et al., 1989; Lavillette et al., 1998), where binding of the RBD to the receptor (in the case of EboV-NPC1) would trigger membrane fusion. However, it is important to note that with the current findings, we cannot rule out the possibility that other steps remain to be identified in the EboV entry pathway. Indeed, it remains fully possible that a more complex model explains the function of NPC1, a model in which an interaction with NPC1 may prepare the virus to undergo a subsequent, yet identified fusion-triggering step. Until we develop an *in vitro* fusion assay we cannot rule out the possibility that binding to NPC1 potentiates the GP for further cysteine protease cleavage or an interaction with another cellular host factor as has been proposed as potential triggers for membrane fusion (Wong et al., 2009; Brecher et al., 2012).

In order to begin to rigorously test the role of NPC1 function in EboV entry we must first set up a series of *in vitro* biochemical and structural assays. A highly detailed structural map of the EboV GP1 RBD bound to its NPC1 ligand is an essential step to understanding the ways in which the RBD binds to NPC1 and how the binding mutants K114A, K115A, and K140A may disrupt this interaction (Dube et al., 2009; Miller et al., 2012). At first, this seems to be a daunting task, given the hydrophobicity, complexity,

and size of the full length NPC1 protein. However, the difficulties in handling the full-length proteins can potentially be circumvented, as a soluble version of the second lumenal loop of NPC1 (soluble lumenal loop 2 or sLL2) appears sufficient to mediate binding to GP (J.M. unpublished data; Miller et al., 2012). Although an atomic resolution structure of the RBD bound to its NPC1 ligand would provide valuable insight into the manner in which the two proteins interact, we must also develop useful *in vitro* assays with which we can interrogate the role of each component of the entry pathway. To this end, our lab is pursuing the development of *in vitro* assays for EboV GP that are akin to the ones used to carefully dissect the ALV-A entry mechanism (Mothes et al, 2000; Smith and Cunningham, 2007; Delos et al., 2008). We should be able to take advantage of a recently developed liposome binding assay for soluble EboV GP trimer that measures the amount of fusion peptide association with liposomes (Brecher et al., 2012), and expand these studies to test for the effect of NPC1 on liposome association. We are also pursuing developing a liposome-virus fusion assay to measure if NPC1 alone or in combination with low pH and proteases is capable of mediating virion-liposome fusion. We will be able to use a recently described HR2 derived peptide (Miller et al., 2011) as a control in both of these experiments to assay for the formation of an extended intermediate and the fusion peptide mutant F535R to reveal the role that the fusion peptide insertion may have in these associations (Ito et al., 1999). Regardless of the exact molecular role that GP binding to NPC1 may play in virus entry, our findings have demonstrated that this interaction is an essential functional step in the entry process, and dissection of the molecular consequences of this interaction are key to understanding its role in entry.

D. Small molecule mediated inhibition of the GP-NPC1 interaction

This thesis describes the identification and characterization of chemical probes used to interrogate the interaction between GP and NPC1 in biochemical, functional, and genetic assays. In Chapter 3 informative derivatives of compound 3.0 were used as probes that help to establish that these compounds target NPC1 in a manner that prevents the binding of cleaved GP to NPC1 containing membranes. Compound 3.98, a photoactivatable derivative of 3.0 that contains a specific site for covalent labeling by click chemistry to enable target identification, crosslinked to NPC1 indicating a direct, though, not exclusive interaction with NPC1, as several other cellular proteins were labeled in CHO_{null} derived membranes. Furthermore, derivatives of 3.0 were able to inhibit binding of cleaved GP in the membrane binding assay in a dose dependent manner that closely correlated with the antiviral activities of the compounds, thus, suggesting that the interaction between cleaved EboV GP and NPC1 is important for virus entry. The functional importance of the interaction between NPC1 and protease cleaved GP was further corroborated by recent findings that mutations in the RBD known to attenuate Ebola virus infectivity result in a GP that binds with lower affinity to the NPC1 ligand and that overexpression of NPC1 can compensate for the low affinity interaction (Miller et al., 2012). Similarly, we found that overexpression of NPC1 mediated resistance to our compounds, but did not increase overall infectivity in these cells. Taken together these findings indicate that in certain cases, either decreased affinity of a mutant RBD for NPC1 or through an inhibitor mediated decrease in the

numbers of NPC1 that can mediate binding to the RBD, the NPC1-GP interaction can become the limiting step in virus entry, thus highlighting the importance of this step.

We have established that the 3.0 derived inhibitors are capable of blocking a NPC1-GP interaction that is essential for virus entry. However, the mechanism by which these compounds inhibit GP binding to NPC1 remains elusive. At least two models exist for the possible mechanism of action of the small molecule entry inhibitors; these compounds can act through a competitive or a non-competitive inhibition model. In a competitive inhibition model, the compounds would have to bind to and compete directly with the GP binding site on NPC1. This mechanism of inhibition would be analogous to the way in which derivatives of the endogenous chemokine RANTES interferes with the binding of CCR5 tropic HIV-1 gp120 with its co-receptor (Lederman et al., 2004). By contrast, the non-competitive model for small molecule inhibition would involve inhibitor binding to an allosteric binding site on NPC1, which could stabilize a conformation of NPC1 that is unable to bind to GP. This type of inhibition would be analogous to inhibition of HIV-1 by maraviroc and other non-competitive inhibitors of CCR5 co-receptor binding (Watson et al; 2005; Kondru et al., 2008; Garcia-Perez et al., 2011). Currently, we cannot distinguish between these two models of inhibition; however, recent findings that a sub-domain of NPC1 may be responsible for GP binding has made it possible to perform biochemical experiments that may be able to distinguish between these two models.

As mentioned above, recent work from our lab and others have found that LL2 of NPC1 is necessary and sufficient for binding to cleaved GP and that a soluble tagged version of this loop is able to pull down cleaved GP through co-immunoprecipitation,

suggesting a direct interaction between GP and the sLL2 (J.M. unpublished data; Miller et al., 2012). We can use a tagged-sLL2 and the soluble GP to interrogate the manner in which sLL2 binds to GP by using surface plasmon resonance (SPR) to quantitatively determine the dissociation constant (K_D) of GP with sLL2. Furthermore, if the inhibitors are able to disrupt co-immunoprecipitation of the cleaved GP trimer to sLL2 then this would indicate that we could use these compounds in similar SPR studies to quantitatively determine the effect of the inhibitors on the K_D between GP and sLL2, a method that has been used to measure the small molecule mediated disruption of the protein-protein interaction between cyclophilin A and cyclosporin A (Wear et al., 2005). Additionally, we are currently trying to use the crosslinkable derivative 3.98 to interrogate exactly where the inhibitors bind to NPC1. In these studies we are crosslinking 3.98 to NPC1 as was done in Chapter 3 and, then, using mass spectroscopy to identify exactly which residues on NPC1 contain the covalent modification. Once we have identified the key residues, we can then mutate those sites in NPC1 and investigate the impact that these sites have on EboV entry, EboV GP binding, and small molecule inhibition. If the sites for inhibitor binding lie within the LL2 and the subsequent mutagenesis reveals that these sites are key contributors to the binding affinity of GP for NPC1, then this would provide direct proof that the inhibitors are competitive inhibitors of binding. Conversely, if these experiments reveal that the target of 3.98 is outside of LL2 and the small molecule inhibitor is unable to disrupt binding of sLL2 to GP then it is likely that these inhibitors act in a non-competitive manner. Regardless of which model the inhibitors use to block GP association with NPC1, understanding the molecular basis with which resistant GPs bind to NPC1 in the

presence of compound should give us mechanistic insights into the manner in which GP1 engages with NPC1, and reveal possible ways in which the virus could overcome the inhibition of this potential therapeutic candidate.

Because EboV is a BSL4 pathogen, selecting for virus mutations that confer resistance to potential antiviral compounds in the context of full-length replication competent virus is both costly and potentially dangerous. Instead, we decided to look to the naturally occurring sequence variations within various filoviridae GPs to identify specific coding mutations that confer resistance to the compounds. We discovered that the SudV GP was resistant to compound 3.47 and, using a series of systematic chimeras, we were able to map the resistance to two residues (A141 and Q142) that are surface exposed after protease cleavage and located near the top outer edge of the GP1 RBD. Notably, these residues can also confer sensitivity to the compound, as replacing the residues with V141 and S142 from EboV could render SudV GP sensitive to 3.47. Whether or not these mutations lead to an overall change in the affinity of the mutant GP for a NPC1 ligand, thus making them either more or less capable of directly competing with the inhibitor for ligand binding, remains to be demonstrated. If resistant GPs demonstrate a greater binding affinity for NPC1 than their sensitive counterparts, this would indicate a resistance mechanism that has arisen from a direct mutant GP mediated competition with the inhibitor binding site, analogous to the HIV resistance mutations to PSC-RANTES (Dudley et al., 2009). By contrast, if the mutations in the RBD do not affect the overall affinity of the site for NPC1 but instead confer the capability to bind to an inhibitor bound conformation of NPC1, then these resistance mutations are likely to act in a non-competitive manner, a resistance mechanism that is

often seen in resistance mutations located in the V3 loop for HIV for the non-competitive family of CCR5 agonists such as Maraviroc and Vicriviroc (Tsibris et al., 2008). An *in vitro* binding affinity assay, like the SPR described above, must be developed to quantitatively measure the binding affinities of SudV GP, Ebo GP, and chimeric GPs in order to understand the molecular mechanism of resistance.

E. NPC1 as a potential therapeutic target

The studies described in this thesis have not only contributed to the Ebola virus entry field through the identification of NPC1 as an essential host factor for entry but they have also contributed to the very early stages of antiviral drug development. Through the identification and validation of NPC1-GP binding as a 'druggable' target, we have identified a potential starting point for the development of therapeutics for the treatment of EboV infection. Ebola is a virus for which control of outbreaks and treatment of patients is limited to isolation, containment, and palliative care for the patient, as no therapeutics or vaccines are currently available to prevent the spread of the virus. Though we will have a long way to go from the identification of a small molecule inhibitor of entry to the development of therapeutics that can treat infection, the data presented in this thesis can, at least, serve as a starting point for further optimization of potential inhibitors of entry. Our initial tests of the sensitivity of different filovirus species to the EboV inhibitors show that there is natural variability in how the virus may respond to the inhibitors. If we can gain structural insight into how the EboV and SudV RBD interact with NPC1 in the presence of inhibitors, then we can use these findings to rationally design a compound that has a broader range of activity against the

different filovirus GPs. We are currently trying to expand the 3.47 studies to include animal trials for pharmacokinetics and inhibition of EboV pathogenesis. If these entry inhibitors were ever to be used as actual therapeutics it would be important to combine them with inhibitors of other EboV proteins, such a the polymerase L proteins, to minimize resistance mutations, analogous to combination therapies for HIV and HCV. However, it is important to note that since Ebola virus produces an acute infection (2-21 days) rather than a chronic infection, the amount of time that a patient maybe exposed to therapy and that a virus has to mutate maybe significantly less than that of chronic infections like HIV or HCV. Although conclusions from evolutionary studies of EboV and MarbV must be approached with a great deal of caution due to the relatively low sample size of sequences, one study has estimated that rate of nonsynonymous mutations in the virus GP is about 100-fold lower than that of HIV or influenza (Suzuki and Gojobori, 1997), suggesting that the virus may be slightly less prone to acquiring resistant mutations.

Conclusions

Our work showing that NPC1 is essential for EboV entry has implications for the EboV entry field as well as virus entry in general. In our studies, we describe a mechanism for entry that involves a multi-step process that ultimately leads to productive infection. As we have continued to uncover each of the layers to the puzzle of how filoviruses get into their host cells, we are revealing new insights into how viruses use host factors to mediate virus entry. In 2005, our lab was the first to identify cathepsins as important entry host factors (Chandran et al., 2005). Follow up work and

an atomic resolution pre-fusion structure of EboV GP revealed that this cleavage event, which removes a heavily glycoslated immunoprotective domain, has the functional consequence of revealing the RBD. Subsequent studies of the role of cathepsins in entry of other enveloped viruses indicates that these endosomal proteases may have role in the entry of viruses such as Sars-CoV and Nipah/ Hendra virus, suggesting that endosomal proteases may have a more expansive role in enveloped virus entry than initially appreciated (Simmons et al., 2005; Huang et al., 2006; Pager and Dutch, 2005; Pager et al., 2006).

Our recent studies pick up where the story for the role of cathepsin inhibitors in EboV entry left off. In this work we go from a small molecule lead, identified by high-throughput screening, to discovering that the target of the compound is NPC1, and confirming that NPC1 binds to the post-cathepsin cleaved GP. Thus, we have simultaneously identified a novel host factor involved in virus entry while confirming that the factor is a potential therapeutic target. To our knowledge, this is the first example of an enveloped virus receptor that binds to its viral ligand in an intracellular compartment rather than at the cellular membrane. Given that several viruses require the low pH environment of the endosome, it will be interesting to see if other viruses have adopted this unique mechanism of protecting highly conserved RBDs. Although, there remain several unanswered questions in filovirus entry, these studies have gotten us one step closer to understanding the host triggers that mediate fusion, and one step closer to developing antiviral therapeutics to this deadly pathogen.

Appendix A

Materials and Methods

Methods Summary: Screening of small molecules was performed at the New England Regional Centers of Excellence for Biodefense and Emerging Infectious Diseases at Harvard Medical School. Infection was assayed using VSV pseudotyped viruses encoding GFP or luciferase. Experiments with native ebolavirus were performed under BSL-4 conditions at the United States Army Medical Research Institute for Infectious Diseases. Cells were infected with EboV Zaire-Mayinga GFP and growth was measured by mean fluorescence. EboV $GP_{\Delta TM}$ and SudV $GP_{\Delta TM}$ are derivatives of EboV GP or SudV GP in which the transmembrane domain has been replaced by a GCN4-derived trimerization domain followed by a His6 tag for purification. Late endosomes/lysosomes (LE/LY) were isolated by differential centrifugation and further purified by Percoll density gradient centrifugation. LE/LY were disrupted by incubation with methionine methyl ester and coated onto high binding ELISA plates. Following attachment, unbound LE/LY membranes were removed and plates were blocked. Bound membranes were incubated with the indicated amounts of native or thermolysin-cleaved EboV $GP_{\Delta TM}$ or SudV $GP_{\Delta TM}$ protein. Unbound $GP_{\Delta TM}$ protein was removed, membranes were washed and bound $GP_{\Delta TM}$ protein was recovered in SDS loading buffer and analyzed by immunoblot using GP1 antiserum. Where applicable, membranes were pre-incubated with 3.0, 3.47, 3.18 or vehicle prior to the addition of $GP_{\Delta TM}$. To analyze EboV $GP_{\Delta TM}$ binding to NPC1, LE/LY membranes were dissolved in 10mM CHAPSO, NPC1 was recovered by immunoprecipitation, and the immune complexes were analyzed by immunoblot probed with EboV GP1 antiserum.

Cell lines. Vero, 293T, HeLa (ATCC) and human fibroblasts (Gelsthorpe et al., 2008) (Coriell) were maintained in DMEM (Invitrogen) supplemented with 5% FetalPlex, 5% FBS (Gemini) or 10% FBS (HeLa, human fibroblasts). All CHO derived cell lines were grown as previously described (Millard et al., 2000; Millard et al., 2005). We have designated the CHO-K1 cell line as CHO_{wt}, CHO-M12 as CHO_{null}, CHO-wt8 as CHO_{NPC1}, and the CHO-derived cell lines expressing NPC1 mutants as CHO NPC1 P692S, CHO NPC1 L657F, and CHO NPC1 D787N. CHO/NPC1-1, designated here as CHO hNPC1, expresses high levels of human NPC1 (Millard et al., 2000). Human fibroblasts from patients with lysosomal storage disorders were obtained from Coriell and are designated in this study as follows: healthy donor fibroblasts (GM05659) as wt, Niemann-Pick disease type C2 patient fibroblasts (GM18429) as NPC2-, Niemann-Pick disease type C1 patient fibroblasts (GM17914) as NPC1-(A), Niemann-Pick disease type C1 patient fibroblasts (GM03123) as NPC1-(B), and Niemann-Pick disease type A patient fibroblasts (GM16195) as ASM-. Genotypes of each of patient derived fibroblasts are described in Figures 2-7 and 2-8.

Antibodies. Rabbit polyclonal anti-serum was raised against a peptide corresponding to residues 83 to 98 of ebolavirus Zaire Mayinga GP1 (TKRWGFRSGVPPKVVC). Antibodies to the following ligands were obtained commercially from the indicated manufacturer: anti-NPC1 (Abcam), anti-ORP5 (Abcam), anti-V-ATPase B1/2 (Santa Cruz), anti-AC (BD Biosciences), anti-Alix (Biolegend), and anti-Alexa Fluor 488 (Invitrogen). Anti-ASM 1H7 was a gift from Genzyme. The monoclonal antibody against BMP was a kind gift from Toshihide Kobayashi.

Expression plasmids. Mucin domain-deleted EboV Zaire Mayinga GP (EboV GP) and VSV G were previously described (Chandran et al., 2005). Plasmids encoding Côte d'Ivoire-Ivory Coast GP, Sudan-Boniface GP, Reston-Penn. GP and Marburg-Musoke GP were obtained from Anthony Sanchez and the mucin domain-deleted (ΔMuc) derivatives were created: ZaireΔMuc GP (Δa.a. 309-489), Côte d'IvoireΔMuc GP (Δa.a. 310-489), SudanΔMuc GP (Δa.a. 309-490), and RestonΔMuc GP (Δa.a. 310-490). Bundibungyo-Uganda viral RNA was Trizol extracted and PCR used to generate a construct that expresses a mucin-deleted GP (Δa.a. 309-489). This PCR added a silent Xba I site at the deletion site in each GP. A plasmid encoding Lassa fever virus GP1 was kindly provided by Gary Nabel. A codon-optimized sequence encoding GP2 was generated and combined with the GP1 sequence in pCAGGS to complete a GP expression vector.

Production and purification of pseudotyped virions. VSV-ΔG pseudotyped viruses were created as described previously (Chandran et al., 2005). LacZ-encoding retroviral pseudotypes bearing the designated envelope glycoproteins were prepared as previously described (Soneoka et al., 1995).

Thermolysin digestion of virus and $GP_{\Delta TM}$. Purified EboV $GP_{\Delta TM}$ (50μg/mL) or VSV particles pseudotyped with EboV GP were incubated at 37°C for 1 hour with the metalloprotease thermolysin (Sigma, 0.2mg/ml) in NT buffer (10 mM Tris.Cl [pH 7.5], 135 mM NaCl). The reaction was stopped using 500 mM Phosphoramidon (Sigma) at 4°C. Cleaved EboV $GP_{\Delta TM}$ was stored in phosphate buffered saline supplemented with

1 mM EDTA, 1 mM PMSF (Sigma) and 1X EDTA-Free Complete Protease Inhibitor Cocktail (Roche). Digestions of purified SudV $GP_{\Delta TM}$ (50mg/mL) or VSV particles pseudotyped with SudV GP were carried out exactly as described for EboV GP except that the time of incubation with thermolysin was only 30 minutes because SudV GP seems to be more sensitive to protease cleavage.

Infection assays with pseudotyped virus. VSV pseudotyped viruses expressing GFP were added to cells in serial 10-fold dilutions and assayed using fluorescence microscopy. An infectious unit (i.u.) is defined as one GFP-expressing cell within a range where the change in GFP-positive cells is directly proportional to the virus dilution. For VSV expressing the luciferase reporter, pseudotyped virus was added to cells and luciferase activity was assayed 6-20 hours post-infection using the firefly luciferase kit (Promega). Signal was measured in relative luminescence units (RLU) using an EnVison plate reader (Perkin Elmer). In experiments involving inhibitors, stock solutions of 3.0 (20mM), 3.47 (10mM), 3.18 (10mM), 3.98 (10mM) and 3.0 (-) amine (10mM) in DMSO were diluted to a final concentration of 1% DMSO in media. All other inhibitors tested were dissolved into DMSO to make stock solutions of 20mM. Inhibitory activity was stable in the media of cultured cells for >72hours as assessed using single cycle entry assays. Infection of target cells with LacZ-encoding retroviral pseudotypes was performed in the presence of 5 mg/ml polybrene (Sigma). Seventy-two hours post-infection, cells were stained for LacZ activity and titer was determined by counting positive foci and expressed as focus forming units (FFU) per ml of virus.

Ebolavirus infections under BSL-4 conditions. Vero cells or CHO cells were seeded to 96-well plates and exposed to EboV-GFP (Towner et al., 2005). For experiments investigating the growth of virus on CHO_{wt}, CHO_{Null}, and CHO_{NPC1} cells, virus was added to CHO cells at a moi of 1 (as measured on Vero cells). For experiments accessing the antiviral activity of our compounds against replication competent EboV, Vero cells were incubated with 3.0 (40 mM), 3.47 (40 mM), E-64-d (150 mM) or 1% DMSO 90 minutes prior to the addition of virus (moi=0.1). Virus-encoded GFP fluorescence was determined using a SpectraMax M5 plate reader (Molecular Devices) at Ex 485nm, Em 515nm, cutoff 495nm at 22.5, 42, 71 and 97 hours post-infection.

Screen for Ebola virus entry inhibitors. Screening of small molecules was performed at the New England Regional Centers of Excellence for Biodefense and Emerging Infectious Diseases at Harvard Medical School. Vero cells were seeded in 384-well plates at a density of $5x10^4$ cells per well using a Matrix WellMate (Thermo Scientific). The BIOMOL ICCB Known Bioactives1, NINDS Custom Collection, ChemBridge3, ChemDiv4, ChemDiv5 and Enamine2 compound libraries were transferred by robotics to the assay plates using stainless steel pin arrays. The compounds were screened at a constant dilution to achieve a final concentration between 10mM and 60mM. After incubation for 2 hours at 37 °C, viruses were dispensed into each well (moi =1) and incubated for an additional 6 hours to allow virus gene expression. Cells were lysed by addition of Steady-Glo (Promega) and after 10 minutes at room temperature luminescence was measured using an EnVision plate reader. Each compound was tested in duplicate. Candidate compounds that inhibited EboV GP infection by more

than 80% were analyzed for potency, selectivity and absence of cytotoxicity (using Cyto-Tox assay, Promega) and 3.0 (2-((3r,5r,7r)-adamantan-1-yl)-N-(2-(4-benzylpiperazin-1-yl)-2-oxoethyl)acetamide) was identified. Other compounds also identified from the small molecule screen include 4.0, 5.0, 6.0, 7.0, 8.0 and their structures are given in Table 2-1. The bioactive screen identified tamoxifen (Sigma), alverine (Sigma), sertraline (Sigma), and U18666A (Cayman Chemical) as antiviral compounds. The antiviral activity of the inhibitors was verified on human cells (HeLa, A549, 293T), mouse embryonic fibroblasts, and Chinese hamster ovary cells.

Virus pre-incubation experiments with EboV inhibitors. Vero cells were seeded onto 12-well cell culture plates. Compounds 3.47 (1μM), 4.0 (10μM), 5.10 (2μM), 6.0 (1μM), 7.0 (2μM), 8.0 (10μM) and a vehicle control (DMSO) were added to cells or virus (VSV-GFP EboV GP or EboV GP_{THL}) in the following three manners. Cells were pre-treated with media containing the inhibitors at 37°C for two hours prior to infection and virus was added to the cells in the presence of the inhibitor. Virus and inhibitors were added to cells simultaneously and inhibitors remained on the cells during infection. Virus was pre-incubated with the inhibitors in a small volume at 37°C for two hours before the addition of the mixture to the cells. The mixture was diluted 100x when added to the cells. GFP-positive cells were counted 18 hours post-infection and infectivity was calculated relative to cells exposed to DMSO vehicle alone.

Inhibitor time of removal assays. Vero cells were incubated for one hour at 37°C with compounds 3.0, 4.0 , 5.0, 6.0, 7.0, 8.0 (20 μM), the lysosomatropic agent

ammonium chloride (NH_4Cl, 30mM), or vehicle control (DMSO). Cells were then cooled to 25°C and VSV-GFP EboV-GP virus was added to allow the particles to bind in the presence of compounds. Cells were incubated with virus and inhibitors for 30 minutes at 25°C. Wells were washed 2x with PBS to remove unbound virus and media containing the inhibitor was added back to the wells. Infection was initiated by raising the temperature to 37°C. At the indicated times post infection, media containing the compounds was replaced with media containing no inhibitors. GFP-positive cells were counted 18 hours post-infection. Infectivity is reported as percent GFP-positive cells relative to cells exposed to DMSO vehicle alone.

Inhibitor time of addition assays. Vero cells were exposed to VSV-GFP EboV GP for 30 minutes at room temperature. Wells were then washed 2x with PBS to remove unbound virus, and infection was initiated by raising the temperature to 37°C. Media was replaced with inhibitor containing media at the indicated times post-infection. Concentrations of compounds and measurement of infectivity are the same as in the washout experiments described above.

LysoTracker Red accumulation assay. Vero cells were grown on Lab-Tek (Thermo) chamber-slides. Cells were incubated for one hour with media containing the following compounds at their antiviral IC99, 3.0 (20μM), 4.0 (10μM), 5.0 (10μM), 6.0 (5μM), 7.0 (5μM), 8.0 (20μM), chloroquine (20μM), NH_4Cl (10mM) or vehicle control (DMSO) at 37°C. The known lysosomatropic agents chloroquine and NH_4Cl were used as positive controls for endosomal pH disruption. The cells were exposed to 100 nM of

LysoTracker Red (Invitrogen) and Hoechst stain (500ng/mL) in the continued presence of the compounds for ten minutes at 37°C. Images of stained cells were obtained using epifluorescence microscopy (Nikon Eclipse TE2000U). The images were processed using ImageJ software.

Synthesis of 3.0 derivatives. Compound 3.47 (methyl 4-((2-((4-(2-(2-((3r,5r,7r)-adamantan-1-yl)acetamido)acetyl)piperazin-1-yl)methyl)phenoxy)methyl)benzoate) was prepared via a multi-step synthesis starting from N-Cbz-piperazine. Thus, coupling of N-Cbz-piperazine with N-Boc-glycine followed by removal of the Boc group under acidic conditions yielded 4-Cbz-piperazine glycinamide. After acylation of the terminal amine with adamantan-1-acetyl chloride, the Cbz group was removed by hydrogenolysis to give (1-(adamantan-1-yl)acetamido)acetyl)piperazine. The piperazine was then benzylated via reductive amination with 2-(4-methoxycarbonyl)benzyloxybenzaldehyde using sodium triacetoxyborohydride to provide 3.47. Compound 3.18 and 3.0 (-) amine was synthesized in a similar fashion. Compound 3.98 was prepared via a multi-step synthesis as follows. First, 2-hydroxy-5-nitrobenzaldehyde was alkylated by 4-ethynylbenzyl bromide in the presence of potassium carbonate in DMF. Resulting benzyloxy aldehyde underwent reductive amination with 2-((3r,5r,7r)-adamantan-1-yl)-*N*-(2-oxo-2-(piperazin-1-yl)ethyl)acetamide using sodium triacetoxyborohydride. The nitro group was then reduced to aniline ($SnCl_2$), diazotized ($NaNO_2$), and the diazonium finally converted to azide to yield 3.98.

Protease inhibitors and protease activity assays. The measurement of cathepsin B activity and the use of the inhibitor CA074 (Sigma) have been previously described (Chandran et al., 2005).

Detection of intracellular cholesterol. Cells were stained with filipin (50 μg/ml, Cayman Chemical) as previously described (Millard et al., 2005). Images of stained cells were obtained using epifluorescence microscopy (Nikon Eclipse TE2000U). The images were processed using ImageJ software.

Production and purification of EboV and SudV $GP_{\Delta TM}$ soluble protein. EboV $GP_{\Delta TM}$ is a derivative of the mucin-deleted EboV Zaire-Mayinga GP in which the transmembrane domain and C-terminus (a.a. 657-676) has been replaced by a GCN4-derived trimerization domain (MKQIEDKIEEILSKIYHIENEIARIKKLIGEV) and a His6 tag. An expression vector encoding a mucin-deleted SudV $GP_{\Delta TM}$ that is fused to GCN4 trimerization/His tag was also prepared (residues 1-309,491-657). The expression plasmid encoding EboV or SudV $GP_{\Delta TM}$ was transfected into 293T cells using lipofectamine2000. Eighteen to twenty-four hours later the culture medium was replaced with 293SFMII (Invitrogen) supplemented with 1X non-essential amino acids and 2 mM $CaCl_2$ and harvested daily for four days. Media containing soluble $GP_{\Delta TM}$ was filtered and PMSF (1 mM)/ 1X EDTA-Free Complete Protease Inhibitor Cocktail was added. $GP_{\Delta TM}$ was purified by affinity chromatography using Ni-NTA agarose beads (Qiagen), dialyzed against PBS using a 3kDa dialysis cartridge (Pierce) and stored at -80^{o}C. Purity and integrity of EboV and SudV $GP_{\Delta TM}$ were analyzed by SDS-PAGE.

Membrane Binding Assay. Indicated cells were washed with PBS x2, scraped in homogenization (HM) buffer (0.25 M sucrose, 1 mM EDTA, 10 mM Hepes pH7.0), and disrupted with a Dounce homogenizer. Nuclei and debris were pelleted by centrifugation at 1000 x g for 10 min. The post-nuclear supernatant was centrifuged at 15000 x g for 30 min at 4°C and the pellet, containing the LE/LY, was resuspended in a total volume of 0.9ml composed of 20% Percoll (Sigma) and 0.4% BSA (Sigma) in HM and centrifuged at 36000 x g for 30 min at 4°C. Fractions (0.150 ml) were collected from the bottom to the top of the tube and those containing the highest β-N-acetylglucosamidase activity, as assessed by release of 4-methylumbelliferone from 4-methylumbellifferyl-N-acetyl-b-D-glucosaminide (Sigma), were pooled and incubated in 20mM methionine methyl-ester (Sigma) for 1 hour at room temperature. Following LE/LY disruption, 1 X EDTA-Free Complete Protease Inhibitor Cocktail and 1 mM PMSF was added. The amount of purified LE/LY membranes used for the binding assay was normalized using the activity of the marker β-N-acetylglucosamidase and validated by immunoblot using V-ATPase B1/2 antibody.

Disrupted LE/LY membranes were coated on high-binding ELISA plates (Corning) overnight at 4°C. Unbound membranes were removed and wells containing bound membranes were blocked for 2 hours at room temperature with binding buffer (PBS, 5% FBS, 1 mM PMSF, 1mM EDTA, 1X Complete Protease Inhibitor Cocktail). The indicated amount of purified EboV $GP_{\Delta TM}$, pretreated or not with thermolysin, was added to each well in binding buffer and incubated for 1 hour at room temperature. Unbound proteins were removed and wells were washed 3 times with PBS. Membrane bound EboV $GP_{\Delta TM}$ was solubilized in SDS-loading buffer. Bound and unbound EboV

$GP_{\Delta TM}$ were detected by immunoblot using the EboV GP1 anti-serum, which recognizes an epitope an in GP1 that is conserved for all Ebola virus species. For binding assays in the presence of inhibitors, the immobilized membranes were pre-incubated at room temperature with the inhibitor or vehicle (10% DMSO) in binding buffer. After 30 minutes, thermolysin cleaved EboV or SudV $GP_{\Delta TM}$ was added in the continued presence of compound and bound and unbound or input GP was measured as described above.

Co-Immunoprecipitation. CHO_{null} and CHO_{hNPC1} cells were homogenized as described above. The 15000 x g membrane pellet was resuspended in HM buffer and protein content was measured using the BCA assay (Pierce). The LE/LY membranes contained in the 15000 x g resuspended pellet were disrupted by incubation with 20 mM methionine methyl-ester for 1 hour at RT. Membranes of equal protein content were incubated with indicated amounts of EboV $GP_{\Delta TM}$, pre-treated or not with thermolysin, for 1 hour at RT in the presence of Complete Protease Inhibitor Cocktail (Roche) and incubated for an additional hour on ice before the addition of membrane lysis buffer (12.5mM CHAPSO, 150mM NaCl, 1mM EDTA, 10mM Tris/HCl pH7.4) for a final concentration of 10mM CHAPSO. Proteins were solubilized on ice for 20 min and debris was removed by centrifugation at 12000 x g for 10 min at 4°C. The soluble membrane lysates were incubated with anti-NPC1 antibody for 1 hour at 4°C and then incubated with Protein A-agarose beads (Sigma) for an additional 4 hours at 4°C. Beads were then washed 3 times with 8mM CHAPSO, 150 mM NaCl, 1mM EDTA, 10 mM Tris/HCl pH7.4 and immunoprecipitated product was eluted by incubation in 0.1M glycine pH 3.5

for 5 min at RT. The eluted complex was then neutralized and analyzed by immunoblot using the indicated antibody.

Photoactivation and click chemistry. Photoactivation and click chemistry were performed as described previously with some modifications (Ban et al., 2010). CHO_{null} and CHO hNPC1 were homogenized in HM buffer as described above. Membranes in the 15,000g pellet were used without further purification and protein concentration was determined using the BCA protein quantification assay (Pierce). Membranes (250µg of protein content) were incubated with 25µM of 3.98 for 10min at room temperature, UV-exposed for 1min on ice, and centrifuged at 15,000g for 30min at 4°C. Membranes were then lysed in lysis buffer (1% Triton X-100, 0.1% NP-40, 150mM NaCl, 0.4mM EDTA, 50mM Tris pH 8.0) containing protease inhibitors (Roche). Lysates were pre-cleared by centrifugation at 10,000g for 10min at 4°C and the soluble proteins were used in the click chemistry reaction.

For labeling of the whole membrane lysates, 50ug of protein was used for the click reaction of 3.98 with 20µM of Alexa Fluor 488 azide (Invitrogen) using the Click-iT Protein Buffer Reaction Kit (Invitrogen). Proteins were precipitated in methanol/chloroform/water (60:15:40), washed in methanol, dried, and resuspended in sample buffer prior to analysis by immunoblot. Labeled proteins were assayed using an anti-Alexa Fluor 488 antibody (Invitrogen) and an anti-NPC1 antibody was used for detection of NPC1 in membrane lysates.

For analysis of NPC1 labeling, 200ug of proteins were incubated with 80µM of Alexa Fluor 488 azide, 7.5µM ascorbic acid, and 1.5µM copper sulfate for 30 min at

room temperature. NPC1 was purified by immunoprecipitation using anti-NPC1 (Abcam) and protein A-agarose beads (Sigma). The immunoprecipitate was eluted from the beads using 0.1M glycine pH3.5 for 5min at room temperature. Samples were neutralized before the addition of the sample buffer for immunoblot analysis using an anti-Alexa Fluor 488 antibody (Invitrogen) to detect labeled purified NPC1 and an anti-NPC1 antibody to access success of the pull-down.

Creating chimeric SudV and EboV GPs. EboV GP1-SudV GP2 and SudV GP1-EboV GP2 chimeras were generated by restriction digestion of the pCAGGS plasmids encoding the mucin-deleted versions of the parental proteins with Xba I (New England Biolabs) to liberate GP1 and GP2 containing fragments for each virus GP. The fragments were gel purified and ligated using T4 DNA ligase (New England Biolabs). Chimeras of the GP1 functional domains were created using overlapping PCR to create fusion proteins of SudV and EboV GP1 at the appropriate junctions. $Z_{90}S$ encodes for a SudV GP whose first 90 AA have replaced with AA 1-90 from EboV GP. The inverse is true for $S_{90}Z$. For the internal GP1 chimeric domain proteins the indicated fragment from the donor GP is placed within the context of the receiving GP. For example, $Z(S_{90\text{-}213})$, $Z(S_{90\text{-}189})$, and $Z(S_{90\text{-}149})$ each encode for an EboV GP where amino acids 90-213, 90-189, and 90-149, respectively, are replaced with the corresponding residues from the SudV GP. Chimeric swaps of one or two amino acid residues between the SudV RBD and EboV RBD were also created using overlapping PCR to introduce the new amino acids at the appropriate site. All GPs were then were cloned into expression vectors

using standard molecular biology techniques. All vectors were verified by DNA sequencing.

Assay for BMP involvement in EboV entry. Vero cells were plated in a 96-well plate and grown overnight with 5 or 50 μg/ml of an antibody directed against BMP or a mouse monoclonal IgG isotype control (Santa Cruz). After 24 hours, the cells were infected VSV particles encoding GFP pseudotyped with EboV GP, VSV G, or Junin GP in the continued presence of antibody. After 24 hours cells were either counted for GFP-positive cells or were washed, fixed (4% paraformadehyde in PBS), and stained with a Cy3-anti-mouse secondary antibody to assay for uptake of the BMP specific antibody into treated cells. Virus infection is reported as percent of GFP-positive cells relative to cells exposed to the isotype control antibody.

Appendix B

References

References

Alakoskela J-M, Vitovic P, Kinnunen PKJ. (2009). Screening for the drug-phospholipid interaction: correlation to phospholipidosis. ChemMedChem **4**,1224-51.

Albritton LM, Kim JW, Tseng L, Cunningham JM. (1993). Envelope-binding domain in the cationic amino acid transporter determines the host range of ecotropic murine retroviruses. J Virol **67**,2091-6.

Albritton LM, Tseng L, Scadden D, Cunningham JM. (1989). A putative murine ecotropic retrovirus receptor gene encodes a multiple membrane-spanning protein and confers susceptibility to virus infection. Cell **57**,659-66.

Alpy F, Stoeckel ME, Dierich A, Escola JM, Wendling C, Chenard MP, Vanier MT, Gruenberg J, Tomasetto C, Rio MC. (2001). The steroidogenic acute regulatory protein homolog MLN64, a late endosomal cholesterol-binding protein. J Biol Chem **276**,4261-9.

Alvarez CP, Lasala F, Carrillo J, Muñiz O, Corbí AL, Delgado R. (2002). C-type lectins DC-SIGN and L-SIGN mediate cellular entry by Ebola virus in cis and in trans. J Virol **76**,6841-4.

Anderson N, Borlak J. (2006). Drug-induced phospholipidosis. FEBS Lett **580**,5533-40.

Bale S, Dias JM, Fusco ML, Hashiguchi T, Wong AC, Liu T, Keuhne AI, Li S, Woods VL, Chandran K and others. (2012). Structural basis for differential neutralization of ebolaviruses. Viruses **4**,447-70.

Bale S, Liu T, Li S, Wang Y, Abelson D, Fusco M, Woods VL, Saphire EO. (2011). Ebola virus glycoprotein needs an additional trigger, beyond proteolytic priming for membrane fusion. PLoS Negl Trop Dis **5**,e1395.

Ban HS, Shimizu K, Minegishi H, Nakamura H. (2010). Identification of HSP60 as a primary target of o-carboranylphenoxyacetanilide, an HIF-1alpha inhibitor. J Am Chem Soc **132**,11870-1.

Barnett AL, Davey RA, Cunningham JM. (2001). Modular organization of the Friend murine leukemia virus envelope protein underlies the mechanism of infection. Proc Natl Acad Sci USA **98**,4113-8.

Barrientos LG, Rollin PE. (2007). Release of cellular proteases into the acidic extracellular milieu exacerbates Ebola virus-induced cell damage. Virology **358**,1-9.

Beniac DR, Melito PL, Devarennes SL, Hiebert SL, Rabb MJ, Lamboo LL, Jones SM, Booth TF. (2012). The organisation of Ebola virus reveals a capacity for

extensive, modular polyploidy. PLoS ONE **7**,e29608.

Blom TS, Linder MD, Snow K, Pihko H, Hess MW, Jokitalo E, Veckman V, Syvänen A-C, Ikonen E. (2003). Defective endocytic trafficking of NPC1 and NPC2 underlying infantile Niemann-Pick type C disease. Hum Mol Genet **12**,257-72.

Bosch V, Pawlita M. (1990). Mutational analysis of the human immunodeficiency virus type 1 env gene product proteolytic cleavage site. J Virol **64**,2337-44.

Brindley MA, Hughes L, Ruiz A, McCray PB, Sanchez A, Sanders DA, Maury W. (2007). Ebola virus glycoprotein 1: identification of residues important for binding and postbinding events. Journal of Virology **81**,7702-9.

Brown MS, Goldstein JL. (1986). A receptor-mediated pathway for cholesterol homeostasis. Science **232**,34-47.

Bullough PA, Hughson FM, Skehel JJ, Wiley DC. (1994). Structure of influenza haemagglutinin at the pH of membrane fusion. Nature **371**,37-43.

Carette JE, Raaben M, Wong AC, Herbert AS, Obernosterer G, Mulherkar N, Kuehne AI, Kranzusch PJ, Griffin AM, Ruthel G and others. (2011). Ebola virus entry requires the cholesterol transporter Niemann-Pick C1. Nature.

Chandran K, Sullivan NJ, Felbor U, Whelan SP, Cunningham JM. (2005). Endosomal proteolysis of the Ebola virus glycoprotein is necessary for infection. Science **308**,1643-5.

Chen J, Lee KH, Steinhauer DA, Stevens DJ, Skehel JJ, Wiley DC. (1998). Structure of the hemagglutinin precursor cleavage site, a determinant of influenza pathogenicity and the origin of the labile conformation. Cell **95**,409-17.

Chernomordik LV, Kozlov MM. (2003). Protein-lipid interplay in fusion and fission of biological membranes. Annual review of biochemistry **72**,175-207.

Chevallier J, Chamoun Z, Jiang G, Prestwich G, Sakai N, Matile S, Parton RG, Gruenberg J. (2008). Lysobisphosphatidic acid controls endosomal cholesterol levels. J Biol Chem **283**,27871-80.

Choe H, Farzan M, Sun Y, Sullivan N, Rollins B, Ponath PD, Wu L, Mackay CR, LaRosa G, Newman W and others. (1996). The beta-chemokine receptors CCR3 and CCR5 facilitate infection by primary HIV-1 isolates. Cell **85**,1135-48.

Côté M, Misasi J, Ren T, Bruchez A, Lee K, Filone CM, Hensley L, Li Q, Ory D, Chandran K and others. (2011). Small molecule inhibitors reveal Niemann-Pick C1 is essential for Ebola virus infection. Nature.

Dalgleish AG, Beverley PC, Clapham PR, Crawford DH, Greaves MF, Weiss RA. (1984). The CD4 (T4) antigen is an essential component of the receptor for the AIDS retrovirus. Nature **312**,763-7.

Davey RA, Hamson CA, Healey JJ, Cunningham JM. (1997). In vitro binding of purified murine ecotropic retrovirus envelope surface protein to its receptor, MCAT-1. J Virol **71**,8096-102.

Deffieu MS, Pfeffer SR. (2011). Niemann-Pick type C 1 function requires lumenal domain residues that mediate cholesterol-dependent NPC2 binding. Proc Natl Acad Sci USA **108**,18932-6.

Delos SE, Brecher MB, Chen Z, Melder DC, Federspiel MJ, White JM. (2008). Cysteines flanking the internal fusion peptide are required for the avian sarcoma/leukosis virus glycoprotein to mediate the lipid mixing stage of fusion with high efficiency. J Virol **82**,3131-4.

Deng H, Liu R, Ellmeier W, Choe S, Unutmaz D, Burkhart M, Di Marzio P, Marmon S, Sutton RE, Hill CM and others. (1996). Identification of a major co-receptor for primary isolates of HIV-1. Nature **381**,661-6.

Devlin C, Pipalia NH, Liao X, Schuchman EH, Maxfield FR, Tabas I. (2010). Improvement in lipid and protein trafficking in Niemann-Pick C1 cells by correction of a secondary enzyme defect. Traffic **11**,601-15.

Dias JM, Kuehne AI, Abelson DM, Bale S, Wong AC, Halfmann P, Muhammad MA, Fusco ML, Zak SE, Kang E and others. (2011). A shared structural solution for neutralizing ebolaviruses. Nat Struct Mol Biol **18**,1424-7.

Dorr P, Westby M, Dobbs S, Griffin P, Irvine B, Macartney M, Mori J, Rickett G, Smith-Burchnell C, Napier C and others. (2005). Maraviroc (UK-427,857), a potent, orally bioavailable, and selective small-molecule inhibitor of chemokine receptor CCR5 with broad-spectrum anti-human immunodeficiency virus type 1 activity. Antimicrobial Agents and Chemotherapy **49**,4721-32.

Dragic T, Litwin V, Allaway GP, Martin SR, Huang Y, Nagashima KA, Cayanan C, Maddon PJ, Koup RA, Moore JP and others. (1996). HIV-1 entry into CD4+ cells is mediated by the chemokine receptor CC-CKR-5. Nature **381**,667-73.

Du X, Kumar J, Ferguson C, Schulz TA, Ong YS, Hong W, Prinz WA, Parton RG, Brown AJ, Yang H. (2011). A role for oxysterol-binding protein-related protein 5 in endosomal cholesterol trafficking. J Cell Biol **192**,121-35.

Dube D, Brecher MB, Delos SE, Rose SC, Park EW, Schornberg KL, Kuhn JH, White JM. (2009). The Primed Ebolavirus Glycoprotein (19-Kilodalton GP1,2): Sequence and Residues Critical for Host Cell Binding. Journal of Virology

83,2883-2891.

Dube D, Schornberg KL, Shoemaker CJ, Delos SE, Stantchev TS, Clouse KA, Broder CC, White JM. (2010). Cell adhesion-dependent membrane trafficking of a binding partner for the ebolavirus glycoprotein is a determinant of viral entry. Proc Natl Acad Sci USA **107**,16637-42.

Dudley DM, Wentzel JL, Lalonde MS, Veazey RS, Arts EJ. (2009). Selection of a simian-human immunodeficiency virus strain resistant to a vaginal microbicide in macaques. J Virol **83**,5067-76.

Duvvuri M, Konkar S, Funk RS, Krise JM, Krise JP. (2005). A chemical strategy to manipulate the intracellular localization of drugs in resistant cancer cells. Biochemistry **44**,15743-9.

Feng Y, Broder CC, Kennedy PE, Berger EA. (1996). HIV-1 entry cofactor: functional cDNA cloning of a seven-transmembrane, G protein-coupled receptor. Science **272**,872-7.

Furuta RA, Wild CT, Weng Y, Weiss CD. (1998). Capture of an early fusion-active conformation of HIV-1 gp41. Nat Struct Biol **5**,276-9.

Garcia-Perez J, Rueda P, Alcami J, Rognan D, Arenzana-Seisdedos F, Lagane B, Kellenberger E. (2011). Allosteric model of maraviroc binding to CC chemokine receptor 5 (CCR5). J Biol Chem **286**,33409-21.

Geijtenbeek T, Kwon DS, Torensma R, van Vliet SJ, van Duijnhoven GC, Middel J, Cornelissen IL, Nottet HS, KewalRamani VN, Littman DR and others. (2000). DC-SIGN, a dendritic cell-specific HIV-1-binding protein that enhances trans-infection of T cells. Cell **100**,587-97.

Geisbert TW, Hensley LE, Larsen T, Young HA, Reed DS, Geisbert JB, Scott DP, Kagan E, Jahrling PB, Davis KJ. (2003). Pathogenesis of Ebola hemorrhagic fever in cynomolgus macaques: evidence that dendritic cells are early and sustained targets of infection. Am J Pathol **163**,2347-70.

Geisbert TW, Jahrling PB. (2004). Exotic emerging viral diseases: progress and challenges. Nat Med **10**,S110-21.

Gelsthorpe ME, Baumann N, Millard E, Gale SE, Langmade SJ, Schaffer JE, Ory DS. (2008). Niemann-Pick type C1 I1061T mutant encodes a functional protein that is selected for endoplasmic reticulum-associated degradation due to protein misfolding. J Biol Chem **283**,8229-36.

Haines KM, Vande Burgt NH, Francica JR, Kaletsky RL, Bates P. (2012). Chinese hamster ovary cell lines selected for resistance to ebolavirus glycoprotein

mediated infection are defective for NPC1 expression. Virology **432**,20-8.

Hanumegowda UM, Wenke G, Regueiro-Ren A, Yordanova R, Corradi JP, Adams SP. (2010). Phospholipidosis as a function of basicity, lipophilicity, and volume of distribution of compounds. Chem Res Toxicol **23**,749-55.

Harrison SC. (2008). Viral membrane fusion. Nat Struct Mol Biol **15**,690-698.

Hood CL, Abraham J, Boyington JC, Leung K, Kwong PD, Nabel GJ. (2010). Biochemical and structural characterization of Cathepsin L-processed Ebola virus glycoprotein: implications for viral entry and immunogenicity. J Virol.

Huang I-C, Bosch BJ, Li F, Li W, Lee KH, Ghiran S, Vasilieva N, Dermody TS, Harrison SC, Dormitzer PR and others. (2006). SARS coronavirus, but not human coronavirus NL63, utilizes cathepsin L to infect ACE2-expressing cells. J Biol Chem **281**,3198-203.

Hunt CL, Kolokoltsov AA, Davey RA, Maury W. (2011). The Tyro3 receptor kinase Axl enhances macropinocytosis of Zaire ebolavirus. J Virol **85**,334-47.

Huynh KK, Gershenzon E, Grinstein S. (2008). Cholesterol accumulation by macrophages impairs phagosome maturation. J Biol Chem **283**,35745-55.

Ito H, Watanabe S, Sanchez A, Whitt MA, Kawaoka Y. (1999). Mutational analysis of the putative fusion domain of Ebola virus glycoprotein. Journal of Virology **73**,8907-12.

Ito H, Watanabe S, Takada A, Kawaoka Y. (2001). Ebola virus glycoprotein: proteolytic processing, acylation, cell tropism, and detection of neutralizing antibodies. Journal of Virology **75**,1576-80.

Kaletsky RL, Simmons G, Bates P. (2007). Proteolysis of the Ebola virus glycoproteins enhances virus binding and infectivity. J Virol **81**,13378-84.

Kawaoka Y, Webster RG. (1988). Sequence requirements for cleavage activation of influenza virus hemagglutinin expressed in mammalian cells. Proc Natl Acad Sci USA **85**,324-8.

Klatzmann D, Champagne E, Chamaret S, Gruest J, Guetard D, Hercend T, Gluckman JC, Montagnier L. (1984). T-lymphocyte T4 molecule behaves as the receptor for human retrovirus LAV. Nature **312**,767-8.

Ko DC, Gordon MD, Jin JY, Scott MP. (2001). Dynamic movements of organelles containing Niemann-Pick C1 protein: NPC1 involvement in late endocytic events. Mol Biol Cell **12**,601-14.

Kobayashi T, Beuchat MH, Lindsay M, Frias S, Palmiter RD, Sakuraba H, Parton RG, Gruenberg J. (1999). Late endosomal membranes rich in lysobisphosphatidic acid regulate cholesterol transport. Nat Cell Biol **1**,113-8.

Kobayashi T, Startchev K, Whitney AJ, Gruenber J. (2001). Localization of lysobisphosphatidic acid-rich membrane domains in late endosomes. Biol Chem **382**,483-5.

Kobe B, Center RJ, Kemp BE, Poumbourios P. (1999). Crystal structure of human T cell leukemia virus type 1 gp21 ectodomain crystallized as a maltose-binding protein chimera reveals structural evolution of retroviral transmembrane proteins. Proc Natl Acad Sci USA **96**,4319-24.

Kodavanti UP, Mehendale HM. (1990). Cationic amphiphilic drugs and phospholipid storage disorder. Pharmacol Rev **42**,327-54.

Kolokoltsov AA, Saeed MF, Freiberg AN, Holbrook MR, Davey RA. (2009). Identification of novel cellular targets for therapeutic intervention against Ebola virus infection by siRNA screening. Drug Dev Res **70**,255-265.

Kolter T, Sandhoff K. (2010). Lysosomal degradation of membrane lipids. FEBS Lett **584**,1700-12.

Kondratowicz AS, Lennemann NJ, Sinn PL, Davey RA, Hunt CL, Moller-Tank S, Meyerholz DK, Rennert P, Mullins RF, Brindley M and others. (2011). T-cell immunoglobulin and mucin domain 1 (TIM-1) is a receptor for Zaire Ebolavirus and Lake Victoria Marburgvirus. Proc Natl Acad Sci USA **108**,8426-31.

Kondru R, Zhang J, Ji C, Mirzadegan T, Rotstein D, Sankuratri S, Dioszegi M. (2008). Molecular interactions of CCR5 with major classes of small-molecule anti-HIV CCR5 antagonists. Molecular Pharmacology **73**,789-800.

Kornhuber J, Tripal P, Reichel M, Mühle C, Rhein C, Muehlbacher M, Groemer TW, Gulbins E. (2010). Functional Inhibitors of Acid Sphingomyelinase (FIASMAs): a novel pharmacological group of drugs with broad clinical applications. Cell Physiol Biochem **26**,9-20.

Kuhn JH, Radoshitzky SR, Guth AC, Warfield KL, Li W, Vincent MJ, Towner JS, Nichol ST, Bavari S, Choe H and others. (2006). Conserved receptor-binding domains of Lake Victoria marburgvirus and Zaire ebolavirus bind a common receptor. J Biol Chem **281**,15951-8.

Kwon HJ, Abi-Mosleh L, Wang ML, Deisenhofer J, Goldstein JL, Brown MS, Infante RE. (2009). Structure of N-terminal domain of NPC1 reveals distinct subdomains for binding and transfer of cholesterol. Cell **137**,1213-24.

Lavillette D, Maurice M, Roche C, Russell SJ, Sitbon M, Cosset FL. (1998). A proline-rich motif downstream of the receptor binding domain modulates conformation and fusogenicity of murine retroviral envelopes. J Virol **72**,9955-65.

Le Blanc I, Luyet P-P, Pons V, Ferguson C, Emans N, Petiot A, Mayran N, Demaurex N, Fauré J, Sadoul R and others. (2005). Endosome-to-cytosol transport of viral nucleocapsids. Nat Cell Biol **7**,653-64.

Lederman MM, Veazey RS, Offord R, Mosier DE, Dufour J, Mefford M, Piatak M, Lifson JD, Salkowitz JR, Rodriguez B and others. (2004). Prevention of vaginal SHIV transmission in rhesus macaques through inhibition of CCR5. Science **306**,485-7.

Lee JE, Fusco ML, Hessell AJ, Oswald WB, Burton DR, Saphire EO. (2008). Structure of the Ebola virus glycoprotein bound to an antibody from a human survivor. Nature **454**,177-182.

Lemieux B, Percival MD, Falgueyret J-P. (2004). Quantitation of the lysosomotropic character of cationic amphiphilic drugs using the fluorescent basic amine Red DND-99. Anal Biochem **327**,247-51.

Leventhal AR, Chen W, Tall AR, Tabas I. (2001). Acid sphingomyelinase-deficient macrophages have defective cholesterol trafficking and efflux. J Biol Chem **276**,44976-83.

Li K, Zhang S, Kronqvist M, Ekström M, Wallin M, Garoff H. (2007). The conserved His8 of the Moloney murine leukemia virus Env SU subunit directs the activity of the SU-TM disulphide bond isomerase. Virology **361**,149-60.

Li W, Moore MJ, Vasilieva N, Sui J, Wong SK, Berne MA, Somasundaran M, Sullivan JL, Luzuriaga K, Greenough TC and others. (2003). Angiotensin-converting enzyme 2 is a functional receptor for the SARS coronavirus. Nature **426**,450-454.

Lin G, Simmons G, Pöhlmann S, Baribaud F, Ni H, Leslie GJ, Haggarty BS, Bates P, Weissman D, Hoxie JA and others. (2003). Differential N-linked glycosylation of human immunodeficiency virus and Ebola virus envelope glycoproteins modulates interactions with DC-SIGN and DC-SIGNR. J Virol **77**,1337-46.

Makino A, Ishii K, Murate M, Hayakawa T, Suzuki Y, Suzuki M, Ito K, Fujisawa T, Matsuo H, Ishitsuka R and others. (2006). D-threo-1-phenyl-2-decanoylamino-3-morpholino-1-propanol alters cellular cholesterol homeostasis by modulating the endosome lipid domains. Biochemistry **45**,4530-41.

Manicassamy B, Wang J, Jiang H, Rong L. (2005). Comprehensive analysis of ebola virus GP1 in viral entry. Journal of Virology **79**,4793-805.

Manicassamy B, Wang J, Rumschlag E, Tymen S, Volchkova V, Volchkov V, Rong L. (2007). Characterization of Marburg virus glycoprotein in viral entry. Virology **358**,79-88.

Marzi A, Gramberg T, Simmons G, Möller P, Rennekamp AJ, Krumbiegel M, Geier M, Eisemann J, Turza N, Saunier B and others. (2004). DC-SIGN and DC-SIGNR interact with the glycoprotein of Marburg virus and the S protein of severe acute respiratory syndrome coronavirus. J Virol **78**,12090-5.

Matsuno K, Kishida N, Usami K, Igarashi M, Yoshida R, Nakayama E, Shimojima M, Feldmann H, Irimura T, Kawaoka Y and others. (2010). Different potential of C-type lectin-mediated entry between Marburg virus strains. J Virol **84**,5140-7.

Matsuzawa Y, Hostetler KY. (1980). Studies on drug-induced lipidosis: subcellular localization of phospholipid and cholesterol in the liver of rats treated with chloroquine or 4,4'-bis (diethylaminoethoxy)alpha, beta-diethyldiphenylethane. J Lipid Res **21**,202-14.

Maxfield FR, Tabas I. (2005). Role of cholesterol and lipid organization in disease. Nature **438**,612-21.

McCune JM, Rabin LB, Feinberg MB, Lieberman M, Kosek JC, Reyes GR, Weissman IL. (1988). Endoproteolytic cleavage of gp160 is required for the activation of human immunodeficiency virus. Cell **53**,55-67.

Millard EE, Gale SE, Dudley N, Zhang J, Schaffer JE, Ory DS. (2005). The sterol-sensing domain of the Niemann-Pick C1 (NPC1) protein regulates trafficking of low density lipoprotein cholesterol. J Biol Chem **280**,28581-90.

Millard EE, Srivastava K, Traub LM, Schaffer JE, Ory DS. (2000). Niemann-pick type C1 (NPC1) overexpression alters cellular cholesterol homeostasis. J Biol Chem **275**,38445-51.

Miller EH, Harrison JS, Radoshitzky SR, Higgins CD, Chi X, Dong L, Kuhn JH, Bavari S, Lai JR, Chandran K. (2011). Inhibition of Ebola virus entry by a C-peptide targeted to endosomes. J Biol Chem **286**,15854-61.

Miller EH, Obernosterer G, Raaben M, Herbert AS, Deffieu MS, Krishnan A, Ndungo E, Sandesara RG, Carette JE, Kuehne AI and others. (2012). Ebola virus entry requires the host-programmed recognition of an intracellular receptor. EMBO J **31**,1947-60.

Misasi J, Chandran K, Yang J-Y, Considine B, Filone CM, Côté M, Sullivan N, Fabozzi G, Hensley L, Cunningham J. (2012). Filoviruses require endosomal cysteine proteases for entry but exhibit distinct protease preferences. J Virol **86**,3284-92.

Mkrtchyan SR, Markosyan RM, Eadon MT, Moore JP, Melikyan GB, Cohen FS. (2005). Ternary complex formation of human immunodeficiency virus type 1 Env, CD4, and chemokine receptor captured as an intermediate of membrane fusion. J Virol **79**,11161-9.

Mothes W, Boerger AL, Narayan S, Cunningham JM, Young JA. (2000). Retroviral entry mediated by receptor priming and low pH triggering of an envelope glycoprotein. Cell **103**,679-89.

Mpanju O, Towner J, Dover J, Nichol S, Wilson C. (2006). Identification of two amino acid residues on Ebola virus glycoprotein 1 critical for cell entry. Virus Research **121**,205-214.

Mulherkar N, Raaben M, de la Torre JC, Whelan SP, Chandran K. (2011). The Ebola virus glycoprotein mediates entry via a non-classical dynamin-dependent macropinocytic pathway. Virology.

Nanbo A, Imai M, Watanabe S, Noda T, Takahashi K, Neumann G, Halfmann P, Kawaoka Y. (2010). Ebolavirus Is Internalized into Host Cells via Macropinocytosis in a Viral Glycoprotein-Dependent Manner. PLoS Pathog **6**.

Negrete OA, Levroney EL, Aguilar HC, Bertolotti-Ciarlet A, Nazarian R, Tajyar S, Lee B. (2005). EphrinB2 is the entry receptor for Nipah virus, an emergent deadly paramyxovirus. Nature **436**,401-5.

Neumann G, Geisbert TW, Ebihara H, Geisbert JB, Daddario-DiCaprio KM, Feldmann H, Kawaoka Y. (2007). Proteolytic processing of the Ebola virus glycoprotein is not critical for Ebola virus replication in nonhuman primates. J Virol **81**,2995-8.

Ogert RA, Ba L, Hou Y, Buontempo C, Qiu P, Duca J, Murgolo N, Buontempo P, Ralston R, Howe JA. (2009). Structure-function analysis of human immunodeficiency virus type 1 gp120 amino acid mutations associated with resistance to the CCR5 coreceptor antagonist vicriviroc. J Virol **83**,12151-63.

Ohgami N, Ko DC, Thomas M, Scott MP, Chang CCY, Chang T-Y. (2004). Binding between the Niemann-Pick C1 protein and a photoactivatable cholesterol analog requires a functional sterol-sensing domain. Proc Natl Acad Sci USA **101**,12473-8.

Pager CT, Craft WW, Patch J, Dutch RE. (2006). A mature and fusogenic form of the Nipah virus fusion protein requires proteolytic processing by cathepsin L. Virology **346**,251-7.

Pager CT, Dutch RE. (2005). Cathepsin L is involved in proteolytic processing of the Hendra virus fusion protein. J Virol **79**,12714-20.

Radoshitzky SR, Abraham J, Spiropoulou CF, Kuhn JH, Nguyen D, Li W, Nagel J, Schmidt PJ, Nunberg JH, Andrews NC and others. (2007). Transferrin receptor 1 is a cellular receptor for New World haemorrhagic fever arenaviruses. Nature **446**,92-6.

Reaves BJ, Row PE, Bright NA, Luzio JP, Davidson HW. (2000). Loss of cation-independent mannose 6-phosphate receptor expression promotes the accumulation of lysobisphosphatidic acid in multilamellar bodies. J Cell Sci **113 (Pt 22)**,4099-108.

Rosenthal PB, Zhang X, Formanowski F, Fitz W, Wong CH, Meier-Ewert H, Skehel JJ, Wiley DC. (1998). Structure of the haemagglutinin-esterase-fusion glycoprotein of influenza C virus. Nature **396**,92-6.

Saeed MF, Kolokoltsov AA, Albrecht T, Davey RA. (2010). Cellular entry of ebola virus involves uptake by a macropinocytosis-like mechanism and subsequent trafficking through early and late endosomes. PLoS Pathog **6**.

Saeed MF, Kolokoltsov AA, Freiberg AN, Holbrook MR, Davey RA. (2008). Phosphoinositide-3 kinase-Akt pathway controls cellular entry of Ebola virus. PLoS Pathog **4**,e1000141.

Sawada H, Takami K, Asahi S. (2005). A toxicogenomic approach to drug-induced phospholipidosis: analysis of its induction mechanism and establishment of a novel in vitro screening system. Toxicol Sci **83**,282-92.

Schmid S, Fuchs R, Kielian M, Helenius A, Mellman I. (1989). Acidification of endosome subpopulations in wild-type Chinese hamster ovary cells and temperature-sensitive acidification-defective mutants. The Journal of Cell Biology **108**,1291-300.

Schornberg K, Matsuyama S, Kabsch K, Delos S, Bouton A, White J. (2006). Role of endosomal cathepsins in entry mediated by the Ebola virus glycoprotein. J Virol **80**,4174-8.

Schornberg KL, Shoemaker CJ, Dube D, Abshire MY, Delos SE, Bouton AH, White JM. (2009). Alpha5beta1-integrin controls ebolavirus entry by regulating endosomal cathepsins. Proc Natl Acad Sci USA **106**,8003-8.

Shimojima M, Ikeda Y, Kawaoka Y. (2007). The mechanism of Axl-mediated Ebola virus infection. J INFECT DIS **196 Suppl 2**,S259-63.

Shimojima M, Takada A, Ebihara H, Neumann G, Fujioka K, Irimura T, Jones S, Feldmann H, Kawaoka Y. (2006). Tyro3 family-mediated cell entry of Ebola and Marburg viruses. J Virol **80**,10109-16.

Simmons G, Gosalia DN, Rennekamp AJ, Reeves JD, Diamond SL, Bates P. (2005). Inhibitors of cathepsin L prevent severe acute respiratory syndrome coronavirus entry. Proc Natl Acad Sci USA **102**,11876-81.

Skehel JJ, Bayley PM, Brown EB, Martin SR, Waterfield MD, White JM, Wilson IA, Wiley DC. (1982). Changes in the conformation of influenza virus hemagglutinin at the pH optimum of virus-mediated membrane fusion. Proc Natl Acad Sci USA **79**,968-72.

Smith JG, Cunningham JM. (2007). Receptor-induced thiolate couples Env activation to retrovirus fusion and infection. PLoS Pathog **3**,e198.

Sobo K, Le Blanc I, Luyet P-P, Fivaz M, Ferguson C, Parton RG, Gruenberg J, van der Goot FG. (2007). Late endosomal cholesterol accumulation leads to impaired intra-endosomal trafficking. PLoS ONE **2**,e851.

Soneoka Y, Cannon PM, Ramsdale EE, Griffiths JC, Romano G, Kingsman SM, Kingsman AJ. (1995). A transient three-plasmid expression system for the production of high titer retroviral vectors. Nucleic Acids Res **23**,628-33.

Supekar VM, Bruckmann C, Ingallinella P, Bianchi E, Pessi A, Carfí A. (2004). Structure of a proteolytically resistant core from the severe acute respiratory syndrome coronavirus S2 fusion protein. Proc Natl Acad Sci USA **101**,17958-63.

Suzuki Y, Gojobori T. (1997). The origin and evolution of Ebola and Marburg viruses. Mol Biol Evol **14**,800-6.

Takada A, Robison C, Goto H, Sanchez A, Murti KG, Whitt MA, Kawaoka Y. (1997). A system for functional analysis of Ebola virus glycoprotein. Proc Natl Acad Sci USA **94**,14764-9.

Tetko IV, Gasteiger J, Todeschini R, Mauri A, Livingstone D, Ertl P, Palyulin VA, Radchenko EV, Zefirov NS, Makarenko AS and others. (2005). Virtual computational chemistry laboratory--design and description. J Comput Aided Mol Des **19**,453-63.

Towner JS, Paragas J, Dover JE, Gupta M, Goldsmith CS, Huggins JW, Nichol ST. (2005). Generation of eGFP expressing recombinant Zaire ebolavirus for analysis of early pathogenesis events and high-throughput antiviral drug screening. Virology **332**,20-7.

Towner JS, Sealy TK, Khristova ML, Albariño CG, Conlan S, Reeder SA, Quan P-L, Lipkin WI, Downing R, Tappero JW and others. (2008). Newly discovered ebola virus associated with hemorrhagic fever outbreak in Uganda. PLoS Pathog **4**,e1000212.

Tsibris AMN, Sagar M, Gulick RM, Su Z, Hughes M, Greaves W, Subramanian M, Flexner C, Giguel F, Leopold KE and others. (2008). In vivo emergence of vicriviroc resistance in a human immunodeficiency virus type 1 subtype C-infected subject. J Virol **82**,8210-4.

Volchkov VE, Feldmann H, Volchkova VA, Klenk HD. (1998). Processing of the Ebola virus glycoprotein by the proprotein convertase furin. Proc Natl Acad Sci USA **95**,5762-7.

Wallin M, Ekström M, Garoff H. (2004). Isomerization of the intersubunit disulphide-bond in Env controls retrovirus fusion. EMBO J **23**,54-65.

Wallin M, Ekström M, Garoff H. (2005). The fusion-controlling disulfide bond isomerase in retrovirus Env is triggered by protein destabilization. Journal of Virology **79**,1678-85.

Wallin M, Ekström M, Garoff H. (2006). Receptor-triggered but alkylation-arrested env of murine leukemia virus reveals the transmembrane subunit in a prehairpin conformation. J Virol **80**,9921-5.

Wang S-F, Huang JC, Lee Y-M, Liu S-J, Chan Y-J, Chau Y-P, Chong P, Chen Y-MA. (2008). DC-SIGN mediates avian H5N1 influenza virus infection in cis and in trans. Biochem Biophys Res Commun **373**,561-6.

Watanabe S, Takada A, Watanabe T, Ito H, Kida H, Kawaoka Y. (2000). Functional importance of the coiled-coil of the Ebola virus glycoprotein. Journal of Virology **74**,10194-201.

Watson C, Jenkinson S, Kazmierski W, Kenakin T. (2005). The CCR5 receptor-based mechanism of action of 873140, a potent allosteric noncompetitive HIV entry inhibitor. Molecular Pharmacology **67**,1268-82.

Wear MA, Patterson A, Malone K, Dunsmore C, Turner NJ, Walkinshaw MD. (2005). A surface plasmon resonance-based assay for small molecule inhibitors of human cyclophilin A. Anal Biochem **345**,214-26.

Weis W, Brown JH, Cusack S, Paulson JC, Skehel JJ, Wiley DC. (1988). Structure of the influenza virus haemagglutinin complexed with its receptor, sialic acid. Nature **333**,426-31.

Weissenhorn W, Carfí A, Lee KH, Skehel JJ, Wiley DC. (1998). Crystal structure of the Ebola virus membrane fusion subunit, GP2, from the envelope glycoprotein ectodomain. Mol Cell **2**,605-16.

Weissenhorn W, Dessen A, Harrison SC, Skehel JJ, Wiley DC. (1997). Atomic structure of the ectodomain from HIV-1 gp41. Nature **387**,426-30.

Westby M, Smith-Burchnell C, Mori J, Lewis M, Mosley M, Stockdale M, Dorr P, Ciaramella G, Perros M. (2007). Reduced maximal inhibition in phenotypic susceptibility assays indicates that viral strains resistant to the CCR5 antagonist maraviroc utilize inhibitor-bound receptor for entry. J Virol **81**,2359-71.

White JM, Delos SE, Brecher M, Schornberg K. (2008). Structures and mechanisms of viral membrane fusion proteins: multiple variations on a common theme. Critical Revs. in Biochem. & Mol. Biol. **43**,189-219.

Wilson IA, Skehel JJ, Wiley DC. (1981). Structure of the haemagglutinin membrane glycoprotein of influenza virus at 3 A resolution. Nature **289**,366-73.

Wong A, Sandesara R, Mulherkar N, Whelan S, Chandran K. (2009). A forward genetic strategy reveals destabilizing mutations in the ebolavirus glycoprotein that alter its protease dependence during cell entry. J Virol.

Wool-Lewis RJ, Bates P. (1998). Characterization of Ebola virus entry by using pseudotyped viruses: identification of receptor-deficient cell lines. Journal of Virology **72**,3155-60.

Wool-Lewis RJ, Bates P. (1999). Endoproteolytic processing of the ebola virus envelope glycoprotein: cleavage is not required for function. J Virol **73**,1419-26.

Yang Z-Y, Huang Y, Ganesh L, Leung K, Kong W-P, Schwartz O, Subbarao K, Nabel GJ. (2004). pH-dependent entry of severe acute respiratory syndrome coronavirus is mediated by the spike glycoprotein and enhanced by dendritic cell transfer through DC-SIGN. J Virol **78**,5642-50.

Yoshikawa H. (1991). Effects of drugs on cholesterol esterification in normal and Niemann-Pick type C fibroblasts: AY-9944, other cationic amphiphilic drugs and DMSO. Brain and Development **13**,115-20.

Yoshimura A, Kuroda K, Kawasaki K, Yamashina S, Maeda T, Ohnishi S. (1982). Infectious cell entry mechanism of influenza virus. J Virol **43**,284-93.

Zampieri C, Sullivan N, Nabel G. (2007). Immunopathology of highly virulent pathogens: insights from Ebola virus. Nat. Immunol.